DISSERTATION

MIR-137 REGULATES PTP61F, AFFECTING INSULIN SIGNALING, METABOLIC HOMEOSTASIS, AND STARVATION RESISTANCE IN *DROSOPHILA MELANOGASTER*

Submitted by

Hana Ibrahim Saedi

Department of Biomedical Sciences

In partial fulfillment of the requirements

For the Degree of Doctor of Philosophy

Colorado State University

Fort Collins, Colorado

Summer 2023

Doctoral Committee:

Advisor: Susan Tsunoda

Frederic Hoerndli
Gregory Amberg
Santiago Di Pietro

ABSTRACT

MIR-137 REGULATES PTP61F, AFFECTING INSULIN SIGNALING, METABOLIC HOMEOSTASIS, AND STARVATION RESISTANCE IN *DROSOPHILA MELANOGASTER*

miR-137 is a highly conserved brain-enriched microRNA (miRNA) that has been associated with neuronal function and proliferation. Here, we show that *Drosophila miR-137* null mutants display increased body weight with enhanced triglyceride and glucose levels and decreased locomotor activity. When challenged by nutrient deprivation, *miR-137* mutants exhibit reduced motivation to feed and significantly prolonged survival. Together, these phenotypes suggest a new role for *miR-137* in energy homeostasis. Genetic epistasis experiments show that the starvation resistance of *miR-137* mutants involves the insulin signaling pathway, and that loss of *miR-137* results in drastically reduced phosphorylation/activation of the single insulin receptor, InR, in *Drosophila*. We explore the possibility that the protein tyrosine phosphatase61F (PTP61F), ortholog of TC-PTP/PTP1B, known to dephosphorylate InR across species, is a potential *in vivo* target of *miR-137*. We show that loss of *miR-137* results in upregulation of an endogenously tagged PTP61F protein, and that genetically increasing levels of PTP61F mimics the loss of phosphorylated InR and increased starvation resistance seen in *miR-137* mutants. Finally, we show that the enhanced starvation resistance of *miR-137* mutants is normalized by activation of the insulin signaling pathway in the nervous system. Our study introduces *miR-137* as a new player in the regulation of central insulin signaling and metabolic homeostasis.

ACKNOWLEDGEMENTS

I am incredibly thankful to my Ph. D advisor Professor. Susan Tsunoda for giving me the opportunity to be part of her lab, for her help and encouragement, and for giving me the freedom to shape my project. I am also grateful to all the members of Tsunoda lab, whom I had great pleasure working with during my project.

I want to express my deepest appreciation to my committee members.

I would like to thank my family and friends. Special thanks to my loving and supporting husband, Mahir, and my two wonderful children, Qusay and Ruby, who provide endless love, encouragement, and inspiration.

Thank you all for making my dream come true.

TABLE OF CONTENTS

LIST OF TABLES

LIST OF FIGURES

CHAPTER 1: INTRODUCTION

1. Non-Coding RNA.

In molecular biology, the fundamental concept of the central dogma is based on transcribing genetic information from DNA sequence (coding DNA) to mRNA, and translating the mRNA to functional proteins. This part of the transcriptome is called protein-coding RNA, and includes about 1% of the genome and encodes more than 20,000 genes in humans (Dunham et al., 2012). However, many transcripts do not follow this protein-coding role and produce non-coding RNA. Researchers in the last decade have made great efforts to separate the non-coding RNA from the junk RNA concept and provide evidence to prove the importance of non-coding RNA for the organism's biology and survival (Fu, 2014; J. Li & Liu, 2019; Statello et al., 2021). Non-coding RNAs come in several different types, including microRNA (miRNA), small nucleolar RNA (snoRNA), short interfering RNA (siRNA), piwi-interacting RNA (piRNA), small nuclear RNA (snRNA), and long non-coding RNA (long ncRNA), all of which have very critical functions in cellular biology (Fu, 2014).

1.1 MicroRNAs (miRNAs).

The most abundant kind of non-coding RNAs are miRNAs. miRNAs are evolutionarily conserved in their sequence in the eukaryotes (Hammond, 2015a; Schanen & Li, 2011). miRNAs were first discovered 30 years ago, in 1993, during the study of the *lin-4* gene in *Caenorhabditis elegans* (*C. elegans*) (Ambros, 1989; Chalfie et al., 1981; R. C. Lee et al., 1993). *Lin-4* RNA was found not to encode a protein, but to translationally repress the expression of another gene, *lin-14*, when it complementarily bound to the 3’

untranslated region (3' UTR) sequence of *lin-14* mRNA (R. C. Lee et al., 1993; Mondol & Pasquinelli, 2012). After another decade in 2000, the functional significance of the miRNA become more evident in studies of the developmental timing in *C. elegans*. A miRNA called *lethal-7* (*let-7*) was found to be a key developmental regulator that highly conserved between *C. elegans*, fruit flies, zebrafish, and humans (Reinhart et al., 2000; Slack et al., 2000). *Let-7* was identified as the first known human miRNA, and the discovery of the let-7 gene was the revolution that revealed miRNA biogenesis, and their many functions. Between 1993 and now, more than 2000 miRNAs have been discovered in humans.

miRNAs are short, endogenous, single-stranded, non-coding RNA sequences with a length of 19-24 nucleotides (nt). MiRNAs mediate gene expression at the post-transcriptional level and are critical for cell development, proliferation, differentiation, metabolism, in various signaling pathways, and cell death processes (apoptosis) (Hammond, 2015b; O'Brien et al., 2018). miRNAs can directly or indirectly modify translated genes after they leave the nucleus. The canonical action of the miRNA is to silence gene expression. miRNAs partially complement and bind to a target messenger RNA (mRNA) at its 3' UTR region, causing the decay of the mRNA target or interference its translation into protein, thereby inhibiting or modifying protein expression levels (O'Brien et al., 2018). However, miRNAs can also cause gene up-regulation under certain circumstances (Vasudevan, 2012).

1.2 miRNA Biogenesis.

miRNA biogenesis starts inside the nucleus. Genes that code for miRNAs are transcribed by RNA polymerase II (PoII), generating a stem-loop hairpin structure single-

stranded RNA called primary-miRNA (pri-miRNA). The pri-miRNA is then processed into a smaller (~70 nt) precursor miRNA (pre-miRNA) by an RNase III endonuclease called Drosha and RNA binding proteins called DiGeorge Syndrome Critical Region 8 protein (DGCR8) (Pasha in *Drosophila*) (Kuehbacher et al., 2007; Y. Lee et al., 2003). The Drosha and DGCR8 cleavage results in a 2 nt overhang on the 3' end of the pre-miRNA. This overhang region at the pre-miRNAs will be recognized and help the transfer of the pre-miRNA to the cytoplasm through nuclear pores with the help of a transporter protein called exportin-5 (EXP-5) (Yi et al., 2003). After translocating to the cytoplasm, a large RNase protein called Dicer associates with its co-factor TRBP (transactivation response element RNA-binding protein) and cleaves the pre-miRNA stem-loop of the hairpin to form a short double-stranded RNA molecule (Kuehbacher et al., 2007). Next, the argonaut protein (Ago2) interacts with Dicer and binds to the miRNA, unwinding the RNA duplex to release one strand that is then degraded. The strand selection is determined by the asymmetric thermodynamic stability of the RNA double strands. The strand with the lower stability at the 5' region interacts and loads on Ago2 and other proteins, to produce a miRNA-induced silencing complex (miRISC). This strand length is ~19-24 nt and functions as the mature RNA (Ghildiyal & Zamore, 2009; Hammond, 2015b; Wahid et al., 2010).

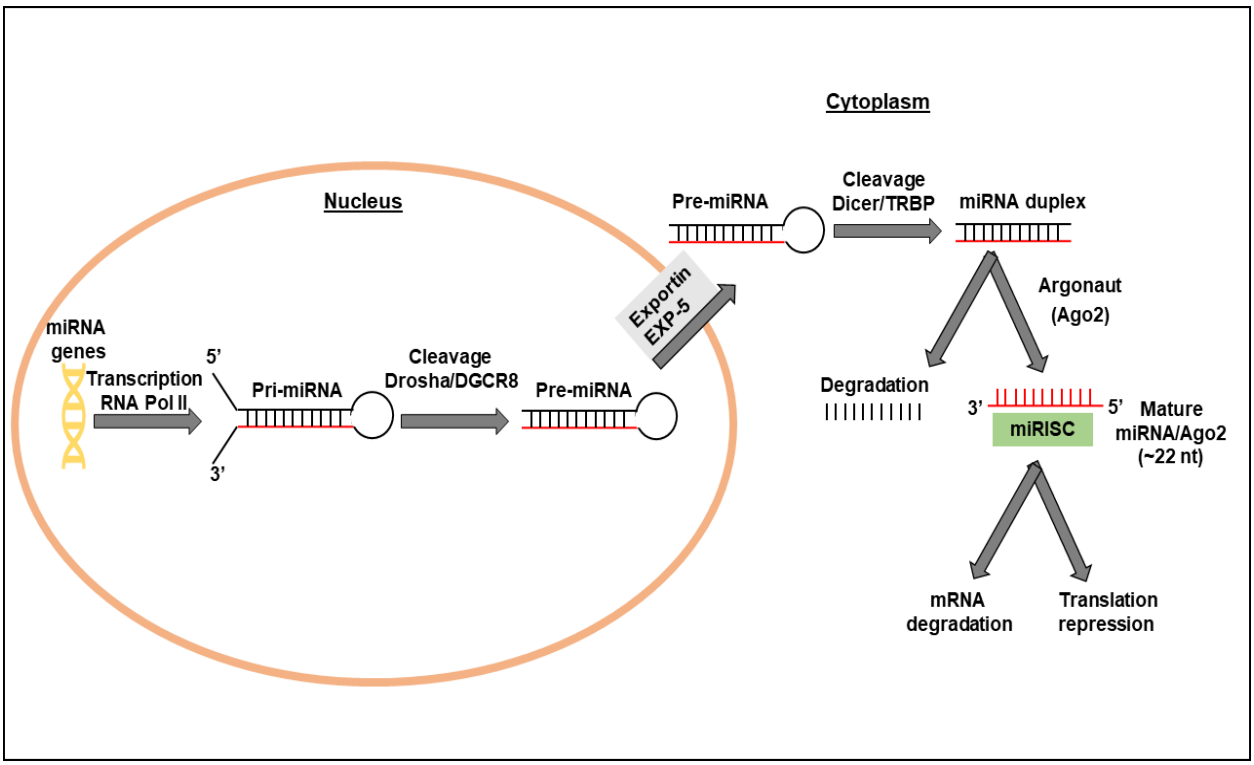

Figure 1. miRNA biogenesis pathway and canonical function. miRNA is transcribed inside the nucleus by RNA pol II transcription factor to pri-miRNA, a hairpin loop structure. Then Drosha and DGCR8 (Pasha in *Drosophila*) micro-process the pri-miRNA to a smaller ~ 70 nt pre-miRNA. Exp-5 transfers the pre-miRNA double-stranded RNA out from the nucleus. In the cytoplasm, the pre-miRNA stem-loop is cleaved by RNase III, known as Dicer, and TRBP unwinds the double-stranded RNA and releases the mature miRNA (19-24 nt). The mature single-stranded miRNA product has a 3' arm and 5' arm that will incorporate with the argonaute protein (Ago2), included in an RNA-induced silencing complex (miRISC) that mediates gene regulation by targeting the 3' UTR region of target mRNAs. Complementary miRNA base pairing of the 6 nt sequence from 2 to 8 (seed sequence) to the 3' UTR sequence results in degradation of the mRNA or inhibition of protein translation, through deadenylating or decapping, respectively.

1.3 miRNA-Mediated Gene Regulation.

Bioinformatics studies estimate that miRNAs regulate the expression of up to 80% of human genes (Lu & Clark, 2012; Mahmoudi & Cairns, 2017). Dysregulation of miRNAs can lead to severe consequences and diseases such as neural disorders and cancers. A

miRNA interacts with the effector complex (microribonucleoprotein miRNP) and the sequence-specific recognition of the target site (called cognate mRNA) to produce its effect on a target gene (Orang et al., 2014; Siomi & Siomi, 2009). miRNAs can rapidly cause gene silencing or transiently fine-tune gene expression depending on cellular and extracellular conditions (Peng & Croce, 2016; Wright et al., 2016). miRISC binds to a 6 nucleotide sequence from nucleotide 2 to nucleotide 8 called the “seed sequences” in the 3’ UTR of a target mRNA. miRISC mediates gene expression at the post-transcriptional level by inhibiting the translation of the mRNA into protein. miRISC interaction with deadenylase or decapping complexes causes mRNA poly-A tail removal (deadenylation) or decapping (Fabian & Sonenberg, 2012). At the translational level, gene silencing may occur directly or indirectly by different mechanisms. For example, gene silencing may occur at the early translation inhibition before elongation, premature termination, or post-initiation inhibition of mRNA translation. In addition, the miRNP could interfere with the ribosome subunit by preventing its joining or promoting its dissociation. The miRNP could also recruit different enzymes, such as deadenylase, exonuclease, and endonucleases resulting in the degradation of the mRNA. As a post-initiation mechanism, miRNP can also obstruct the translation elongation and termination of translation by antagonizing the elongation factors causing protein decay (Fabian & Sonenberg, 2012; Gu & Kay, 2010; Orang et al., 2014; Ruby et al., 2007). However, the exact mechanism of how miRISC regulates its targets remains debatable.

Until recently, gene repression has been the exclusive mechanism studied for miRNAs. However, miRNAs have now been found to post-transcriptionally up-regulate gene expression in response to specific stress conditions, in specific cell types, during

different developmental periods, or with particular co-factors (Vasudevan, 2012). How exactly miRNAs up-regulate gene expression is more complicated. A miRNA can up-regulate gene expression directly by associating with miRNP factors, or indirectly by abolishing the inhibitory action of the miRISC (Orang et al., 2014). Some miRNAs can mediate both up-regulation and down-regulation in a context-dependent manner. For example, *miR-206* can regulate the *Krüppel-like factor4* (*KLF4*) transcription factor in a regulatory feedback loop that is the opposite during normal versus cancer conditions. In normal conditions, *miR-206* promotes the expression of transcription factor *KLF4* and promotes proliferation of non-cancerous cells. (Lin et al., 2011) have reported that in breast and gastric cancer cells, *miR-206*, however, represses the expression of *KLF4* and *miR344-1*. Furthermore, at the oocyte stage, *miR-206* and *miR-16* activate the two key factors responsible for stimulating translation, *KLF4* and *Myelin transcription factor 1* (*Myt1*), by Ago2 and *fragile-X-metal retardation-related protein 1* (*FXR1*). *KLF4* and *Myt1* can regulate mRNA translation by associating with a factor needed for mRNA translational activation (TNFα-AU-rich 3'UTR) (Orang et al., 2014). In a similar manner, *miR-369-3* is associated with *TNFα* and causes translational activation, but only under conditions of serum starvation (Rusk, N. 2008). Another example, *miR-346* can up-regulate a transcription coregulator called receptor-interacting protein 140 (RIP140), required for metabolic processes via binding to the 5' UTR of its mRNA and facilitating mRNA-polysomes interaction (Tsai et al., 2009). Interestingly, the up-regulation of RIP140 protein expression occurs without affecting RIP140 mRNA levels (Tsai et al., 2009). Another miRNA mechanism of increasing translation involves its pairing to the 5' UTR. For example, *miR-10* can bind to the 5' UTR of the ribosomal protein (*RP*) mRNA

increasing global ribosomal biogenesis, thereby enhancing global protein synthesis and controlling the cell's transformation capacity (Ørom et al., 2008).

Increasing evidence shows that gene expression can be either up-regulated or down-regulated post-transcriptionally depending on the cell type and cell condition. In addition, hundreds of genes can be regulated by a single miRNA, and multiple miRNAs can regulate a single gene. This complexity has made the identification of the exact mechanisms by which miRNAs regulate gene expression to be very challenging.

1.4 miRNA Recognition and Seed Sequence.

At the present time, the mechanism of miRNA recognition and targeting mRNA has been well characterized. As a result, a number of computational prediction algorithms capable of predicting miRNA-mRNA interactions have been developed, such as miRbase, DIANA-microT-CDS, cmiR, a-mir-SVR and TargetScan (Peterson et al., 2014). However, the most commonly used target prediction tool is TargetScan (https://www.targetscan.org/). The standard features of target prediction methods are based on several main factors, including the matching between the seed sequence of the miRNA and mRNA sequence, the conservation of the sequences across species, the predicted stability of the mRNA-miRNA structure, the binding site accessibility, and the energy required (Peterson et al., 2014). The seed sequence is the first 2-8 nucleotides from the miRNA 5' end (Lewis et al., 2005). The miRNA seed sequence can bind to the 3' UTR of a mRNA with precise base pairing or with partial complementary base pairing. The precise base pairing is where adenosine A is bound to uracil U and guanine is bound to cytosine C, while partial complementary binding occurs when at least 6 nucleotides are

complementary. Databases generated to predict targets are mainly based on seed sequence identification. Computational prediction algorithms list putative targets based on organism type, miRNA name, gene name, seed match, and conservation probability. Overall, miRNA-mRNA target prediction tools have advanced gene expression regulation research.

1.5 *miR-137*.

miR-137 is one of many miRNAs that have a critical role in mammalian cellular biology. *miR-137* was first discovered by Lagos-Quintana and his colleagues in 2002. *miR-137* is expressed in various human and animal tissues, but mainly in the nervous system, where it is highly expressed in the brain with a high concentration at synapses (Guella et al., 2013; Landgraf et al., 2007). The gene coding for *miR-137* is 61 kilobase (Kb) long and located on chromosome 1p22 within a long non-coding host gene called *MIR137HG* in the human genome (Lagos-Quintana et al., 2002; Mahmoudi & Cairns, 2017). Like all the other miRNAs, the *miR-137* gene is transcribed in the nucleus and processed into a smaller hairpin *precursor-miR-137* (*pre-miR-137*). The *pre-miR-137*, which is 102 base pair long, then leaves the nucleus through nuclear pores, and is then cleaved into the smaller mature *miR-137*. The mature *miR-137* form is 23 nt long, UAUUGCUUAAGAAUACGCGUAG (5′ to 3′) (Mahmoudi & Cairns, 2017).

As miRNAs can regulate multiple mRNAs, a problem with a single miRNA can have deleterious effects from mis-regulation of multiple downstream targets resulting in phenotypical effects. *miR-137* is a miRNA that is associated with adult neurogenesis, dendritic development, neural maturation, and cognitive function (Olde Loohuis et al.,

2015a; Strazisar et al., 2015; Thomas et al., 2018). *miR-137* regulates neurodevelopmental processes during development by modulating target genes associated with neural stem cell proliferation, differentiation, and apoptosis. The overexpression of *miR-137* is able to shift cells from proliferation to differentiation of neurons in stem cells (Meza-Sosa et al., 2014). The overexpression of *miR-137* decreases dendritic density and spine growth in newborn neurons, and its inhibition has the opposite effect on dendritic complexity (Smrt et al., 2010a). In addition, *miR-137* levels change during development with levels increasing with age, highest around the age of 25, then continuing to increase as age increases (Pacheco et al., 2019). *miR-137* is required for healthy dendritic development of hippocampal neurons *in vivo* and *in vitro* studies (E. He et al., 2018; Sakamoto & Crowley, 2018). *miR-137* also functions in many signaling pathways, including MAPK/ERK, Nrg/ErbB, and PI3K-AKT-mTOR (Jiang et al., 2019a; Thomas et al., 2017, 2018).

Mis-regulation of *miR-137* is associated with neurological conditions, such as Schizophrenia, Autism, and Bipolar Disease in humans (discussed further in section 1.7). *miR-137* dysregulation also contributes to several cancers like neuroblastoma and glioblastoma multiforme, and it is used as a blood biomarker for cancer in humans (Bier et al., 2013; Silber et al., 2008). Epigenetic hypermethylation causes loss of *miR-137* in primary endometrial tumors (Kashani et al., 2019). The down-regulation of *miR-137* has been proven to increase cancer progression as it is a stimulant of cell differentiation (Bier et al., 2013; Mahmoudi & Cairns, 2017). Overall, genetic overexpression of *miR-137* suppresses the growth and proliferation of tumors and reduced tumor size (J. Wang et al., 2021; Y. Wang et al., 2020).

1.6 Putative and Validated Targets of *miR-137*.

By using bioinformatic analysis approaches, over 1300 potential target genes are predicted to be regulated by *miR-137,* including ion channels and many signaling proteins (Agarwal et al., 2018; Yin et al., 2014). TargetScan identifies 1314 putative targets in humans, 1274 in mice, and 532 in the fly. More than fifty genes have been experimentally confirmed to be direct targets for *miR-137*, either by western blot, RT-qPCR, or luciferase assay in various cell lines (Mahmoudi & Cairns, 2017). For example, *miR-137* directly influences the protein kinase B, AKT1, AKT2, AKT3, and DRD2, essential components of the mTOR pathway (Howell & Law, 2020; L. Li et al., 2020). Interestingly, substantial genes that have roles in the etiology of schizophrenia and brain function such as, CSMD1, C10orf26, CACNA1C, TCF4, ZNF804A, ERBB4, GABRA1, GRIN2A, GRM5, GSK3B, NRG2, and HTR2C, have also been validated as targets of *miR-137* (Wright et al., 2013). More validated targets of *miR-137,* include RORα, D2R, TCF4, NRXN1, SHANK2, SCN2A, genes that associated with autism spectrum disorder, neurological disorders, and cancer (Jiang et al., 2019b; Mahmoudi & Cairns, 2017; Pacheco et al., 2019; Yin et al., 2014a).

1.7 *miR-137* Roles in Neurodevelopment, Mental, and Behavioral Disorders.

Validated targets suggest a potential association of *miR-137* with the etiology of psychiatric disorders. A genome-wide association study (GWAS) has linked single nucleotide polymorphisms (SNPs) in *miR-137* to cognitive disorders such as schizophrenia (SZ) and autism spectrum disorder (ASD) in humans (Sakamoto & Crowley, 2018). Many genetic polymorphisms have been associated with the adult onset

of schizophrenia (AOS), and the *miR-137HG* gene is the top associated gene with SZ SNP (*rs1625579, rs1198588, rs2660304, rs1702294*) (Pacheco et al., 2019). SZ is a chronic mental illness that causes a person to disconnect from reality, affecting feelings, thinking, and behavior. Patients with SZ suffer from cognitive and memory difficulties (Manoach & Stickgold, 2015). SZ is a highly hereditable disorder that runs through the family (He et al., 2018; Siegert et al., 2015; Strazisar et al., 2015). The SNP *Rs1625579* was identified within an intron of a putative primary transcript of *miR-137* (Arakawa et al., 2019; Ripke et al., 2011). *Rs1625579* is located 8 kb downstream of the *miR-137* gene and was found to be associated with many SZ phenotypes, including memory deficit and cognitive dysfunction (Yin et al., 2014b). *miR-137* likely contributes to the etiology of neurodevelopmental deficits as it regulates adult neurogenesis, glutamate receptor signaling, and synaptic plasticity (Olde Loohuis et al., 2015b; Siegert et al., 2015b; Smrt et al., 2010b). *miR-137* expression is decreased in the prefrontal cortex by about 30% in patients with SZ and Bipolar disorder (Guella et al., 2013), and increased at hippocampal synapses (Arakawa et al., 2019). These studies hypothesize that *miR-137* gain of function is associated with the risk of SZ.

ASD is a group of neurodevelopmental disabilities characterized by abnormal social communication, limited interest, and stereotypical repetitive behavior. ASD susceptibility is linked to genetic components. Multiple reports suggest that microdeletion of *miR-137* is a potential contributor to ASD (Cheng et al., 2018; Siegert et al., 2015). Retinoic acid-related orphan receptor alpha gene (*RORα*) has been implicated as one of the candidate genes linked to ASD. Even though several other brain regions are affected, the cerebellum, where *RORα* is most highly expressed, is the area of the brain

most affected by the neuropathology of ASD. *miR-137* was found to be targeting the 3' UTR of *RORα* and directly regulates its expression (Devanna & Vernes, 2014). Taken together, these data suggest there is a possibility that *miR-137* and autism candidate gene *RORα* are related to ASD.

The primary diagnosis for neuropsychiatric disorders is impaired social behaviors and memory deficit, and evidence shows that *miR-137* dysregulation is associated with phenotypes showing deficits in cognitive functions. Patients with the *miR-137 Rs1625579* allele showed an alteration in front-amygdala activity (Yin et al., 2014b). In memory tests and fear behavioral tasks that measure memory recall of a stimulus (tone) followed by foot shock, mice with *miR-137* overexpression showed a reduced freezing response compared to control mice (Siegert et al., 2015). Further data showed that *miR-137* overexpression impaired hippocampal learning and memory in the Morris water maze tests, where mice with *miR-137* overexpression were significantly delayed finding the escape platform compared to the control mice (Siegert et al., 2015). These results indicate that *miR-137* overexpression, which is associated with SZ, impaired hippocampus-dependent memory.

On the other hand, mice with loss of *miR-137* also reveal impaired learning and memory. *miR-137* partial knockdown mice showed a significant delay in finding the escape platform compared to the wild type In Morris water maze tests (Cheng et al., 2018). In the Barnes maze, where mice were trained to find a hidden box to escape the maze, *miR-137* partial knockdown mice revealed a significantly longer time to find fewer boxes than the wild type (Cheng et al., 2018). Together, these data indicate that the loss of *miR-137* results in learning and memory deficits.

The loss of *miR-137* mice resulted in repetitive behaviors, such as burying extra marbles and extended self-grooming, especially when in contact with new mice (Cheng et al., 2018). In addition, *miR-137* partial knockdown mice showed increased anxiety-like behavior and less interest in exploring new mice (Sakamoto & Crowley, 2018). In conclusion, the loss of *miR-137* significantly affects memory, cognitive, and social behavior.

miR-137 expression appears early in life, and studies have provided strong evidence that *miR-137* is essential for development. Cheng et al., 2018, showed that *miR-137* knockout mice exhibit complete embryonic lethality, as none of the homozygote *miR-137* knockout mice survived. Mice needed at least one copy of *miR-137* to live. He et al., 2018, showed that *miR-137* homozygous knockout mice exhibit postnatal lethality, where mice only survived until 21 days and suffered from significant brain and body weight loss. The partial loss of *miR-137* in the CNS causes issues in synaptic plasticity, repetitive behavior, and impaired learning and memory (Cheng et al., 2018). Together, these studies show that *miR-137* plays a vital role in neurodevelopment, and its function is critical for survival.

1.8 The Implication of miRNAs and *miR-137* in Response to Different Kinds of Stress.

Under stress, cells deviate from the normal state to a new state that threatens cellular homeostasis. Stress results in neurological, physiological, and behavioral modifications that help the cell tolerate change to a new cellular condition and/or restore itself to the previous homeostasis (Clark & Fucito, 1998). Depending on the severity and

the duration of the stressor, cells attempt to survive by repairing damaged macromolecules, changing gene expression, arresting growth, or triggering cell death (apoptosis). miRNAs are important candidates involved in the stress response as they can modulate gene expression in multiple signaling pathways by targeting mRNAs or regulating protein translation (Olejniczak et al., 2018). miRNA biogenesis is also altered under conditions of stress. For example, Ago2 complexes associate with miRNAs and localize stress granules to different subcellular compartments upon stress (Leung & Sharp, 2007). Deletion of specific miRNAs does not always produce a significant phenotype under normal conditions, however, the same miRNA mutants sometimes exhibit deleterious phenotypes under stress conditions (van Rooij et al., 2007).

miR-137 is essential for significant aspects of cellular and physiological processes, such as neural cell proliferation and differentiation. For example, *miR-137* attenuated oxidative stress, apoptosis, and inflammatory responses through the MAPK signaling pathway. *miR-137* knockout increases the oxidative stress response, indicated by the level of reactive oxygen species (ROS) and inflammatory factors in the brain tissues of *miR-137* knockout mice (Tian et al., 2019). *miR-137* inhibits the MAPK signaling pathway in ischemic stroke by complementary binding to the 3' UTR of gene products, including *Src*, a proto-oncogene non-receptor tyrosine kinase. Src induces the activation of *ERK1/2* as well as *p38-MAPK/JNK* signaling pathways, which are responsible for the regulation of cell apoptosis (Tian et al., 2019). Therefore, it is possible that *miR-137* may also be involved in regulating the stress response by regulating the synthesis of proteins or targeting the transcripts involved in stress responses.

On the other hand, *miR-137* knockdown alleviates oxidative stress injury of neurons in a mouse model of Parkinson's disease by up-regulating oxidation resistance protein 1 (*OXR1*) (Jiang et al., 2019). *OXR1* is a vital protein that acts protectively by regulating the sensitivity of neuronal cells to oxidative stress. Mice lacking *OXR1* display increased neurodegeneration (Oliver et al., 2011). Our understanding of the underlying mechanisms through which *miR-137* participates in these responses is still under intense investigation.

1.9 Molecular Mechanisms Underlying Metabolic Stress in *Drosophila melanogaster*.

The metabolic energy of insects is regulated by three main signaling pathways, similar to mammals: the Glucagon/Adipokinetic signaling pathway, the Insulin/IGF signaling pathway, and the TOR signaling pathway. The functions of these pathways facilitate cell development, proliferation, production of proteins, mobilization and storage of nutrients, and survival. These pathways are conserved from flies to humans and coordinate tissue growth and metabolism depending on nutrient availability.

1.9.1 Glucagon/Adipokinetic Signaling Pathway (AKH).

The major hormonal pathways that control metabolism, growth, and survival are conserved throughout the animal kingdom. In mammals**,** the nutrient-sensing glucagon and insulin hormones are controlled by blood glucose level and regulate fat and glucose metabolism. When blood glucose levels are low (starvation), the level of insulin hormone decreases while the level of glucagon hormone increases. The increase in glucagon

hormone level promotes the breakdown of glycogen and lipids to maintain survival. In *Drosophila*, the functional analog of the glucagon hormone is the Adipokinetic hormone (AKH). AKH is a metabolic neuropeptide hormone released from the neuroendocrine ring gland called corpus cardiaca in the brain of *Drosophila*. AKH is involved in metabolic regulation during metabolic stress (G. Lee & Park, 2004; Schooneveld et al., 1983)**.** AKH binds with high affinity to the Adipokinetic hormone receptor (AKHR), located on the plasma membrane of fat body cells. The fat body in insects is the main site of energy storage and serves a similar purpose as the liver and adipose tissue in mammals (Aguila et al., 2007). The AKHR is a G-protein-coupled receptor, and AKH binding to AKHR in the fat body stimulates glycogen phosphorylase, which activates the breakdown of glycogen and increase the release of the primary circulating sugar in the hemolymph of the flies (trehalose) (Graham & Pick, 2017; G. Lee & Park, 2004)**.** AKH activity in the fat body leads to the phosphorylation of lipid storage droplet protein-2 (*LSD2*), a protein primarily associated with lipid droplets in the fat body (Toprak, 2020). Moreover, AKHR activation increases the transcription of the *Drosophila* homolog of triglyceride lipase, called bummer (*bmm*). The phosphorylation of *LSD2* and *bmm* lead to a breakdown of triglycerides into diacylglycerides and transport to the hemolymph (Grö Nke et al.,2007). The lipid movement from the stores during starvation stress is analogous to the mammalian regulation of lipolysis. Overall, AKH signaling in the fat body elevates lipid and trehalose levels in the hemolymph and boosts survival during metabolic stress.

AKH signaling regulates the starvation phenotype of flies. For example, AKH is involved in increasing locomotor activity during starvation. Flies normally exhibit hyperactivity during starvation, a behavioral sign for searching for food. The disadvantage

of starvation-induced hyperactivity is the fast depletion of energy stores, decreasing survival longevity. The AKH mutant flies exhibit a decrease in starvation-induced hyperactivity (Q. He et al., 2020; R. Huang et al., 2020). The genetic mutation in AKH (*Akh*^{1}), is a loss-of function mutation at the second amino acid (Leu) of the N-terminus of *AKH* gene. *Akh*^{1} or AKHR mutant flies exhibit phenotypes of hyperlipidemia, hypertrehalosemia (Mochanová et al., 2018). These AKH-deficient flies are starvation resistant due to increased levels of energy stores, and the increased body mass (G. Lee & Park, n.d.; Mochanová et al., 2018).

Crosstalk between the AKH and insulin signaling pathways depends on nutritional state. *Drosophila* insulin-like peptides (*Dilps*) are released under normal feeding conditions to promote energy storage, while AKH is released in starved conditions to promote energy release (Q. He et al., 2020). An evolutionarily conserved α-glucosidase, a target of brain insulin (*Tobi*), showed a link between the insulin and AKH signaling pathways with both AKH and Dilps regulate it. *Tobi* levels are elevated by dietary protein intake and decreased by dietary glucose intake. *Tobi* regulates the conversion of glycogen to glucose, thereby regulating glycogen content (Ahmad et al., 2020; Buch et al., 2008; Strilbytska et al., 2020). The interaction between AKH and insulin signaling pathways mediates a regulatory role in insect metabolism.

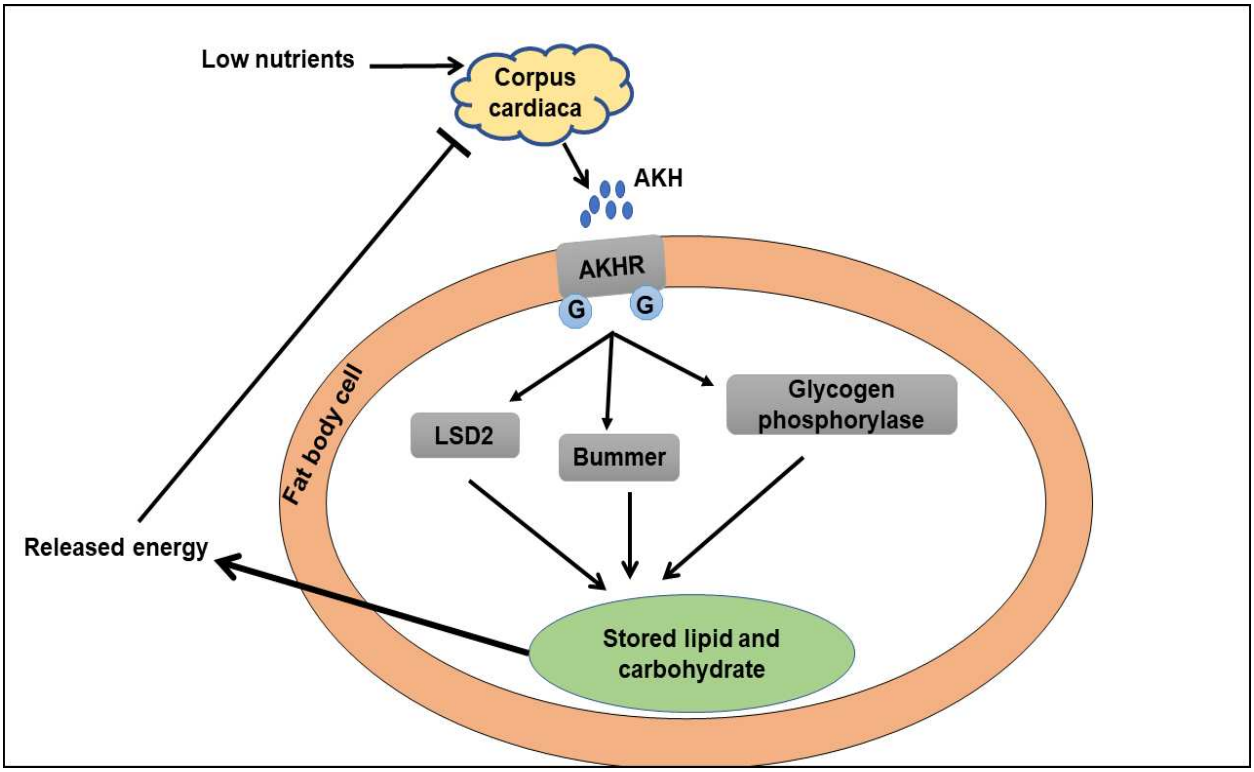

Figure 2. Simplified representation of the AKH signaling pathway. AKH hormone is released from the corpus cardiaca cells in response to low circulating trehalose. In the fat body, AKH will bind to G-protein-coupled receptors (AKHR) and activate glycogen phosphorylase, LSD2, and Bummer lipases, allowing the mobilization of stored energy. As a result of the released energy, feedback inhibition of AKH release will occur.

1.9.2 Insulin/IGF Signaling Pathway (IIS).

In addition to AKH, the other two major players that sense, control, store, and metabolize nutrients in animals are the insulin/IGF (IIS) and TOR pathways. Among all animal species, the insulin/PI3K/AKT pathway is highly conserved and implicated in regulating cellular growth, proliferation, fat storage, and survival (Liu & Lehmann, 2006; Scanga et al., 2000). After a meal, food is digested into sugar, amino acids, and fatty acids. The pancreas releases the hormone insulin to regulate blood glucose levels after digestion. In mammals, the insulin receptor (InR) can be activated by insulin hormone, insulin-like growth factor I (IGF-1), and insulin-like growth factor II (IGF- II) (Boucher et

al., 2010). Insulin interacts with the insulin receptor located on the surface of target cells like liver cells, skeletal muscle cells, and adipose cells to promote glucose uptake.

The InR/IGF is composed of a proprioceptor polypeptide that undergoes proteolytic modification to generate a dimer of two extracellular alpha subunits and two transmembrane beta subunits that are joined by disulfide bonds (Baserga, 1999; Fernandez et al., 1995). Insulin binding to the InR extracellular alpha subunits triggers the activation of the cytoplasmic C-terminal tyrosine kinase domain contained in the beta subunits and causes InR autophosphorylation. InR β-subunit is phosphorylated at 3 major tyrosine residues (Tyr1131, Tyr1135, and Tyr1136) and two kinases domains Y1162/1163, all of which are essential for InR activation (Baserga, 1999; Hernandez-Sanchez et al., 1995; Lopaczynski et al., 2000; C. L. Wu et al., 2011a). The phosphorylated InR generates a docking site for adaptor molecules and can phosphorylate a number of downstream targets, including the Insulin receptor substrate (IRS). IRS has 4 isoforms in mammals (IRS1-4), with only one isoform in *Drosophila* called chico. IRS/chico proteins contain different binding domains, such as a phosphotyrosine binding domain (PTB) and an N-terminal pleckstrin homology (PH) domain. The PTB domain site is associated with the phosphorylated InR, resulting in IRS/chico phosphorylation. A PH domain in IRS/chico can also act as a docking site for SH2-containing proteins. Phosphorylation of IRS/chico initiates a phosphorylation cascade. The IRS/chico phosphorylation recruits a p85 adaptor unit for phosphatidylinositol 3 kinase (PI3K) phosphorylation. After PI3K is phosphorylated, it will phosphorylate a membrane phospholipid, PIP2, and convert it into PIP3. The phosphorylated site on PIP3 subsequently be recognized by a 3-phosphoinositide-

dependent kinase (PDK) and activate protein kinase B, called AKT. Full activation of AKT depends on Thr308 phosphorylation by PDK1 (Thr342 in *Drosophila*) and Ser473 phosphorylation (Thr505 in *Drosophila*) within the carboxy terminus of PDK2 (Alessi et al., 1996). AKT also promotes glycogen synthesis by repressing glycogen synthesis kinase 3β (GSK-3 β) (Shaggy in *Drosophila*) (Hietakangas & Cohen, 2009; Jacinto et al., 2006; S. Lee & Dong, 2017). Upon AKT activation, Forkhead Box O (FOXO) will be repressed. FOXO is a transcription factor that plays a critical role in response to several physiological stresses (Ni et al., 2007). *Drosophila* has a single FOXO gene called dFOXO, representing the FOXO family in mammals (Puig et al., 2003). Phosphorylated AKT can phosphorylate FOXO at three sites: Thr44, Ser190, and Ser259 (Regazzetti et al., 2009). Phosphorylated FOXO is bound by 14-3-3 proteins in the cytoplasm that will mask the DNA binding interface in FOXO and prevent it from translocating into the nucleus (Nielsen et al., 2008). The phosphorylation of FOXO decreases the expression of the translation repressor protein initiation factor 4E binding protein (4E-BP), increasing protein translation (Y. Liu & Lehmann, 2006). Eventually, AKT promotes the translocation of the glucose transporter (GLUT) to the cell membrane in liver, adipose tissue, and muscles, allowing glucose to enter the cell and reducing blood glucose levels.

Drosophila has a single InR/IGF gene that shares 32.5% and 33.3% amino acids identity with the mammalian InR and IGF proteins, respectively, and the level of amino acids identity is even higher (up 50%) when beta subunits are compared (Ruan et al., 1995). Despite the homology, the *Drosophila* InR/IGF can only be activated by the insulin-like peptide (Dilps) but not mammalian IGF (Fernandez-Almonacid & Rosen, 1987). There

are eight insulin-like-peptide genes (Dilps 1-8) that have been identified (Semaniuk, Piskovatska, et al., 2021). Dilps are released into the fly hemolymph and interact with the single *Drosophila* InR/IGF. In response to circulating nutrients, Dilps 2,3 and 5 are produced from two symmetric clusters of seven neurosecretory cells in the brain called insulin-producing cells (IPCs), while Dilp6 is released from the fat body (Semaniuk et al., 2021; Ikeyaet al. 2002). AKH and Dilp6 work together to increase lipolysis, while Dilp 2, 3, and 5 activate lipogenesis (Toprak, 2020). During starvation, Dilp3 and Dilp5 are down-regulated while Dilp2 accumulates in the IPCs (S. Broughton et al., 2008; Kannan & Fridell, 2013). In addition to nutrients, several other factors regulate the release of Dilps from the IPCs, like temperature, circadian rhythms, short neuropeptide F (sNPF), and miRNAs (Luo et al., 2012; Semaniuk, Strilbytska, et al., 2021). For example, *miR-14* regulates metabolism and nutrient content (lipid and glycogen) in the fly by controlling the release of Dilps from IPCs (Varghese et al., 2010).

The insulin signaling pathway supports cellular growth during infection and starvation (Britton et al., 2002; Kannan & Fridell, 2013; Semaniuk, Piskovatska, et al., 2021). During nutrient limitation, insulin signaling is suppressed, and AKT activation is decreased. As a result, the transcription factor FOXO is dephosphorylated, translocating into the nucleus and promoting its downstream targets' transcription. The increase in FOXO levels has been associated with increased resistance to stress and extended lifespan during the decrease in insulin signaling (Barthel et al., 2005; Y. Liu & Lehmann, 2006). In addition, the increase in FOXO level upon starvation can directly feedback and up-regulate transcription of the InR mRNA, thereby increasing insulin sensitivity (Puig et

al., 2003). Overall, the insulin signaling pathway is well-conserved and critical for maintaining homeostasis against environmental stress.

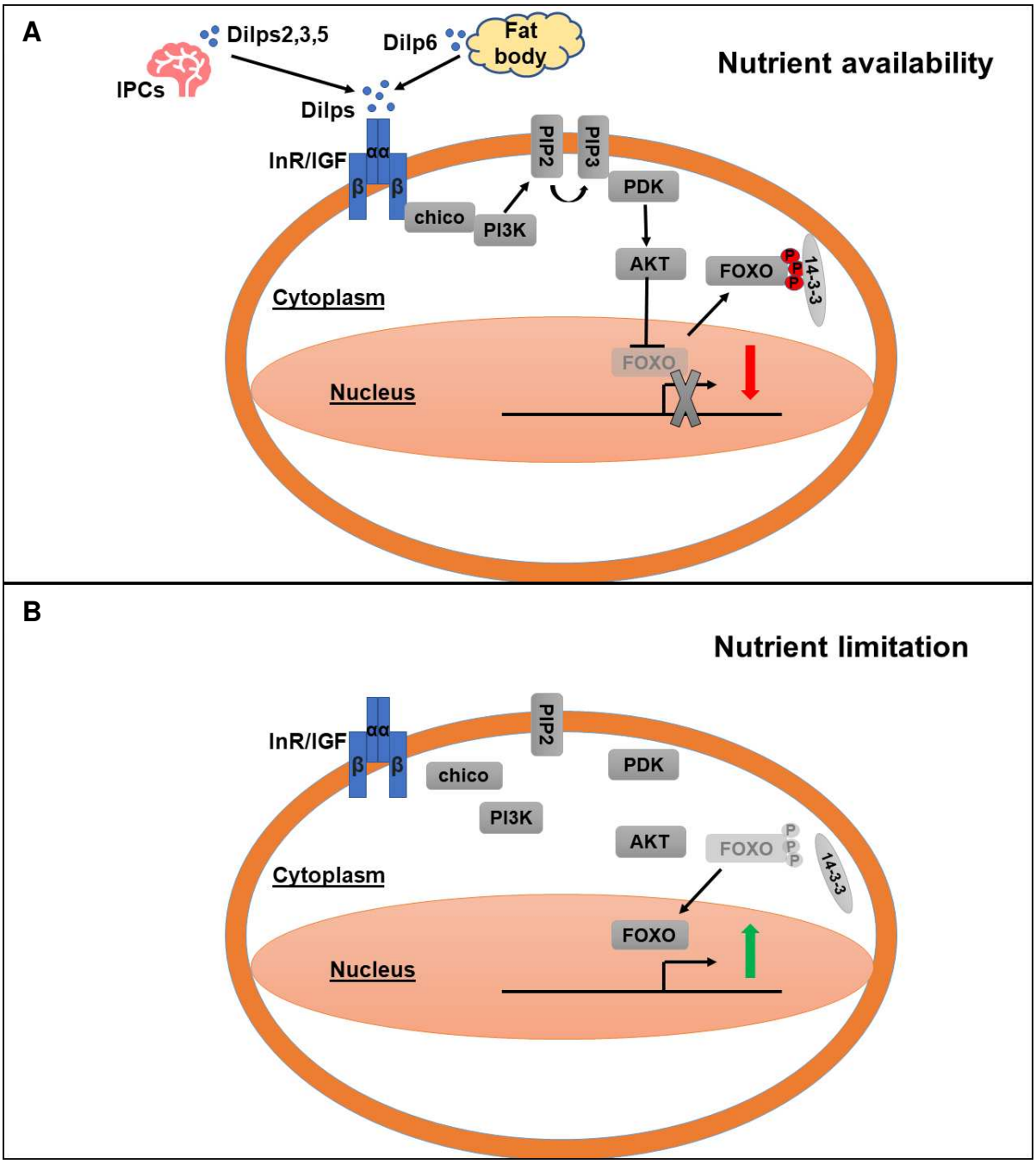

Figure 3. Simplified representation of the highly conserved Insulin/PI3K/AKT signaling pathway. ***A.*** During nutrient availability (fed state), activation of InR/IGF initiates a phosphorylation cascade that ends by repressing FOXO transcription factors by nuclear exclusion. ***B.*** Under nutrient limitation (starved state), FOXO repression is relieved, and FOXO can translocate into the nucleus and start transcription of multiple target genes.

1.9.3 TOR Signaling Pathway.

Target of the Rapamycin (TOR) pathway is a nutrient-sensitive pathway that is activated by PI3K/AKT signaling. The TOR pathway is a conserved signaling pathway from yeast to humans and regulates growth and metabolism at the cellular level (González & Hall, 2017). TOR detects information about nutrients directly from the level of amino acids, and then regulates two direct downstream targets: 4E-BP and S6 kinase. Accumulation of amino acids activates TOR signaling and increases the uptake of amino acids through an amino acid transporter called Slimfast. TOR is composed of two proteins, TOR complex 1 (TORC1) and TOR complex 2 (TORC1) (Loewith et al., 2002). Increase in intracellular amino acids activates TORC1 proteins. TORC1 stimulation controls protein synthesis by phosphorylating 4E-BP and serine kinase 6 (S6K), two critical translation mediators that regulate cellular metabolism and growth (Kapahi & Zid, 2004). The phosphorylation of 4E-BP causes its release from eIF4E and allows cap-dependent mRNA translation to proceed (González & Hall, 2017; Oldham, 2011). On the other hand, S6K phosphorylation promotes the interaction of the small ribosomal subunit with the start codon and initiates translation. Furthermore, activated S6K phosphorylates several proteins, including eIF4B, eIF4A, and 40S ribosomal protein S6 (rpS6), causing an increase in ribosomal synthesis, thereby increasing global protein synthesis (Pallares-Cartes et al., 2012).

IIS and TOR signaling directly or indirectly interfere with global protein translation by modulating ribosome biogenesis. For instance, insulin induces activation of the TOR pathway through phosphorylation of AKT at Ser473, a site that has been identified as a

target of the mammalian target of rapamycin (mTOR) (Jacinto et al., 2006; Malsam et al., 2005). AKT activation relieves the inhibition of tuberous sclerosis complex 1/2 (TSC1/2) and activates a small GTPase Rheb, a positive regulator of rapamycin (TOR) (J. Huang & Manning, 2009; Jacinto et al., 2006). IIS and TOR pathways have been shown to undergo crosstalk dependent on nutrient status in a mechanism that leads to the conservation of cellular energy when nutrient levels are low. TOR and IIS have opposite effects on 4E-BP. In the case of insulin and nutrient availability (fed state), TOR activation inhibits the translation inhibitor 4E-BP and mediates cellular and organism growth and size phenotypes (Hietakangas & Cohen, 2009; Kapahi & Zid, 2004; Tsokanos et al., 2016). In contrast, during nutrient limitation, FOXO positively regulates 4E-BP, inhibiting translation and promoting survival (Puig et al., 2003; Teleman et al., 2005a; Tettweiler et al., 2005a). In addition, insulin levels stimulate a decrease in Proline-rich AKT substrate 40 (PRAS40), a binding partner for TORC1. Decreasing PRAS40 inhibits TORC1 kinase activity, thereby enhancing 4E-BP levels (L. Wang et al., 2007). Lastly, dFOXO, a downstream target of IIS, has been identified to regulate the expression of the transcription factor Myc, a downstream target of the TOR pathway. Myc expression regulates cell division and growth (Teleman et al., 2008).

In summary, the IIS and TOR pathways play key roles in regulating metabolic processes and have been strongly linked to the starvation response. Due to complex interactions between IIS and TOR, mutations of any component of either pathway can produce severe phenotypes.

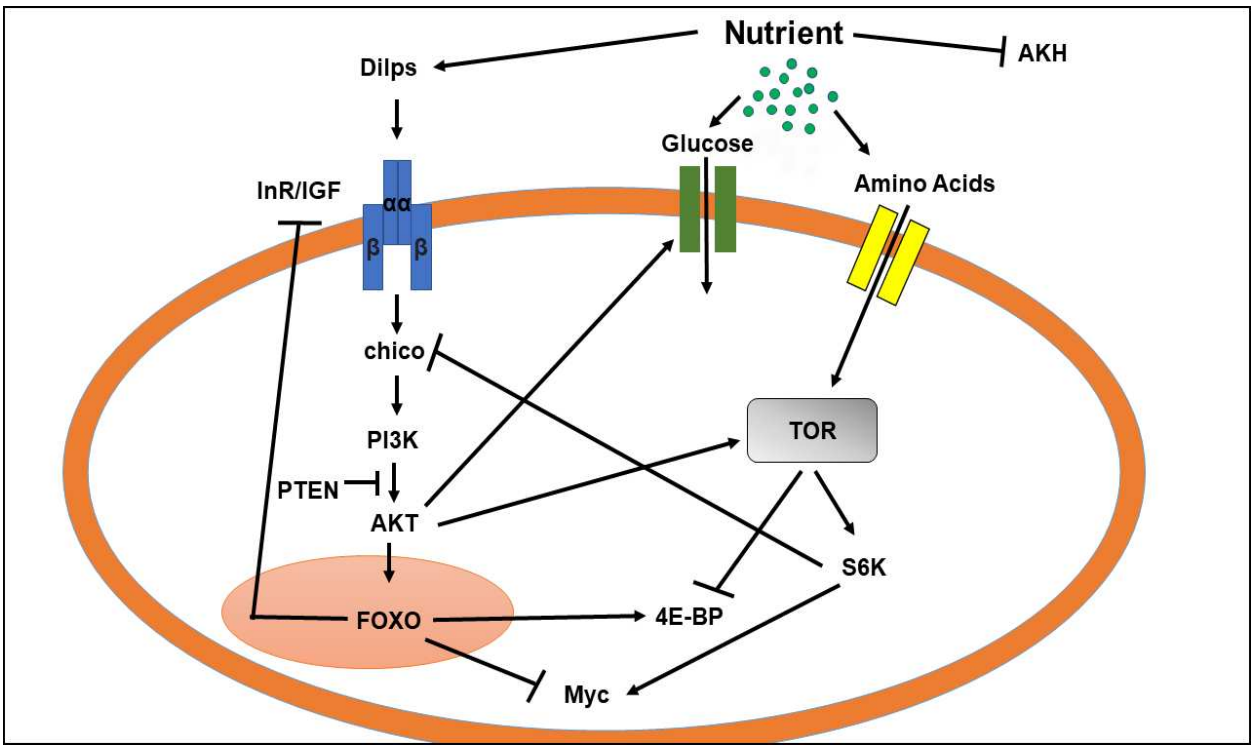

Figure 4. Simplified representation of the TOR signaling pathway. The availability of extracellular amino acids activates TOR kinases and leads to the phosphorylation of S6K and inhibition of 4E-BP, which results in increased protein translation and cellular growth.

1.10 Negative Regulators of the IIS

Although the activity of insulin signaling is somewhat clear, the factors involved in negative regulation of IIS are less well understood. Mechanisms underlying the regulation of insulin signaling can happen on the insulin receptor level or at any step in the pathway.

The InR and IRS can be negatively regulated by ligands, protein tyrosine phosphatase (PTP), serine phosphorylation, and negative feedback loops. For example, a prolonged increase in insulin levels (hyperinsulinemia) leads to internalization and/or degradation of the InR and IRS (Watson et al., 2022). A decrease in the number of InR in

the cell membrane, a mutation in the *InR* gene, or a decrease in IRS leads to a severe condition of insulin resistance in animals, where failure to maintain blood glucose levels results in diabetes, kidney and heart failure and a shortened lifespan (Graham & Pick, 2017b; Lizcano & Alessi, n.d.; Um et al., 2006). On the other hand, growth factor receptor-bound proteins (Grb10) and (Grb14) are also known to bind to the auto-phosphorylated InR and inhibit its tyrosine kinase activity towards IRS (Depetris et al., 2005; Ding et al., 2020; Gual et al., 2005; Holt & Siddle, 2005). IRS can be negatively regulated by serine phosphorylation which causes IRS degradation. For example, phosphorylation of a serine residue of the IRS by S6K, a serine kinase downstream of AKT, causes IRS inhibition and degradation (Manning, 2004; Um et al., 2006). Another example of the negative regulation of IRS by serine phosphorylation is by c-Jun-N-terminal kinases (JNK). Increasing IIS activity stimulates JNK activity that leads to phosphorylation of IRS at Ser307, which mediates feedback inhibition of IIS activity (Y. H. Lee et al., 2003). In addition, Protein Phosphatase 2A (PP2A), and Phosphatase 2B (PP2B), also known as calcineurin, are involved in the dephosphorylation of some downstream IIS components like AKT (Hatzihristidis et al., 2015; Padmanabhan et al., 2009). Phosphatase tension homolog (PTEN) inhibits IIS by negatively regulating PI3K activity. PIP3 acts as a docking site for the pleckstrin homology domain (PH domain) of PI3K, which recruits protein phosphatase PTEN (Georgescu, 2010a; Y. Z. Li et al., 2020). SHIP2 is another phosphatase that can negatively regulate IIS by catalyzing the de-phosphorylation of PIP3 to regulate phospho-Thr308-AKT activity (Soeda et al., 2010). *InR* mRNA transcription can also be regulated by a feedback loop mediated by the FOXO1 transcription factor (Durmaz et al., 2019; Puig et al., 2003). Other modulators of the IIS

are Suppressors of Cytokine Signaling (SOCS) proteins. There are seven SOCS, and SOCS1, SOCS3, SOCS6, and SOCS7 function by binding to the InR and preventing its signaling, or targeting IRS for degradation (Cao et al., 2018; Krebs et al., 2002; Ueki et al., 2004).

The main regulator of IIS activity involves protein tyrosine phosphatases (PTPs) that dephosphorylate the InR and IRS (Band et al., 1997). The first type of PTPs are receptor-type protein tyrosine phosphatases (RPTPs). There are 21 RPTPs, including Leukocyte Antigen Related (LAR), and CD45 (Galic et al., 2003; Hatzihristidis et al., 2015; Jacob et al., 2010; Xu & Fisher, 2012), both capable of negatively regulating IIS. The other type of PTP is the non-receptor protein tyrosine phosphatase. There are 17 protein tyrosine phosphatases, including PTEN, Protein Tyrosine Phosphatase 1B (PTP1B), and T Cell Protein Tyrosine Phosphatase (TCPTP). PTP1B (encoded by *PTPN1*) and TCPTP (encoded by *PTPN2*) are the major protein tyrosine phosphatases that recognize and dephosphorylate the InR (Hatzihristidis et al., 2015; Xu & Fisher, 2012). In *Drosophila*, protein tyrosine phosphatase dPTP61F is homologous to PTP1B and TCPTP. dPTP61F negatively regulates insulin signaling activity by dephosphorylating the activated site of InR/IGF (Willoughby et al., 2017; Wu et al., 2011). dPTP61F has also been identified as a negative regulator of the TOR pathway and involved in the organism's size (P. Liu et al., 2022). *Drosophila* PTP61F null mutants showed multiple phenotypes in flies, including developmental delay, an increase in body and wing size, a decrease in locomotor activity, a shortened lifespan, and an increase in resistance to paraquat and hypoxia conditions compared with wild type (Buszard et al., 2013; P. Liu et al., 2022). Overall, mechanisms

by which the IIS is negatively regulated are likely to contribute to physiological and pathological conditions in the organism, and much remains to be understood.

1.11 Implications of Insulin Signaling in Diseases.

Because of its pivotal role in glucose homeostasis, insulin is linked with several metabolic disorders, such as diabetes and hyperglycemia. Diabetes type 2 is a significant disease associated with the insulin signaling pathway and affects multiple body organs. Besides lifestyle and environmental factors, the two main reasons for diabetes are insulin resistance, which is attributed to dysfunction of the InR, and dysregulation of insulin release/production in response to glucose (Baenas & Wagner, 2022; Graham & Pick, 2017). IIS dysfunction in the brains of diabetic patients increase the risk of developing neurodegenerative disorders like Alzheimer's disease (Akomolafe et al., n.d.; Y. Huang et al., 2019). Additionally, a rare recessive genetic disorder called Rabson-Mendenhall can result from *InR* gene mutations and is characterized by severe insulin resistance (Semple et al., 2011). Similar to diabetes and insulin resistance in mammals, ablation of IPCs, down-regulation of InR, or mutation of *chico* in flies results in an increase in circulating glucose, glycogen, and lipid levels (S. Broughton et al., 2008; S. J. Broughton et al., 2005; Hall et al., 2020; S. Lee & Dong, 2017; Semple et al., 2011; Toprak, 2020). In summary, mutations in the *InR* gene affect a proper insulin response, causing insulin resistance, and impairment in muscle and adipose tissue development (Arcidiacono et al., 2012; Semple et al., 2011).

A great number of studies have confirmed that the insulin pathway plays a significant role in metabolic phenotypes. For example, defects in the production of Dilps

in *miR-278* mutant flies result in several phenotypes, including lean body size, insulin resistance, and elevated circulating glucose that is mobilized from energy stores (Teleman & Cohen, 2006). Furthermore, mutation of the insulin receptor substrate IRS1 in mice or *chico* in flies results in a decrease in body size, decrease in cell size and number, an extension of lifespan, and delayed aging (Böhni et al., 1999). Conditional knockdown of the InR in the adipose tissue in mice extends their life (Blüher et al., 1977). In *C. elegans*, reduced IIS caused by loss of *daf-2*, the homolog of the InR/IGF receptor, causes increased lifespan (Kimura et al., 1997). Mutations in the *InR* gene in *Drosophila* prolongs lifespan (Tatar et al., 2001). Increasing the expression of *dFOXO* in the fat body positively regulates *Dilp6* mRNA in the adult fat body. The increase in *Dilp6* represses *Dilp5* and *Dilp2* mRNA expression in the brain and reduces the release of *Dilp2* in the hemolymph. Consequently, the decrease in Dilp2 and the increase in the expression of dFOXO causes an increase longevity (Bai et al., 2012).

The insulin/TOR signaling pathway affects both metabolic function and growth-promoting function. IIS protein activity promotes cell proliferation and stops apoptosis (Chen et al., 2018; Georgescu, 2010). Multiple reports have also shown that abnormal IIS leads to cancer development and progression (Baserga, 1999; Georgescu, 2010a; Peng & Croce, 2016). In *Drosophila*, loss of PTEN, which also functions as a tumor suppressor, results in an increase in the activity of PI3K and causes an increase in organ size, and an increase tumor growth (C. Y. Chen et al., 2018; Nowak et al., 2013). Phosphorylation of TOR has two downstream targets: S6K and 4E-BP. The phosphorylation of S6K and 4E-BP increases mRNAs' global translation, activating growth and development. Overall, a

mutation in various IIS components in *Drosophila* and mammals generates similar consequences demonstrating these pathways' importance in organisms' normal biology.

1.12 Physiological Mechanisms of Starvation Resistance.

Food deficiency is a common challenge in the natural environment. Species that adapt to this environmental challenge will have a higher probability of survival and will likely develop evolutionary traits that will be passed on to the following generations as a result of that experience. Starvation resistance is examined by placing groups of flies in a vial where they have access to a source of hydration, but no nutritional source, then recording times until death (Harshman et al., 1999). During times of nutrient deprivation, the flies that are able to survive longer are considered starvation resistant (Chippindale et al., 1996; Kawecki et al., 2021).

Potential mechanisms by which an organism can increase starvation resistance are increased energy resources and minimized energy expenditure. Increase in energy resources results in a larger size with starvation endurance (Chauhan et al., 2021). Animals can store energy in the form of lipids, carbohydrates, and proteins. Starvation resistance positively correlates with lipid content (Brown et al., 2019; Chauhan et al., 2021; Harshman et al., 1999). Starved animals utilize their glycogen stores initially, then switch to lipid metabolism, and only after lipid stores are depleted, protein breakdown starts to promote survival (K. P. Lee & Jang, 2014). Humidity affect energy stores and starvation resistance in the organism. Flies that are reared under high humidity (85%RH) have higher lipid levels that contribute to longer survival during starvation (Parkash et al., 2014). On the other hand, lipid content is greatly affected by temperature. Flies that were

starved at 33 ºC (high temperature) had a significant decrease in energy stores (glycogen and lipids) compared to flies that were starved at 13 ºC (Klepsatel et al., 2019). In summary, an increase in energy resources, specifically lipid content, has been a consistent marker that is correlated with starvation resistance.

Starvation affects adult flies' movement. Food deprivation induces an increase in locomotor activity as a sign of food-seeking behavior. Consequently, the increase in locomotor activity disadvantages survival by depleting energy resources faster. The food-seeking behavior is mediated by IIS through S6K or AKH to enhance locomotor activity (Q. He et al., 2020; R. Huang et al., 2020). Flies that showed starvation resistance are less active, have lower fecundity, and exhibit developmental delay compared with control flies (E. B. Brown et al., 2019; Yang et al., 2015). Overall, there is a strong relationship between metabolic rate, available energy resources, and starvation resistance.

Feeding behavior varies during the different development stages. In *Drosophila*, the life cycle starts with eggs that will hatch into larvae. The larval stage is characterized by extensive feeding that supports fast growth and leads to the accumulation of energy stores in the larval fat body (Aguila et al., 2007; Rehman & Varghese, 2021a). Then the larvae enter into the non-feeding pupal stage, where the larvae go through metamorphosis for approximately 4-5 days. During pupation, about 50% of the energy stored in the larval fat body during the feeding and growth stage is consumed (Aguila et al., 2007). The larval fat body cells continue to be present in the flies during early adulthood for up to 3 days after eclosion. Due to that, the ability of newly eclosed flies to resist starvation is nearly three times higher compared to older flies (Aguila et al., 2007;

Rehman & Varghese, 2021a). Genetic blocking of cell death of larval fat cells increases starvation resistance in older flies (Aguila et al., 2007). This evidence supports the idea that fat body cells have a fundamental role in post-metaphoric energy metabolism and provide an effective energy source that contributes to increased resistance to starvation (Aguila et al., 2007; Chippindale et al., 1996; Rehman & Varghese, 2021). After that, adult flies that emerge from the pupae enter a feeding but non-growing stage. Adult feeding supports organism reproduction and survival (Park et al., 2018). Upon conditions of starvation stress, flies normally tend to increase their feeding rate when they return to food. One odd feeding behavior that can occur during starvation stress is that flies that are the last to die cannibalize on the carcasses of the flies that have died earlier during starvation (E. B. Brown et al., 2019; Huey et al., 2004).

To sum up, these findings suggest that the increase in lipid content, food intake, food storage, and reduced physical activity contribute to increased starvation resistance.

1.13 *Drosophila melanogaster* as a Model Organism

The fruit fly, *Drosophila melanogaster*, is an excellent model organism for studying systemic changes in miRNAs, gene expression, and behavior in response to environmental challenges (Agarwal et al., 2018; Epiney et al., 2021). *Drosophila melanogaster* has many advantages as a model organism starting with its small size, relatively fast life cycle, fast reproduction time, low cost, and advanced genetic accessibility. *Drosophila* is a simple organism with only four pairs of chromosomes, which facilitates genetic manipulation. The first chromosome is the sex chromosome, while the other three chromosomes are autosomes (Leister et al., n.d.). The ability to design

mutations in flies is well established and has helped study the influence of genetics on behavior. The *Drosophila melanogaster* genome exhibits 60% DNA sequence homology with the human genome. Approximately 75% of genes responsible for various kinds of disorders in humans are found in *Drosophila* with at least 50% protein sequence homology (Chien et al., 2002; Reiter et al., 2001), including metabolic disease (Mirzoyan et al., 2019).

miRNAs are ideal for studying stress response factors as they mediate gene expression and fine-tune the proteins that help the cell restore homeostasis. *Drosophila* has proved to be one of the most amenable animal models to understand miRNA biogenesis, expression pattern, and function *in vivo* and *in vitro*. *Drosophila* has a wide range of genetic and molecular tools for manipulating miRNA levels *in vivo*, which helps to analyze miRNA function. Some miRNA knockouts do not always exhibit physiological or developmental phenotypes. However, the same miRNA mutant sometimes exhibits a phenotype under stress conditions (Leung & Sharp, 2010a). *miR-137* is highly conserved in its seed sequence, as well as its mature miRNA sequence across different animal species (Ez-Ventoso et al., 2008). Therefore, *Drosophila* is an ideal organism to survey mutations and screen for interesting phenotypes of *miR-137*.

In the last decade, *Drosophila* has emerged as a powerful tool for studying several aspects of biology, such as metabolism, stress responses, and cancer (Chien et al., 2002; Hardy et al., 2018; Nichols et al., 2012; Rudrapatna et al., 2012). *Drosophila* is widely used to experiment with stress resistance. *Drosophila* is an excellent model to study the insulin signaling pathway due to the high conservation of genes and biological function of

the insulin signaling molecules between *Drosophila* and mammals. Insulin-like peptides are similar to mammalian insulin (Brogiolo et al., 2001; Garofalo, 2002). The biological function of insulin signaling in *Drosophila* is also similar to mammals, and includes the regulation of protein synthesis, fat storage, cell growth, nutrition sense, aging, proliferation, stress, and apoptosis (Nijhout & McKenna, 2018; Teleman et al., 2008). To sum up, mammalian organism models are greatly useful, yet using *Drosophila* as a model to study miRNAs and metabolic signaling *in vivo* has proven advantageous in many ways.

1.14 PROJECT, AIM, and OBJECTIVES.

Despite studies demonstrating that *miR-137* is associated with numerous functions such as cancer repression, development, learning and memory, and neural proliferation, nothing is known about *miR-137* as a regulator of energy homeostasis. Starvation resistance can be due to a variety of complex traits that allow the organism to survive. Investigating the molecular mechanism by which *miR-137* regulates metabolic pathways and contributes to their ability to adapt to starvation is likely to give valuable understanding into energy homeostasis. Furthermore, this thesis gives insight into novel *miR-137* regulation for the insulin signaling pathway through its role of *Drosophila*-only *PTPP61F* gene, the ortholog of TCPTP/PTP1B known to dephosphorylate the InR, as a conical target for *miR-137 in vivo*. To sum up, this project is expected to broaden our knowledge of the genetic and physiological mechanism/s underlying starvation resistance in *miR-137* mutants.

Aims.

This thesis aims to examine the role of *miR-137* in regulating central insulin signaling, metabolic homeostasis, and lifespan under nutrient stress in *Drosophila melanogaster*.

Objectives.

The primary objectives we addressed in this thesis are summarized as follows.

1. Characterization of *miR-137* expression in *Drosophila melanogaster*.
2. Analysis of the role of *miR-137* under nutritional and oxidative stress.
3. Analysis of the effect of the loss of *miR-137* on energy storage**.**

4. Genetic epistasis analysis to identify in which pathway *miR-137*-mediated starvation phenotype.
5. Analysis of PTP61F as a target for *miR-137*, affecting the activation of the insulin receptor and starvation resistance.
6. Normalization of starvation sensitivity to *miR-137* mutants by activating the insulin signaling pathway in the nervous system.

CHAPTER 2: MATERIAL AND METHODS

2.1 Fly Work.

2.1.1 Fly Rearing and Stocks.

Drosophila melanogaster flies were reared on standard *Drosophila* food made of cornmeal, yeast, and agar. Fly stocks were maintained in a controlled environment with a 12/12 hrs light/dark cycle, and experiments were conducted at 25 ºC and 65% humidity.

Drosophila melanogaster strains were obtained from the Bloomington *Drosophila* Stock Center (BDSC), Vienna *Drosophila* Resource Center (VDRC), and individual laboratories, as indicated in (Table 1):

Table 1. Fly Stocks.

Genotype	Obtained from
w^{1118}	BDSC # 5905
Elav-Gal4	BDSC # 458
Elav-Gal4;;Gal80^{ts}	BDSC # 7017
miR-137^{KO}	BDSC # 58893
miR-137^{CR}	Tsunoda's lab
UAS-miR-137	Second # 59881
UAS-miR-137	BDSC # 59882
Akh^{1}	A kind gift from Dr. Michal Zurovec and Dr. Dalibor Kodrik
UAS-InR Dominant-negative	BDSC # 8253
UAS-InR-RNAi	VDRC # 991
chico^{1}	BDSC # 10738
UAS-AKT-RNAi	VDRC # 2902
UAS-PI3K Dominant-negative	BDSC # 8288

FOXO$^{\Delta 94}$	BDSC # 42220
Thor^{2} (4E-BP mutant)	BDSC # 9559
UAS-PTP61F	BDSC # 22229
UAS-PTP61F	BDSC # 56194
UAS-PTP61F-RNAi	BDSC # 56036
UAS-PTP61F-RNAi	BDSC # 32426
UAS-PTP61F-RNAi	BDSC # 56510
dAdipoR-RNAi	VDRC # 40936
dAdipoR-RNAi	VDRC # 40935
UAS-Dilp2	BDSC # 280936
UAS-Dilp5	BDSC # 66008
UAS-InR constitutively active	BDSC # 8440
UAS-PI3K	BDSC # 8287
UAS-AKT	FLYORF # 001315
UAS-FOXO	BDSC # 80946
UAS-4E-BP	BDSC # 78108
UAS-4E-BP	BDSC# 77999
PTP61F$^{\Delta}$	Kind gift from Dr. Coral Warr
GFDTF-PTP61F	BDSC # 61756
GFSTF-PTP61F	BDSC # 61767
Cha^{ts2}	(Salvaterra2 & Mccaman, 1985)
UAS-TrpA^{1}	BDSC # 26263
Aβ^{42}	(Iijima et al., 2008)

2.2 Stress Assays.

2.2.1. Temperature Stress.

For temperature stress experiments, 3-day old, mated male wild-type flies were grouped 10 flies per vial that contained standard fly food. Flies were subjected to a high temperature of 33 °C for 3 days, a low temperature of 6 °C for 3 days, or 25 °C for 3 days (the control). Fly heads were collected for RNA extraction from each condition to compare *miR-137* levels by RT-qPCR.

2.2.2 Nutritional Stress.

For nutritional stress assays evaluating *miR-137* levels by RT-qPCR: 7-day old, wild-type flies from a mixed population of males and females were separated by sex and then subjected to 5 days of continuous sugar/ protein starvation or 3 days of total starvation at 25 ºC. Controls were aged-matched wild-type flies fed on standard fly food. Fly heads were collected for RNA extraction from each condition to compare *miR-137* levels by RT-qPCR.

2.2.3 Media for Nutritional Stress.

Starvation media were prepared as follows: Total starvation media was prepared by heating dH_2O to a boil, then adding 1% agar. Sugar starvation media was prepared by heating dH_2O to a boil, adding 1% agar, and once the media cooled down, a fresh yeast paste prepared from dry yeast and dH_2O was added to the side of the vial. Protein starvation media was prepared by heating dH_2O to a boil, then adding 1% agar and 5% sucrose. To inhibit mold growth, 0.3% tegosept and 0.03% propionic acid were added to all starvation media after cooling to 60 ºC. Fresh vials were prepared for each experiment.

2.2.4 Starvation Stress Survival.

Newly-eclosed, less than 24 hrs old flies, were raised on standard fly food for 6-7 days in a mixed population of males and females. Flies were transferred to fresh food every 3-4 days before being sorted for starvation. 6-7day old male and female flies from a given genotype were separated into groups of 10 per vial that contained starvation media, as described above. Flies were raised at 25 °C and 65% humidity. For each experiment, we ran two trials, n=100 per genotype per gender. Under conditions of total starvation, survival was scored every 12 hrs until all flies were dead. In the case of protein and sugar starvation, flies were scored every 1-2 days, and the starvation media was replaced every 5 days. The percentage of flies that died at each time point was calculated, and survival curves were generated using GraphPad Prism 6 (Fig 5). Survival curves were pairwise compared by Log-rank Mantel-Cox 18 test, Chi-square, and Gehan-Breslow -Wilcoxon test using GraphPad Prism 6, and a $P<0.05$ was considered statistically significant.

2.2.5 Oxidative Stress Media and Survival.

Paraquat (PQ) is a highly toxic chemical agent commonly used to induce oxidative stress in flies (Rzezniczak et al., 2011). Adult males 3-5 days old were fed 20 % paraquat (cat. no. 856177, Sigma–Aldrich, St. Louis, MO, USA). 20 g of PQ was dissolved in 100 ml ofdH_2O, that used to prepare ready-used standard cornmeal, yeast, and agar diet. To avoid unnecessary stress, flies were not starved prior to paraquat feeding in this test. Flies were transferred to freshly prepared paraquat food every 6-7 days. Survival was scored every 12 hrs until all flies were dead. Data were analyzed using GraphPad Prism 6. For each genotype, we tested two independent populations of 100 flies. Survival curves

were pairwise compared by Log-rank Mantel-Cox test, Chi-square, and Gehan-Breslow - Wilcoxon test using GraphPad Prism 6, and a P-value of < 0.05 was considered significant.

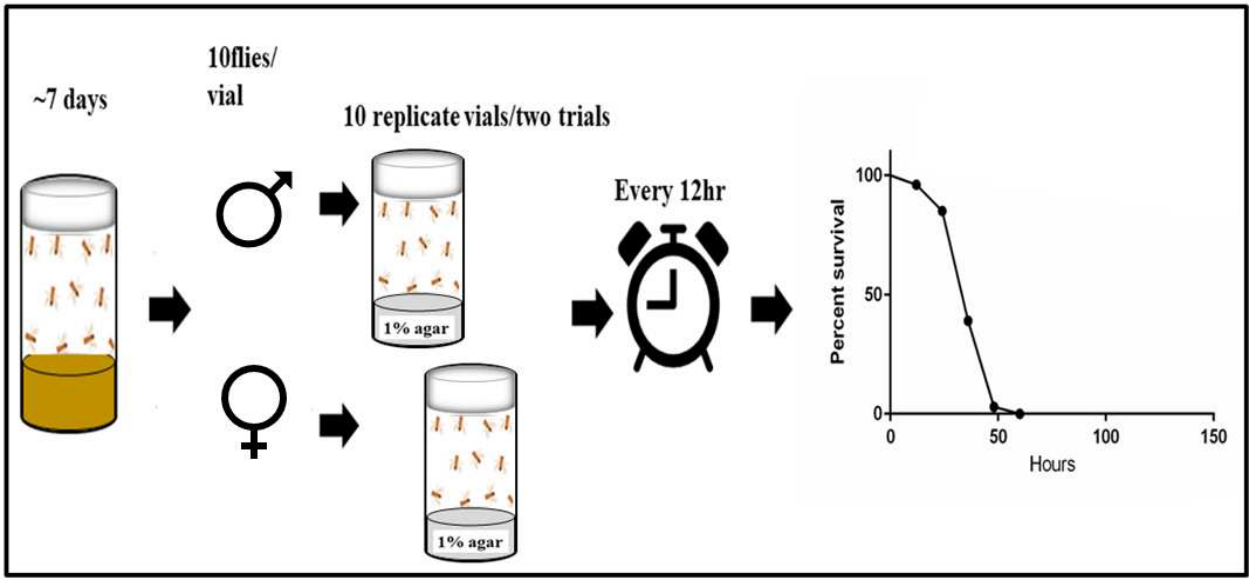

Figure 5. Starvation stress survival. After hatching, the mixed fly populations were raised on standard fly food. After ~7 days, adult males and females from a given genotype were sorted by sex on the experimental media and separated into groups of 10 per vial. Two replicates of population of at least 100 flies per genotype per gender were assayed. Survival was scored every 12 hrs until all flies were dead. The percentage of flies that died at each time point was calculated, and survival curves were generated.

2.3 Gene Expression.

2.3.1 miRNA Expression Analysis by Quantitative Polymerase-Chain-Reaction (RT-qPCR).

Total RNA was extracted from five heads or five bodies per sample using the miRNeasy Mini Kit (Qiagen). The procedure was followed as recommended by the manufacturer's protocol. The total RNA concentrations and the RNA purity were determined by NanoDrop (Fisher Scientific Thermo Scientific Nanodrop Lite

Spectrophotometer). The reverse transcription step used only RNA with acceptable purity (more than 1.90 absorbance A260/280 ratio). 10 ng of total RNA was used in a 15 µl reverse transcription (RT) reaction to generate complementary DNA (cDNA). To assess the expression level of *miR-137*, small RNA controls were used as reference genes. The two reference genes we used were *2S rRNA*, 30 nt long, and *U14*, 51 nt long (Table 2). We verified that reference genes were stable between the studied conditions. Double-stranded cDNA was used as a template to amplify mature *miR-137* and the reference genes separately for each sample. Because the miRNAs do not have a poly-A tail, a small RNA-specific stem-looped RT primer that contains a complementary region to the target miRNA at the end region was used to extend the double-stranded cDNA product (Fig 6). Then cDNAs were amplified using the thermocycler (BIO-RAD T100 Thermal Cycler), per the manufacturer's procedure recommended. TaqMan™ microRNA assays obtained from Applied Biosystems were used to determine the expression of *miR-137* and reference genes. TaqMan™ Fast Advanced Master Mix was used for the LightCycler® 480 for quantification by RT-qPCR. The analysis software determined Ct values, and technical duplicates were averaged. Data were normalized to the reference gene, and the $2^{-\Delta\Delta}$Ct method was used to determine the relative expression of *miR-137*. Significant differences were determined by a P-value less than 0.05, calculated by the two-tailed student's T-test.

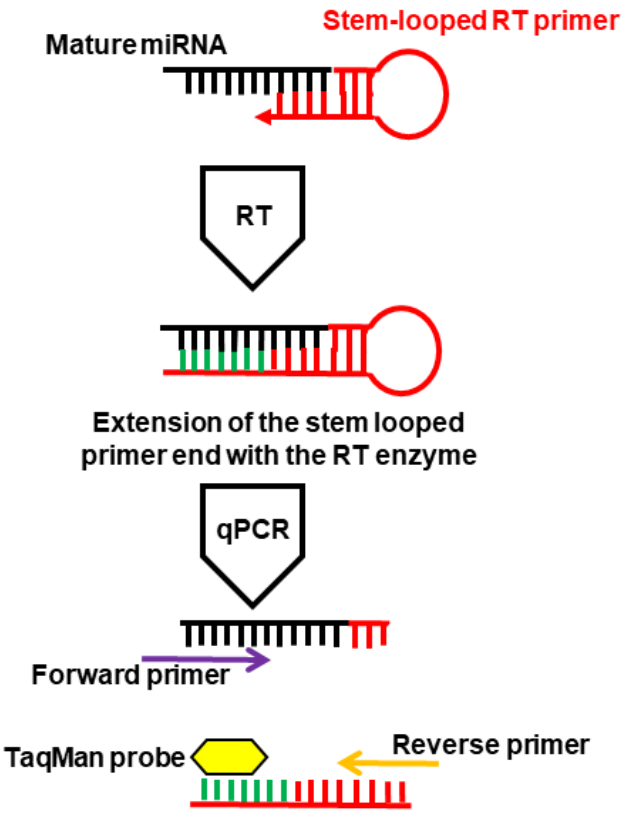

Figure 6. The mature miRNA is short and lacks a poly-A tail. A stem-loop primer is used to generate cDNA. Stem-loop primer has a sticky end that will attach to the mature miRNA, and the reverse transcription enzyme extends and complete the strand, resulting in a hairpin-loop double-standard miRNA.

Table 2. Primer sequences used for RT-qPCR.

Name	Primer Sequence
miR-137-3p	UAUUGCUUGAGAAUACACGUAG
miR-137-stem-loop primer	CAAUCUCCAAUGGCCACGUGUAUGCUCGUAGCUAUAACCUGAAAUCCAAAUGUUAUUGCUUGAGAAUACACGUAGUUCACCGAGAUUUGUU
2S rRNA	TGCTTGGACTACATATGGTTGAGGGTTGTA
U14	GCGGTTTCCACCAGAAAGCTTCGGCTTAATGATGGTCTAAGGCGTCTGACT

2.3.2 mRNA Expression Analysis by RT-qPCR.

Total RNA was extracted from ten heads per sample, and QIAzol Lysis Reagent (Qiagen) was used for homogenization. A clean and sterile pestle was used for homogenization. The procedure was followed as recommended by the manufacturer's protocol. The total RNA concentrations and the RNA purity were determined by NanoDrop (Fisher Scientific Thermo Scientific Nanodrop Lite Spectrophotometer). The reverse transcription step used only RNA with acceptable purity (more than 1.90 absorbance A260/280 ratio). 500 ng of total RNA was reversed transcribed (RT) with High-Capacity Reverse Transcriptase (Applied Biosystems) to generate a 20 µl cDNA reaction. cDNA was then amplified using the thermocycler (BIO-RAD T100 Thermal Cycler), per the manufacturer's recommended procedure. Primers were used to amplify cDNA from genes of interest we obtained from Integrated DNA Technologies (www.idtdna.com), and ribosomal protein (*Rp49*) was used as a reference gene (Table 3). We verified that the reference gene was stable between the studied conditions. The primer's specificity was verified by running the PCR products on the gel electrophoresis and obtaining a single band at the expected molecular size. Power Syber Green Master Mix obtained from Applied Biosystems was used for the LightCycler® 480 for quantification by RT-qPCR to determine the expression of targets and reference genes. RT-qPCR from serial dilutions of the cDNA were then used to verify primers efficiency. Only primers with an acceptable efficiency range of 90-110% were used in this study (Fig 7). The analysis software determined Ct values, and technical duplicates were averaged. Data were normalized to the reference gene, and the $2^{-\Delta\Delta}$Ct method was used to determine the relative expression

of the genes of interest. Significant differences were determined by a P-value less than 0.05, calculated by the two-tailed student's T-test.

Table 3. Primer sequences used for RT-qPCR.

Primer	Forward primer	Reverse primer
Pre-miR-137	CAATGGCCACGTGGTATGCTC	ACAAATCTCGGTGAACTACGTG
eIF1A	TCGTCTGGAGGCAATGTG	GCCCTGGTTAATCCACACC
Dilp2	GGCCAGCTCCACAGTGAAGT	TCGCTGTCGGCACCGGGCAT
Dilp5	GAGGCACCTTGGGCCTATTC	CATGTGGTGAGATTCGGAGTCA
InR	AACAGTGGCGGATTCGGTT	TACTCGGAGCATTGGAGGCAT
FOXO	AGGCGCAGCCGATAGACGAATTTA	TGCTGTTGACCAGGTTCGTGTTGA
4E-BP	CACTCCTGGAGGCACCA	GAGTTCCCCTCAGCAAGCAA
Rp49	GCTAAGCTGTCGCACAAA	TCCGGTGGGCAGCATGTG
PTP61F	ATCGATCCAATTCCAGGCC	CTGTTTGTCCTCGTTCTCCC

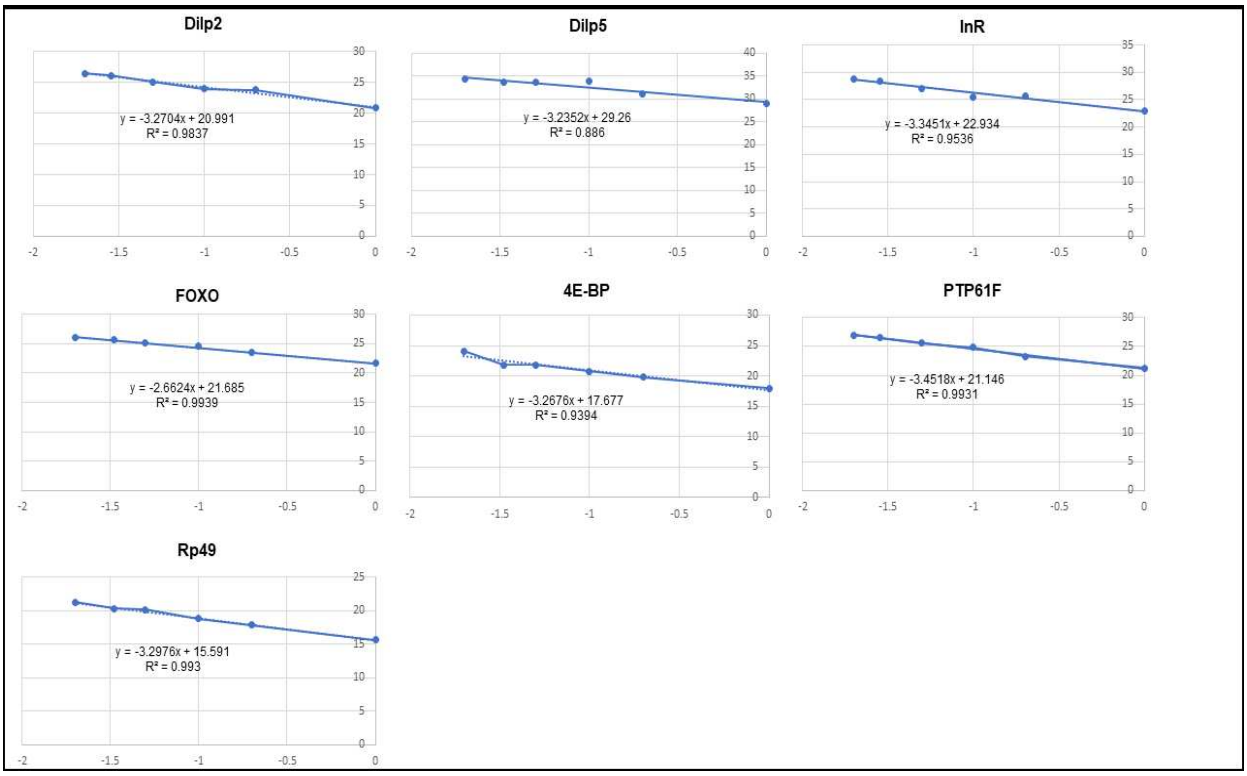

Figure 7: Primers efficiencies. Log of dilution factors plotted against Ct value. Slopes were used to estimate primer efficiencies.

2.4 Heat-Treatment Assay.

Flies with temperature sensitive (*Cha*^{ts2}*, TrpA1*) and *Gal80*^{ts} were raised at 18 ºC. For heat treatment, young adult flies were collected and grouped into 10 flies per vial and exposed to heat treatment at 32 ºC. During extended heat treatment, fly food was replaced periodically to avoid food dehydration. Flies were aged until the desired age then fly heads were collected for RNA extraction to compare *miR-137* levels by RT-qPCR.

2.5 Aging Assay.

Newly-eclosed wild-type males were collected and grouped into 10 flies per vial. The control was collected at 3 days old, and experimental flies groups were aged until 10, 25, and 40 days. Flies were aged in a controlled environment at 25 ºC and 65% humidity

on standard *Drosophila* food. Flies were transferred to fresh food every 3-4 days during the experiments. Fly heads were collected for RNA extraction from each selected age to compare *miR-137* levels by RT-qPCR.

2.6 Time of the Day/ Biological Clock Regulation.

Newly-eclosed male wild-type flies were collected and grouped 10 flies per vial. Flies were entrained under a 12/12 light/ dark zeitgeber time (ZT) cycle for four days, where ZT 0 represents when the light is first turned ON, and ZT 12 represents when the light is turned OFF. After four days of entrainment, fly heads were collected for RNA extraction at ZT 0, ZT 6, ZT 12, and ZT 18 to compare *miR-137* levels by RT-qPCR.

2.7 Body Weight.

Dry body weight was determined by weighing batches of 15 flies from each genotype of interest. A total of 150 flies per genotype were measured. Flies were anesthetized and collected in pre-weighed 1.7 ml tubes. Then the tubes containing the flies were flash frozen immediately in liquid nitrogen and weighed using ultra-sensitive Mettler Toledo AG285 Analytical balance (Marshall Scientific). The average flyweight (mg) was determined by subtracting the pre-tube weight from the weight of the flies and the tube, divided by the number of flies. A P-value less than 0.05 calculated by the two-tailed student's T-test indicated that the two populations were significant difference.

2.8 Triglyceride Quantification.

Triglyceride concentrations were determined as previously described in (Diop et al., 2017). Five adult flies per sample were collected and rinsed several times with 1 ml of cold 1X Phosphate Buffered Saline +0.05 Triton (PBST) to wash away traces of fly food that may stick to the outer fly body. The flies were weighed using ultra-sensitive Mettler

Toledo AG285 Analytical balance (Marshall Scientific) before being rapidly homogenized in 100 µl of cold PBST and centrifuged for 3 min at 4 ºC, 15,000 rpm. The supernatant was transferred into new 1.7 ml tubes. Triglyceride 1 mM standard (cat. MAK266E, Sigma–Aldrich) was used to create 2 mM/µl, 4 mM/µl, 6 mM/µl, and 8 mM/µl with PBST. We used a multi-channel pipette to load 200 µl of the Triglyceride reagent (Triglycerides Reagent Thermo Electron Corp., cat. TR22421) into a clear bottom 96-well spectrophotometer plate. 20 µl of the PBST (blank), standard dilutions, and fly sample supernatants were loaded in triplicate and mixed by pipetting up and down with careful attention not to make bubbles. The plate was then sealed with parafilm and incubated at 37 ºC for 10 min. The absorbance of each well was read using a versa max spectrophotometer microplate reader at 550 nm. The standard curve was generated by plotting the concentration and absorbance, linear regression was performed to generate a linear relationship for quantification. To quantify each sample's Triglyceride concentration (µg/µl), the amount of the Triglyceride in the unknown sample from the standard curve (nM) was divided by sample volume (20 µl) and multiple by the molecular weight of Triglyceride (885.4 ng/nM). A P-value less than 0.05 calculated by the two-tailed student's T-test indicated that the two populations were significantly different.

2.9 Protein Quantification.

Protein concentrations were quantified by using the Pierce™ BCA Protein Assay Kit cat. 23227. Five adult flies per genotype were collected and rinsed several times with 1 ml of cold PBST to wash away traces of any fly food that may stick to the outer fly body. Flies were rapidly homogenized in 100 µl of cold PBST and centrifuged for 3 min at 4 ºC, 15.000 rpm. BCA Protein standard was used to create 1.5 µg/µl, 1 µg/µl ,0.75 µg/µl, 0.5

µg/µl, 0.25 µg/µl,0.125 µg/µl, and 0.025 µg/µl dilution with PBST. The BCA working reagent was prepared as recommended by the manufacturer's protocol. A multi-channel pipette was used to load 200 µl of the working reagent into a clear bottom 96-well spectrophotometer plate. Then, 10 µl of the PBST (blank), standard dilutions, and fly sample supernatants were loaded in triplicate and mixed by pipetting up and down with careful attention not to make bubbles. The plate was then sealed with parafilm and incubated at 37 ºC for 10 min. The absorbance of each well was read using a versa max spectrophotometer microplate reader at 562 nm. The standard curve was generated by plotting the concentration against absorbance fitting point by linear regression. The standard curve was used to determine the protein concentration in each sample. A P-value less than 0.05 calculated by the two-tailed student's T-test indicated that the two populations were significantly different.

2.10 Glucose Quantification.

The Glucose (GO) Assay Kit GAGO20-1KT Sigma was utilized to quantify the glucose levels in the flies. Five adult flies per sample were collected and rinsed several times with 1 ml of cold 1X PBS to wash away traces of the fly food that may stick to the outer fly body. The flies were rapidly homogenized in 100 µl of cold 1X PBS. Samples were heated for 10 minutes at 70 ºC, then centrifuged for 3 minutes at 4 ºC, 15,000 rpm. The supernatant was transferred into new 1.7 ml tubes. Glucose standard was used to generate dilutions of 0.02 µg/µl, 0.04 µg/µl, 0.06 µg/µl, 0.08 µg/µl, and 0.1 µg/µl standard with PBS. A multi-channel pipette was used to load 100 µl of the GO reagent into a clear bottom 96-well spectrophotometer plate. 30 µl of the PBS (blank), standard dilutions, and fly sample supernatants were loaded in triplicate and mixed by pipetting up and down with

careful attention not to make bubbles. The plate was then sealed with parafilm and incubated at 37 ºC for 30 min. After that, 100 µl of sulfuric acid was added to each well to stop the reaction. The absorbance of each well was read using a versa max spectrophotometer microplate reader at 540 nm. The standard curve was generated by plotting the concentration against absorbance fitting point by linear regression. The standard curve was used to determine the glucose concentration in each sample. A P-value less than 0.05 calculated by the two-tailed student's T-test indicated that the two populations were significantly different.

2.11 Feeding Quantification.

Fifteen adult flies (7 days old) per vial were collected and kept free from CO_2 for 24 hrs to avoid the negative impact of anesthesia exposure on feeding behavior. Flies were then either kept on standard fly food (fed) or starved for 18 hrs on 1% agar (starved) before they were transferred to vials containing 1% agar, 5% sucrose, and 2.5% blue food dye (Erioglaucine Disodium Salt, Sigma, cat. # 861146) and allowed to feed for 15 min at 25 ºC. The flies were then collected, flash-frozen immediately in liquid nitrogen, and rapidly homogenized in 1000 µl of cold PBS. Samples were centrifuged at 4 ºC for 25 min at 13200 rpm. To assess the flies' response to the 15 min acute feeding bout, 1 ml of the supernatant was transferred to cuvettes, and each sample absorbance was read at 625 nm by a Beckman Coulter DU730 UV-Vis spectrophotometer reader. A P-value less than 0.05 calculated by the two-tailed student's T-test indicated that the two populations were significantly different.

2.12 Immunoblot Analysis.

For sample preparation for immunoblot analyses, 5 heads of 7-day old adult flies were homogenized in 20 µl SDS sample buffer (0.5 M Tris pH 6.8, 10% SDS, 25% Glycerol, 1 M DDT, and 0.01% Bromophenol blue) and 1% protease/phosphatase inhibitor cocktail (Cell Signaling Technology # 5872). The samples were then sonicated for 16 sec using a signifier (Branson Ultrasonics, Danbury, CT) and centrifuged for 2 min at 4 ºC, 13500 rpm. 16 µl of the samples were loaded onto 10% SDS-PAGE and ran for 1-2 hrs at 100 V. Proteins were then transferred to 0.45 µm nitrocellulose membrane, and the membrane was blocked in 5% non-fat dry milk in 1X Tris-Buffered Saline + 0.1 Tween-20 (1X TBST). The membrane was then incubated with the primary antibody overnight at 4 °C (Table 4). The blots were washed 3 times in 1X TBST for 5 min. Following washes, blots were treated with HRP-conjugated secondary antibodies. The immunoblots were visualized by chemiluminescence (Thermo Scientific Super Signal West Pico PLUS). Bands were visualized using the (Bio-Rad Gel Imager). ImageJ gel analysis was used to quantify the densities of western blot bands. The quantification of bands of interest was normalized to those from Anti-Actin on the same blots. Secondary normalization was made to a control condition before values were combined and compared across the blots.

Table 4. List of primary and secondary antibodies used for immunoblot analysis.

Protein	Primary antibody dilution	Secondary antibody dilution	Source	Cat. No.
Insulin receptor Phospho-InR-β/IGF-I (Tyr1131/Tyr1146)	1:1000	1:2000 Goat α-rabbit	Cell Signaling Technology	3021
AKT	1:1000	1:2000 Goat α-rabbit	Cell Signaling Technology	9272
Phospho-AKT (Ser473)	1:1000	1:3000 Goat α-rabbit	Cell Signaling Technology	9271
dFOXO	1:1000	1:5000 Goat α-rabbit	pAb Abcam	195977
GFP	1:5000	1:5000 Goat α-rabbit	Torrey Pines Biolabs	TP401
Actin	1:10,000	1:5000 α-mouse	MAB	1501

CHAPTER 3: RESULTS

3. Characterize the Expression Pattern of miR-137 in *Drosophila melanogaster*.

3.1 Overview.

miRNAs can be expressed differently in different tissues depending on their function. The expression of a miRNA is often under spatial and temporal restriction depending on its function(s). A miRNA's expression patterns may also give insight into related disease diagnosis and treatment. Studies have shown that miRNAs are highly conserved in their sequence throughout evolution show similar expression patterns and close functions across species (Ha et al., 2008; N. Liu et al., 2008; Ninova et al., 2014; Shi et al., 2012; Stark et al., 2005). Previous studies on *miR-137* have shown that *miR-137* is highly conserved in sequence, and expressed throughout development with high expression in the CNS (Ibáñez-Ventoso et al., 2008; Mahmoudi & Cairns, 2017; Pacheco et al., 2019).

miR-137 is one of the most abundant miRNAs in the brain, with an especially high concentration in the hippocampus (Guella et al., 2013; Pacheco et al., 2019; Thomas et al., 2017). *miR-137* regulates processes associated with SZ, ASD, bipolar disorder, and other major neurological and psychiatric disorders, as well as cancer (Guella et al., 2013; L. Li et al., 2020; Mahmoudi & Cairns, 2017; Ripke et al., 2011; Y. Wang et al., 2020). Studies have shown that in mammals, *miR-137* is highly localized at the synapse and regulates the expression of genes that are essential for mechanisms during neuronal development, differentiation, and apoptosis (Thomas et al., 2017; Yin et al., 2014a). The expression of *miR-137* is associated with neurogenesis, learning, and memory. Since little is known about *miR-137* in *Drosophila*, we chose to characterize the expression

pattern of *miR-137*. We made the following comparisons for *miR-137* expression in wild-type flies: heads versus bodies, males versus females, virgin versus non-virgin females, males at different ages, males at different times of day, males at during changes in neural activity, and under different environmental stressors (e.g., thermal stress, nutritional stress).

3.2 *miR-137* is Enriched in *Drosophila* Brains.

Since *miR-137* is enriched in the mammalian brain, we first examined if *miR-137* was differentially expressed in the head versus the body in *Drosophila*. We performed RT-qPCR from equivalent quantities of RNA isolated from heads and bodies of wild-type *Drosophila* (w^{1118}). We found that *miR-137* is more highly concentrated in heads than in bodies (9-fold increase) (Fig. 8). Similar to mammals, our result suggests that *miR-137* a brain/CNS enriched in flies. These results indicate that the functions of *miR-137* are likely focused on the nervous system. Future studies may look if *miR-137* is enriched in a particular brain region.

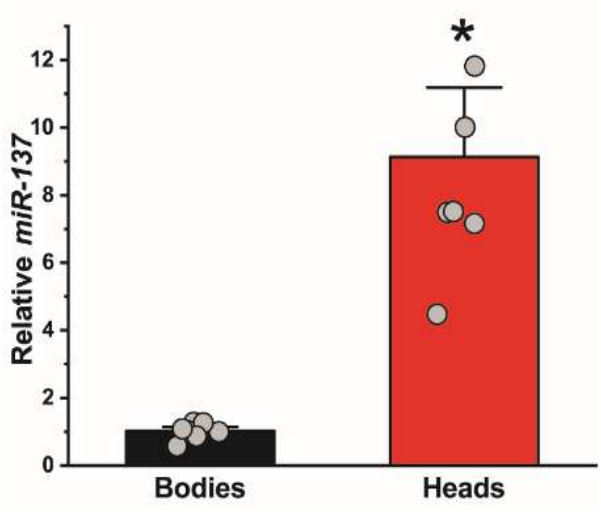

Figure 8. *miR-137* is enriched in *drosophila* brains. Quantification of the relative expression of the mature *miR-137* by RT-qPCR in wild-typed flies (w^{1118}). Results normalized to S2 rRNA. The level of *miR-137* was analyzed using two-tailed student T-test between each independent group and the control group as described in the

experimental procedures. * Indicates significant difference in *miR-137* level ($P<0.05$), error bars indicate SE. RT-qPCR analysis of the mature *miR-137* level in the head vs. bodies shows that *miR-137* was significantly elevated in the heads.

3.3 *miR-137* Expression Between Sexes.

The next question we wanted to address is whether *miR-137* expression is different between the sexes. Males and females differ in disease outcomes and pathogenesis. Sex differences, either hormonal or genetic, can have a significant impact on gene expression. Studies have found that the expression of some miRNAs are regulated by sex steroid hormones as well as X-linked genes (Klinge, 2015; Sharma & Eghbali, 2014). Many miRNA gene promoters contain estrogen-responsive elements where estrogen can bind and regulate miRNA expression (Klinge, 2009, 2015). Differential expression of miRNAs between males and females is important for identifying mechanisms and treating sex-specific diseases (Guo et al., 2017). In cancer, for example, *miR-137* promoter methylation in squamous cell carcinoma is associated with the female gender (Langevin et al., 2010).

To evaluate if *miR-137* expression levels are influenced by gender, sex chromosome, or sex hormone, we quantified levels of *miR-137* from male and female wild-type (w^{1118}) flies. RNA was isolated from the heads of 3 days old flies and were normalized to 2S rRNA. The RT-qPCR results showed no significant change in *miR-137* levels between males and females (Fig. 9).

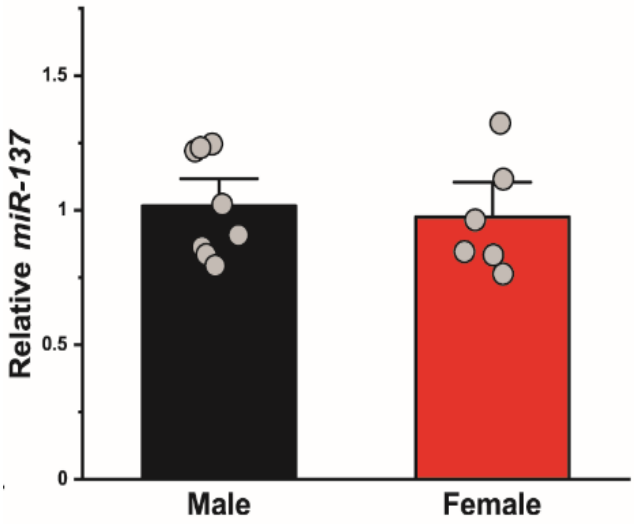

Figure 9. *miR-137* expression between sexes. Quantification of the relative expression of the mature *miR-137* by RT-qPCR in wild-typed flies (w^{1118}). Results normalized to S2 rRNA. The level of *miR-137* was analyzed using two-tailed student T-test between each independent group and the control group as described in the experimental procedures. Error bars indicate SE. RT-qPCR analysis of the mature *miR-137* level in heads between same-aged males and females shows no significant difference.

3.4 *miR-137* Expression Between Virgin and Non-Virgin Females.

The expression of some miRNAs can be robustly altered depending on the mating status of the adult *Drosophila* fly (Saul et al., 2016). Upon mating or gestation, *Drosophila* female flies undergo transcriptional changes and gene regulation that result in different physiology and behavior (Fricke et al., 2014; Newell et al., 2020; Zhou et al., 2014). As such, we wanted to evaluate if *miR-137* expression in the female brain is dependent on mating status. To obtain virgin females, we cleared all adult flies from the flies bottle. In the next 24 hrs, we collected virgins female flies shortly after eclosion, held them in groups of 10 per vial, and aged them for 3 days. Non-virgin females (control) were aged for 3 days in a mixed population of males and females to allow mating. RNA was isolated from the heads and normalized to 2S rRNA. Our RT-qPCR results showed no significant

change in *miR-137* levels between mated females and virgins (Fig. 10). These results suggest that *miR-137* expression was not affected by mating status in adult flies.

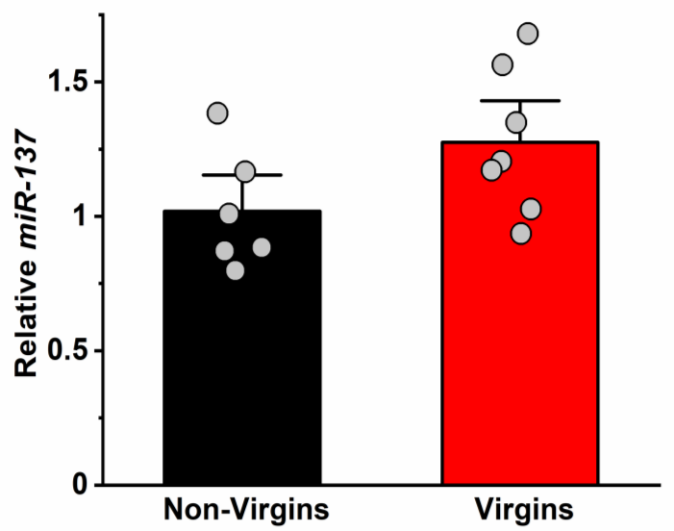

Figure 10. *miR-137* expression between virgin and non-virgin females. Quantification of the relative expression of the mature *miR-137* by RT-qPCR in wild-typed flies (w^{1118}). Results normalized to S2 rRNA. The level of *miR-137* was analyzed using two-tailed student T-test between each independent group and the control group as described in the experimental procedures. Error bars indicate SE. RT-qPCR analysis of the mature *miR-137* level in heads between same-aged virgins and non-virgins females shows no significant difference.

3.5 *miR-137* Expression During Lifespan.

The next question we wanted to address is whether *miR-137* expression changes during adult life. Age determines many physiological changes related to significant diseases. Some age-associated pathologies, such as a defect in the function of vital organs and inflammatory and cardiovascular diseases, are linked to miRNAs (Dimmeler & Nicotera, 2013; Kinser & Pincus, 2020). For example, a brain-enriched miRNA, *miR-34,* is involved in *Drosophila's* age-related neurodegenerative disease and long-term

brain integrity (N. Liu et al., 2012). The loss of *miR-34* increases brain aging, neurodegeneration, increases the accumulation of ubiquitinated proteins in the brain with age and decreases survival (N. Liu et al., 2012). In contrast, the up-regulation of *miR-34* extends lifespan and mitigates neurodegeneration (N. Liu et al., 2012; Newell et al., 2020). Further evidence of miRNAs such as *lin-4, miR-71, miR-238, miR-239,* and *miR-246* report a relation between miRNA and age (Thalyana & Slack, 2012).

We wanted to examine if *miR-137* is influenced by age in *Drosophila*. Since the w^{1118} median lifespan is 54 days (Qiu et al., 2017), we chose to compare levels of *miR-137* at young adult age (3 days), middle age (10 and 25 days), and old age (40 days). *miR-137* expression was quantified from RNA extracted from male heads and showed no difference between the chosen ages (Fig 11), suggesting that *miR-137* expression is not age-dependent and remains stably expressed throughout the adult lifespan of the *Drosophila*.

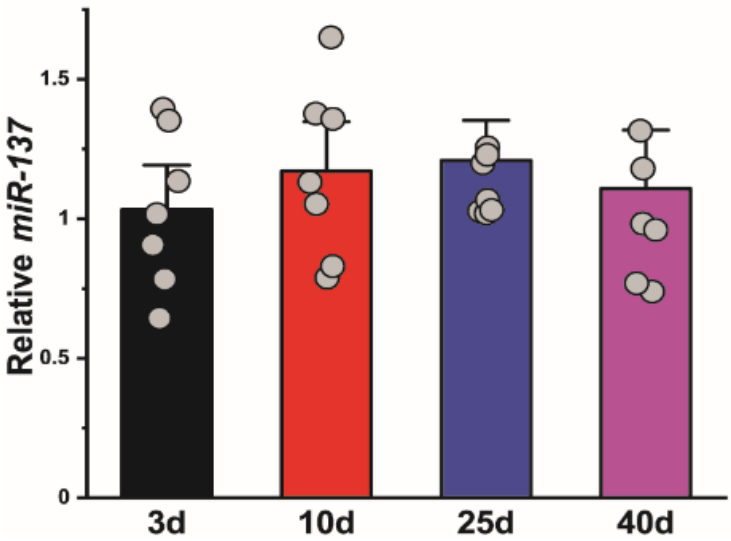

Figure 11. *miR-137* expression during lifespan. Quantification of the relative expression of the mature *miR-137* by RT-qPCR in wild-typed flies (w^{1118}). Results normalized to S2 rRNA. The level of *miR-137* was analyzed using two-tailed student T-test between each independent group and the control group as described in the experimental procedures. Error bars indicate SE. RT-qPCR analysis of the mature *miR-*

137 in WT flies of age 3,10, 25, and 40 days, RT-qPCR performed using male heads. Expression level normalized to 3 days old and shows no significant difference between the groups.

3.6 *miR-137* Expression During Different Times of the Day.

Because miRNAs influence multiple biological pathways and have been increasingly recognized to be involved in circadian rhythm regulation (Kadener et al., 2009; Xue & Zhang, 2018). We wanted to evaluate if *miR-137* expression is under circadian or biological clock regulation. To do this, 3-day old male flies were collected, grouped into 10 per vial, and entrained for four consecutive days under a 12/12 light-Dark cycle. Next, we collected RNA from male heads collected at the indicated times during the day (ZT= Zeitgeber; ZT 0 represents when the light is first turned ON, and ZT 12 represents when the light is turned OFF, ZT 0= time) to compare *miR-137* levels. RNA was isolated from the heads and were normalized to 2S rRNA. RT-qPCR showed that levels of *miR-137* did not show any significant change between selected times of the day. Our results suggest that *miR-137* is not under circadian regulation (Fig 12). Further studies, however, could examine *miR-137* expression in clock gene(s) mutants.

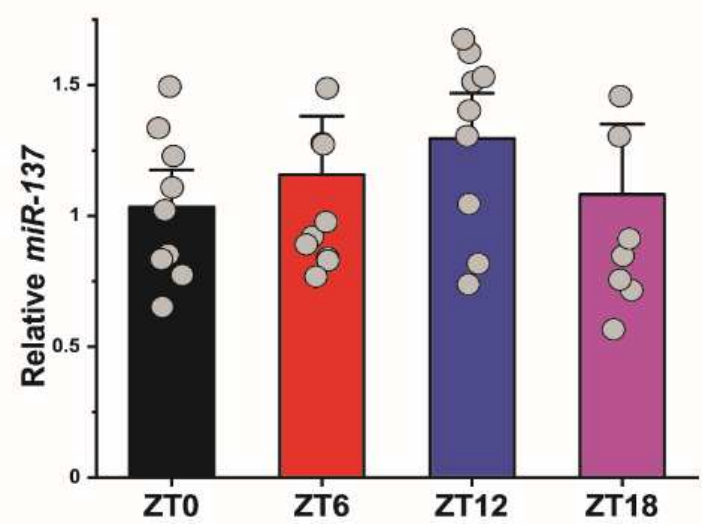

Figure 12. *miR-137* expression during different times of the day. Quantification of the relative expression of the mature *miR-137* by RT-qPCR in wild-typed flies (w^{1118}). Results normalized to S2 rRNA. The level of *miR-137* was analyzed using two-tailed student T-test between each independent group and the control group as described in the experimental procedures. Error bars indicate SE. RT-qPCR quantification of the mature *miR-137* level did not change in fly heads collected at the indicated times during the day (ZT= Zeitgeber; ZT 0 represents when the light is first turned ON, and ZT 12 represents when the light is turned OFF, ZT 0= time).

3.7 Regulation of *miR-137* by Neuronal Activity.

Neural activity-dependent regulation of miRNAs may regulate gene expression in response to synaptic plasticity, learning, and memory function (Hu & Li, 2017; Kiltschewskij & Cairns, 2019; Sim et al., 2014; I. F. Wang et al., 2022). Studies suggest that a possible mechanism by which neural activity could induce miRNAs regulation is by enhancement in Dicer RNase III cleavage activity, thereby enhancing the processing of pre-miRNA into mature miRNA (Lugli et al., 2005). A second possible mechanism is that neural activity regulates transcription factors such as CREB activity (West & Greenberg, 2011). Studies showed that *miR-132* and *miR-212* are regulated through CREB-dependent induction (Nudelman et al., 2010; Remenyi et al., 2013). These studies suggest that miRNA expression could be affected by disturbing neuronal activity.

Since little is known about whether changes in neural activity regulate *miR-137* expression, we manipulated neuronal activity with various protocols *in vivo* and tested if *miR-137* expression levels changed.

3.7.1 Genetically Decreasing Neural Activity with Cha^{ts2}.

Acetylcholine is the major excitatory neurotransmitter in the *Drosophila* CNS (W. W. Liu & Wilson, 2013). We used a temperature-sensitive Choline acetyltransferase mutant allele (Cha^{ts2}) as a tool to decrease neural activity (Greenspan et al., 1980). In

Drosophila, *Cha*^{ts2} mutants produce reduced, but near-normal levels of the neurotransmitter acetylcholine at 18 ºC. However, upon increased temperature to 30 °C, *Cha*^{ts2} mutants inhibit about 75% cholinergic activity *in vivo* by losing all Choline acetyltransferase (Salvaterra2 & Mccaman, 1985; Takagawa & Salvaterra, 1996). We used homozygous *Cha*^{ts2} mutants and subjected them to heat treatment at 32 °C for 3 hrs to inhibit neural activity. For controls, we used *Cha*^{ts2} mutants raised at 18 ºC, which exhibited Choline acetyltransferase activity similar to wild type. For this experiment, we examined the level of the *pre-miR-137*. RNA was collected from the heads immediately after the 3 hrs heat treatment. Rt-qPCR Ct values normalized to those of *elfA1* reference gene and results showed that the levels of *miR-137* in heads did not significantly change in response to decreased neural activity in *Cha*^{ts2} (Fig 13).

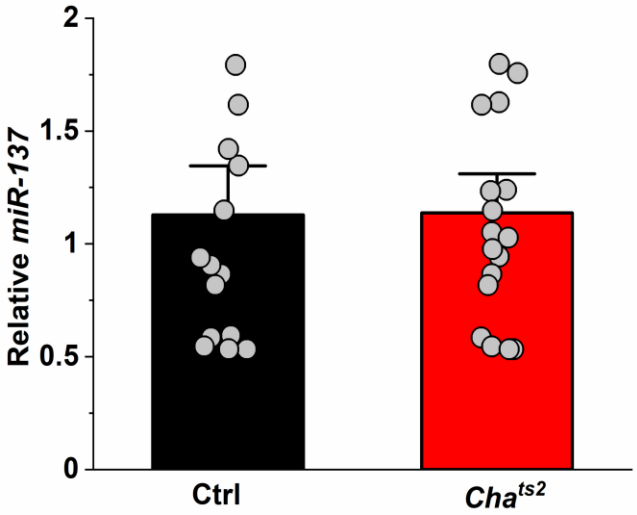

Figure 13. Quantification of the relative expression of the *pre-miR-137* by RT-qPCR in *Cha*^{ts2}mutant flies. Results normalized to *elfA1*. The level of *miR-137* was analyzed using two-tailed student T-test between each independent group and the control group as described in the experimental procedures. Error bars indicate SE. Rt-qPCR results showed that the levels of *miR-137* in heads did not significantly change in response to decreased neural activity in *Cha*^{ts2}.

3.7.2 Genetically Increasing Neural Activity with *TrpA1*.

The Transient Receptor Potential-A1 cation channel (*TRPA1*) gene encodes a nonspecific cation channel that is selectively permeable for Ca+ and Na+ ions and composed of six transmembrane-spanning domains (Kang et al., 2012; Roessingh & Stanewsky, 2017; Venkatachalam et al., 2014). *TrpA1* channels are temperature sensitive channels are best activated by temperatures stimulation between 27 °C and 29 °C (Zhou & Zhang,.1989) or between 30 °C and 36 °C depending on the TRPA1 isoform (Kang et al., 2012; Zhong et al., 2012).

We used *TrpA1* as a genetic tool to increase neural activity *in vivo* (Barbagallo & Garrity, 2015; Bellemer, 2015), and we used a pan-neuronal *elav-Gal4* transgene to drive the expression of *TrpA1* under the control upstream activating sequence (*UAS*) in all neurons. The UAS-GAL4 system is a mechanism taken from yeast (Saccharomyces cerevisiae), and can be used to drive the expression of a particular DNA sequence *in vivo* in flies. The UAS-GAL4 components are carried by two flies strains, and crossing these genotypes results in offspring that carry both parts of the system. *Elav-Gal4>>TrpA1* progeny ≤ 24 hrs were collected and entrained for four days at 12/12 Light/Dark cycle at 18 °C. After that, flies were heat treated at 32 °C for different time periods of 1 hr, 3 hrs, 6 hrs, and 24 hrs. The control flies were *elav-Gal4>>TrpA1* without heat treatment (18 °C). Heads were collected and total RNA was isolated. The RT-qPCR analyses showed that *miR-137* expression was not affected by an increase in neural activity in *TrpA1* (Fig 14).

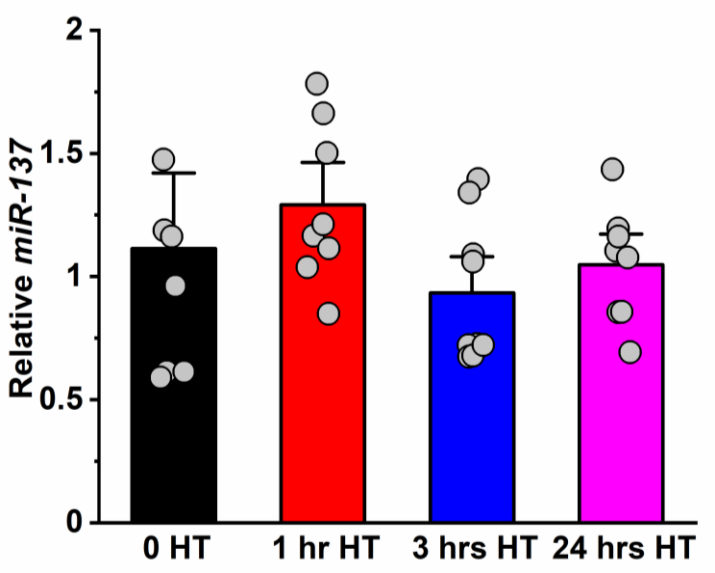

Figure 14. Quantification of the relative expression of the mature *miR-137* by RT-qPCR in *TrpA1* flies. Results normalized to S2 rRNA. The level of *miR-137* was analyzed using two-tailed student T-test between each independent group and the control group as described in the experimental procedures. Error bars indicate SE. Rt-qPCR results showed that the levels of *miR-137* in heads did not significantly change in response to increased neural activity using *TrpA1.*

3.8 *Drosophila* Diseased Models in which Activity is Changed.

Drosophila melanogaster disease models have been utilized to model human brain diseases. These models have been validated to reproduce some aspects of human neurodegenerative disorder and changes in neural activity. Using *Drosophila* disease models may promote an understanding of activity-dependent mediated miRNA regulation. Here, we investigated the levels of *miR-137* in models of Alzheimer's disease and seizure/epilepsy.

3.8.1 Model of Alzheimer's Disease.

Alzheimer's disease (AD) is the most common neurodegenerative disease that is characterized by intracellular accumulation and aggregation of β-amyloid (*Aβ*) oligomers in the brain (Glenner & Wong, 1984; Hardy & Allsop, 1986). In addition, AD has also been

associated with toxicity of the *Aβ* fibrils under certain conditions like age (Eckert et al., 2008). The expression of *Aβ* induces neural activity in the cortical and hippocampal neurons (J. T. Brown et al., 2011). We used a transgenic *Drosophila* line that pan-neuronally expresses a secreted form of the human *β-amyloid*$_{1-42}$ (*Aβ*$_{1-42}$) peptide sequence and is used as a model to study Alzheimer's disease (Iijima et al., 2008). This *Aβ42*-modle exhibits phenotypes such as locomotor dysfunction and age-dependent learning and memory deficit (Iijima et al., 2004). Our lab has previously reported that this model also displays an age-dependent decrease in potassium voltage-gated channels Kv4 (Ping et al., 2015) and early increased hyper-activity (Hahm et al., 2018). *Aβ* accumulation in the brain is much higher in older age compared to young flies suggesting that the overexpression of *Aβ42* in the nervous system results in neurodegeneration in an age-dependent manner (Finelli et al., 2004; Ping et al., 2015). We used young male flies from the Aβ42 model at ages of 3 days (the control) and compared them to 15 days and 25 days old. Heads were collected, and total RNA was isolated. The results of RT-qPCR, however, showed no significant change in *miR-137* expression in Aβ42 flies at 15 and 25 days compared to 3 days old (Fig 15). These results suggest that *miR-137* expression was not affected by increased neural activity in this *Aβ42* Alzheimer's disease model.

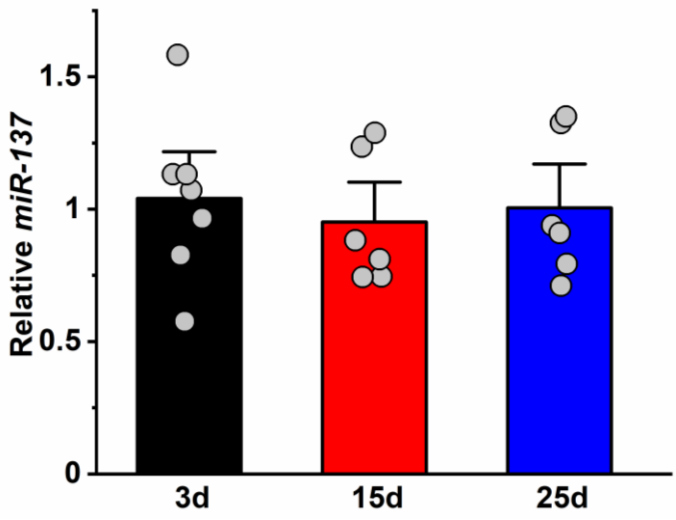

Figure 15. Quantification of the relative expression of the mature *miR-137* by RT-qPCR in Alzheimer's disease model flies (*Aβ42*). Results normalized to S2 rRNA. The level of *miR-137* was analyzed using two-tailed student T-test between each independent group and the control group as described in the experimental procedures. Error bars indicate SE. The results of RT-qPCR show no significant change in *miR-137* expression in Aβ42 flies at 15 and 25 days compared to 3 days old.

3.8.2 Models of Seizure and Epilepsy.

Epilepsy is a neurological disease that results from abnormalities and highly synchronized discharge of brain neurons. More than 45.9 million people around the world suffer from epilepsy (Beghi et al., 2019; Howard & Baraban, 2017). Epilepsy onset involves gene mutations that encode for ion channels, especially genes affecting voltage-gated sodium channels, neurotransmitter signaling, solute carrier, synaptic and vesical structure, and multiple transcription factors that involve metabolic signaling pathways (Fischer et al., 2023; Parker, Howlett, et al., 2011; Song & Tanouye, 2008). Several studies demonstrate that miRNAs are involved in the occurrence, development, and treatment of epilepsy (Henshall et al., 2016; J. Wang & Zhao, 2021).

Drosophila-disease models of epilepsy have been used for many years (Finelli et al., 2004). We used a transgenic *Drosophila* model called bang sensitive (*bss*), which is

a gain-of-function mutation in the paralytic (para) voltage-gated sodium channel gene (Parker, Padilla, et al., 2011). *bss* mutant flies respond with severe seizure-like behavior and paralysis upon mechanical stimulation (bang), such as brief vortexing or tapping vials (Parker, Padilla, et al., 2011; Song & Tanouye, 2008). *bss* is characterized by the most severe seizure phenotype and lowest seizure threshold compared to any other bang-sensitive *Drosophila* epilepsy models.

In this experiment, we used *bss* mutant flies as a diseased model where the neural activity is increased and compared them to w^{1118} as a control. To induce an increase in neural activity, we collected young adult male flies, divided them into groups of 10, placed them in empty vials, and exposed them to mechanical stimulation by vortexing the vial for 10 seconds every 30 minutes for 3 hours. The 30-minute interval between vortexing allows flies to re-acquire their bang sensitivity and completely recover from the initial seizure/paralysis and then respond to the next mechanical stimulation (Kuebler & Tanouye, 2000). w^{1118} controls were given the same stimulation and recovery conditions. Total RNA was collected from heads, and *miR-137* expression was determined by RT-qPCR. The results of RT-qPCR showed no significant difference in *miR-137* levels between the wild-type and the *bss* mutants after 3 hrs of induce an increase in neural activity (Fig 16), suggesting that *miR-137* expression was not affected by increased neural activity in the *bss* epilepsy disease model.

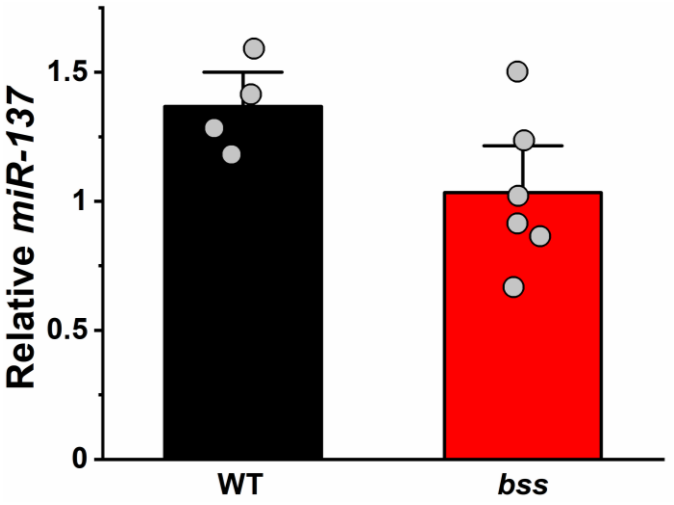

Figure 16. Quantification of the relative expression of the mature *miR-137* by RT-qPCR in wild-typed flies and (*bss*). Results normalized to S2 rRNA. The level of *miR-137* was analyzed using two-tailed student T-test between each independent group and the control group as described in the experimental procedures. Error bars indicate SE. RT-qPCR results showed that the levels of *miR-137* in heads did not significantly change in response to increased neural activity in *bss* epilepsy disease model.

3.9 *miR-137* Expression During Temperature and Starvation Stress.

Environmental stress conditions can impact miRNA biogenesis and function (Leung & Sharp, 2010). Changes in miRNA expression levels may be involved in various stress responses by regulating transcription factors and signaling pathways (Gosline et al., 2016; Mazzelli et al., 2020). Here, we explored if *miR-137* is a stress-responsive miRNA. We quantified *miR-137* levels in wild-type w^{1118} flies after subjecting them to different types of stress, including temperatures and nutrient deprivation.

3.9.1 Temperatures Stress.

Extreme heat or cold temperatures greatly impact animals' physiology, development, behavior, metabolism, and transcriptional mechanisms in order to avoid damage or lethality. *Drosophila* is an exothermal organism that highly depends on the outside temperature to regulate its endogenous temperature. *Drosophila* is a tropical

organism with optimal growth and life span at 25 ºC (Dillon et al., 2009). miRNA expression in *Drosophila* is highly dependent on the temperature in the environment (Fast et al., 2017). Some miRNAs expression may be adjusted to ensure homeostasis and adaptation to outside heat/cold temperature stress. Cold stress causes dehydration and loss of sodium ions, affecting the flies' development and survival (Hazell & Bale, 2011; MacMillan & Sinclair, 2011). Adaptation to cold temperature conditions (6 ºC) could cause extensive changes in global transcription (MacMillan et al., 2016). *miR-31-5p,* for example, is up-regulated during cold stress and involved in cold adaptation (Fast et al., 2017). On the other hand, an increase in temperature ≥ 30 ºC (heat stress) results in a substantial decrease in the fat body stores, increase in metabolism, and decrease in lifespan (Miquel et al., 1976).

We tested the level of *miR-137* in response to temperature stress. 7-day old male flies were collected and divided into groups of 10 per vial. Then we subjected them to a high temperature of 33°C for 3 days, cold temperature of 6 °C for 3 days, while the control was kept at 25 °C for 3 days. After temperature stress treatment, heads were collected, and total RNA was isolated. RT-qPCR results showed that *miR-137* was relatively stable under heat/cold thermal stress in *Drosophila* (Fig 17).

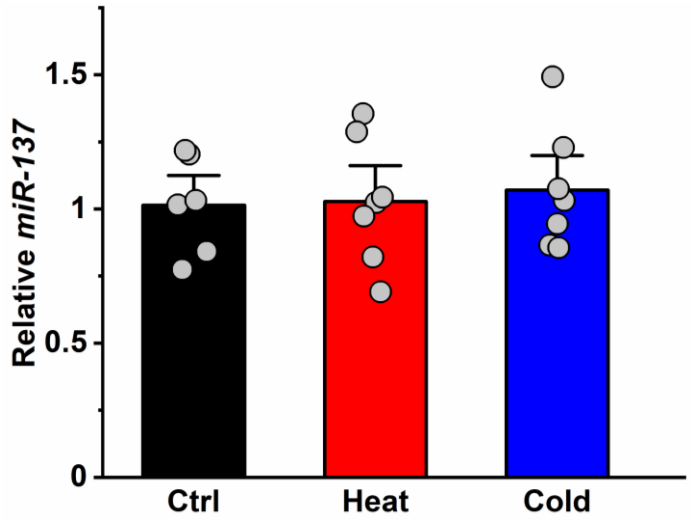

Figure 17. Quantification of the relative expression of the mature *miR-137* by RT-qPCR in wild-typed flies during temperatures stress. Results normalized to S2 rRNA. The level of *miR-137* was analyzed using two-tailed student T-test between each independent group and the control group as described in the experimental procedures. Error bars indicate SE. RT-qPCR results showed that the levels of *miR-137* in male heads did not significantly change in response heat stress 33°C for 3 days, cold stress 6 °C for 3 days, or the control 25 °C for 3 days.

3.9.2 *miR-137* Expression During Dietary Restriction of Protein, Sugar, and Total Starvation.

We next investigated whether *miR-137* levels change in response to different conditions of nutrient restriction (Kálmán et al., 2014). The quantity and the quality of the food consumed by the organism are associated with metabolic stress, reproduction, development, and lifespan. Adaptation to environmental food shortage may induce molecular changes underlying animal physiology and behavior.

For nutritional stress, we evaluated levels of *miR-137* by RT-qPCR in w^{1118} males and females. Flies were raised in a mixed population of males and females for 7 days on standard fly food, then sorted by sex, and divided into groups of 10 per vial. Flies were then placed on media of protein starvation for 5 days or sugar starvation for 5 days.

Because w^{1118} has limited tolerance to total starvation, we only expose the flies to 3 days of total starvation. Control flies were freely fed and age-matched wild type. Heads were collected, and total RNA was isolated. Overall, *miR-137* levels in w^{1118} did not change in response to protein, sugar, or total starvation in males or females (Fig 18). These results indicate that the expression of *miR-137* is relatively stable in response to nutrient stress.

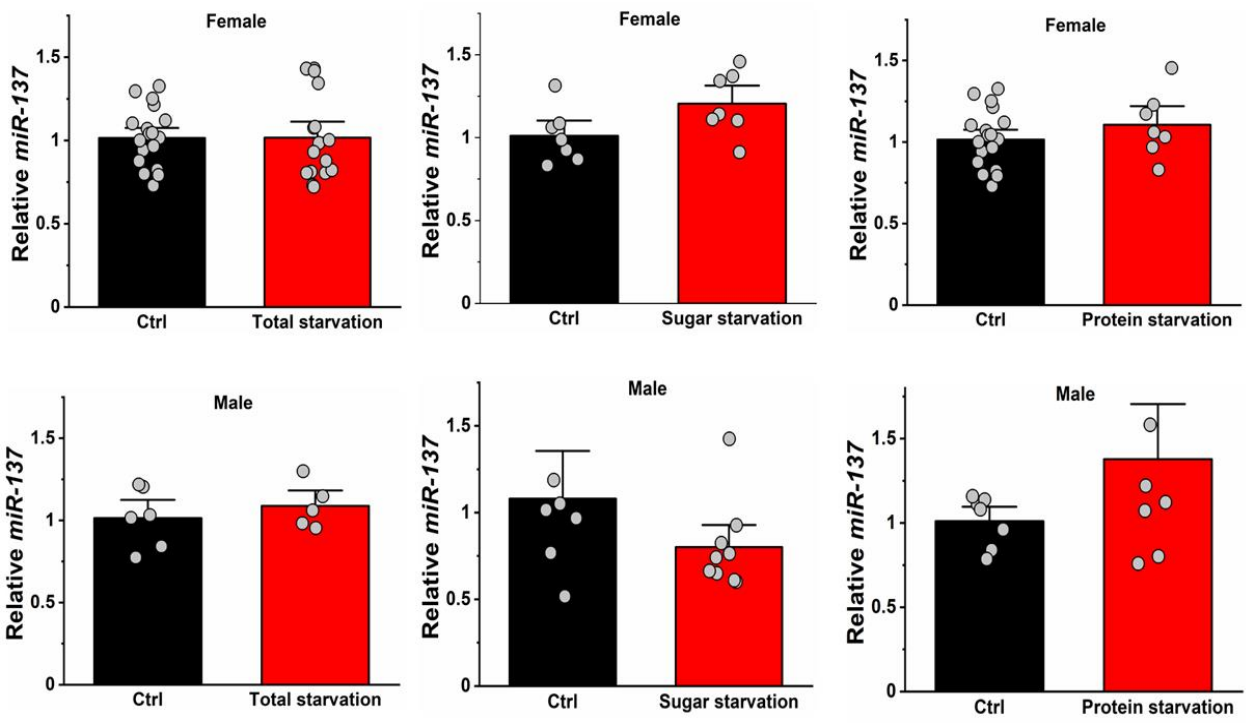

Figure 18. *miR-137* expression during dietary restriction of protein, sugar, and total starvation. Quantification of the relative expression of the mature *miR-137* by RT-qPCR in wild-typed flies. Results normalized to S2 rRNA and U14. The level of *miR-137* was analyzed using two-tailed student T-test between each independent group and the control group as described in the experimental procedures. Error bars indicate SE. *miR-137* levels in w^{1118} did not change in response to 5 days protein starvation, 5 days sugar starvation, or 3 days total starvation in males or females

3.10 Conclusion

In conclusion, we showed by RT-qPCR that the expression level of *miR-137* was highly concentrated in *Drosophila* brains. This result indicates its crucial function in regulating genes in the nervous system. We also showed that *miR-137* has no sex-biased expression and that it is not affected by mating status. We also investigated the expression level of *miR-137* during different times of day (ZT0, ZT6, ZT12, ZT18), and the *miR-137* levels were unchanged, suggesting that the circadian clock does not regulate *miR-137* expression. We further tested the influence of age different kinds of stress on *miR137* expression, and results showed no significant difference in *miR-137*.

Despite evidence that reports miRNAs regulation by neural activity (Sim et al., 2014), our RT-qPCR analysis concluded that *miR-137* expression in the brain was relatively stable and not affected by changes in neural activity. *miR-137* levels have been shown to regulate neuronal development and cognitive function. We showed that decreasing or increasing the neural activity in the CNS by heat treatment of Cha^{ts2} and *TrpA1*, respectively, showed no effect on *miR-137* levels. In addition, some studies showed that *miR-137* was reduced in the serum of patients with AD (Jiang et al., 2018; Kou et al., 2020), and reduced in brain tissues from both patients and mouse models of epilepsy (W. Wang et al., 2018). However, our analysis of *miR-137* levels showed relatively stable levels of *miR-137* in epileptic and Alzheimer's disease *Drosophila* models.

To sum up, *miR-137* expression appears to be enriched in *Drosophila* brains and exhibits relatively stable expression over time and with stress.

CHAPTER 4: miR-137 MUTANTS EXHIBIT METABOLIC PHENOTYPES

4.1 Overview.

The best method to study the biological function of an individual miRNA in a model organism is by mutating/deleting the gene and examining its phenotype. In this chapter, we characterized multiple *miR-137* phenotypes related to energy homeostasis in *Drosophila melanogaster.* Many miRNA mutants exhibit minor defects under normal conditions but then significant phenotypes under stress. In this study, we used two independently made null mutant lines of *miR-137*. The first null mutant line (*miR-137^{CR}*) was generated in our lab by CRISPR/Cas9 following methodology previously described (Gratz, Harrison, et al., 2015; Gratz, Rubinstein, et al., 2015). We used two guide RNAs to direct the endonuclease Cas9 cleavage at two DNA sites, removing sequence including the entire *pre-miR-137* (5'-*CAATCTCCAATGGCCACGTGTATGCTCGTATAACCTG-AAATCCAAATGTTATTGCTTGAGAATACACGTAGTTCACCGAGATTTGTT-3'*) and within it, the mature *miR-137* sequence (underlined). During homology-directed repair (HDR), the *miR-137* sequence was replaced by sequence encoding *DsRed* under the control of a 3xP3 promoter (for selection). Deletion of *miR-137* and replacement with *DsRed* was confirmed by PCR and DNA sequencing. To confirm that phenotype(s) are not a consequence of genetic background, we obtained a second null mutant line, *miR-137^{KO},* which was generated by homologous recombination, replacing *miR-137* with the w [+] gene (Y. W. Chen et al., 2014). Both homozygous *miR-137* mutants are viable with no apparent developmental defects, and RT-qPCR was performed to validate that both lines show virtually undetectable levels of *miR-137* expression (Fig.19).

In this chapter, we tested a range of phenotypes in *Drosophila melanogaster,* including the ability of *miR-137* mutants to survive under different nutrient restrictions, oxidative stress tolerance, body weight, energy storage, and food intake.

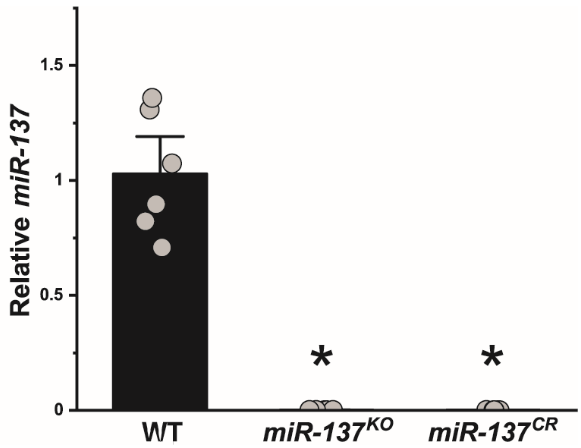

Figure 19. Validation of *miR-137* expression in WT and *miR-137^{CR}* and *miR-137^{KO}* mutant heads. *miR-137* levels are normalized to levels of *S2 rRNA* from the same samples, and $2^{-\Delta\Delta ct}$ values are shown as representations of relative fold-changes compared to control condition which is the group shown on the furthest left of each graph (see Materials and Methods). Pairwise comparisons were made using the Student t-test. *P<0.05, error bars indicate SEM.

4.2 Modulating *miR-137* Levels Affects Lifespan Under Conditions of Nutrient Deprivation.

Animals living in the natural environment often face periods of food limitations. Animals' survival mainly depends on their response to starvation physiologically and behaviorally. To study whether *miR-137* is involved in nutrient sensing regulation, we tested the ability of *miR-137* mutants to survive during different nutrient restrictions. We used populations of *miR-137* mutant flies and compared them to wild-type populations.

4.2.1 *miR-137* Mutants are Starvation Resistant.

miR-137 has been highly studied with regard to neuronal differentiation, proliferation, maturation and development, as well as synapse formation, synaptic transmission, and learning and memory function (Y. W. Chen et al., 2014; Crowley et al., 2015; Olde Loohuis et al., 2015c; Silber et al., 2008; Smrt et al., 2010c; Sun et al., 2011; Szulwach et al., 2010). However, little is known about whether its expression in the brain also contributes to the central regulation of energy homeostasis and survival. We wanted to test how *miR-137* mutant flies react to different nutritional stress compared to wild-type.

To test for survival under protein starvation, populations of newly-eclosed wild-type and *miR-137*^{CR} and *miR137*^{KO} mutants were collected, raised in a mixed population of males and females, and aged to 7 days to avoid any starvation resistance due to the reported persistence of the larval fat body in the young adult (Aguila et al., 2007; Rehman & Varghese, 2021a). Then flies were raised on a media containing a sugar source but no protein source. Ten replicate vials (10 flies per vial) for each sex and two trials of each population of 100 were used to test starvation resistance. The protein starvation survival curve of *miR-137*^{CR} (red line) and *miR-137*^{KO} (blue line) exhibited extended survival compared to control populations (*w*^{1118} in black line) (Log-rank test $p<0.0001$) (Fig. 20A). Median survival of male *miR-137*^{CR} and *miR-137*^{KO} was 10 days and 12 days, respectively; median survival of wild-type was 5 days. *miR-137*^{CR} and *miR-137*^{KO} females also exhibited an increase in survival compared to control populations (Fig. 20B). Median survival of both *miR-137*^{CR} and *miR-137*^{KO} were 11 days, and median survival of wild-type 5 days.

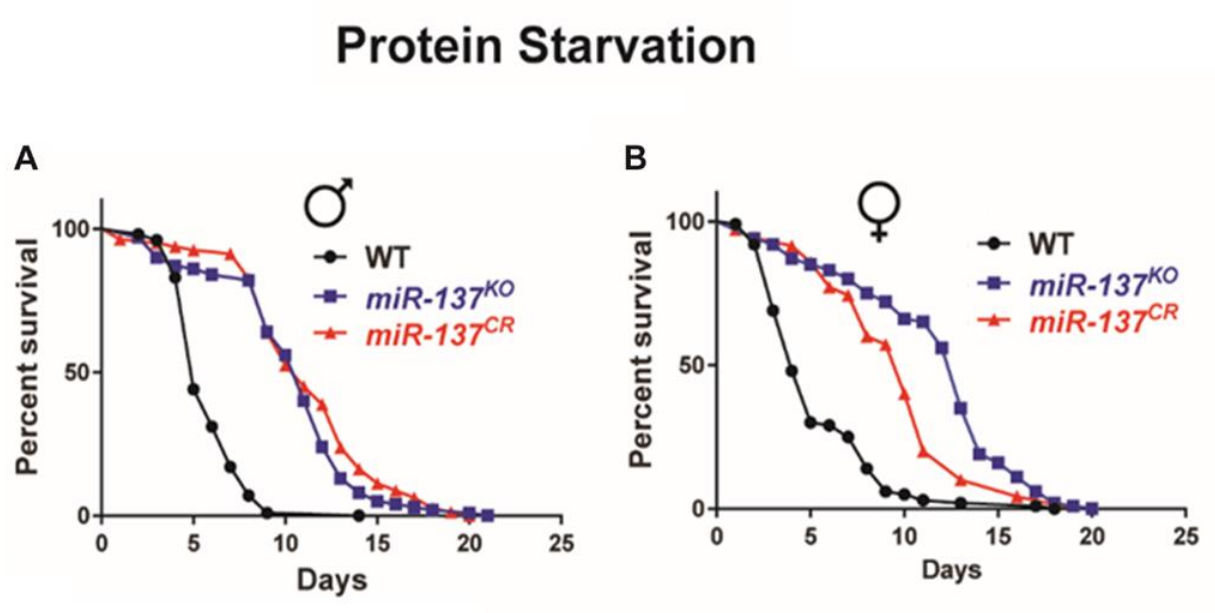

Figure 20. Loss of *miR-137* results in increased resistance to protein starvation. Representative survival curves shown for populations (N=100) of male ♂ (***A***) and female♀ (***B***) wild-type (WT; black), *miR-137*^{KO} (blue), and *miR-137*^{CR} (red), as indicated, under protein starvation conditions (see Materials and Methods). *miR-137*^{KO} and *miR-137*^{CR} lines displayed significantly extended lifespans compared to WT, as analyzed by Log-rank test (P<0.0001).

For sugar starvation, flies were raised on a media containing a source of protein (yeast paste) but no source of sugar. Populations of newly-eclosed wild-type and *miR-137*^{CR} and *miR137*^{KO} mutants were collected, raised in a mixed population of males and females, and aged to 7 days. Ten replicate vials (10 flies per vial) for each sex and two trial of each population of 100 were used to test starvation resistance. Sugar starvation survival curve of *miR-137*^{CR} (red line) and *miR-137*^{KO} (blue line) exhibited extended survival compared to control populations (*w*^{1118} in black line) (Log-rank test p<0.0001). Median survival of both *miR-137*^{CR} and *miR-137*^{KO} males were 19 days, and median survival of wild-type was 13 days (Fig. 21A). *miR-137*^{CR} and *miR-137*^{KO} females also exhibited an increase in survival compared to control populations (Log-rank test

p<0.0001) (Fig. 21B). Median survival of *miR-137*^{CR} and *miR-137*^{KO} was 15 and 20 days, respectively, and median survival of wild-type was 14 days.

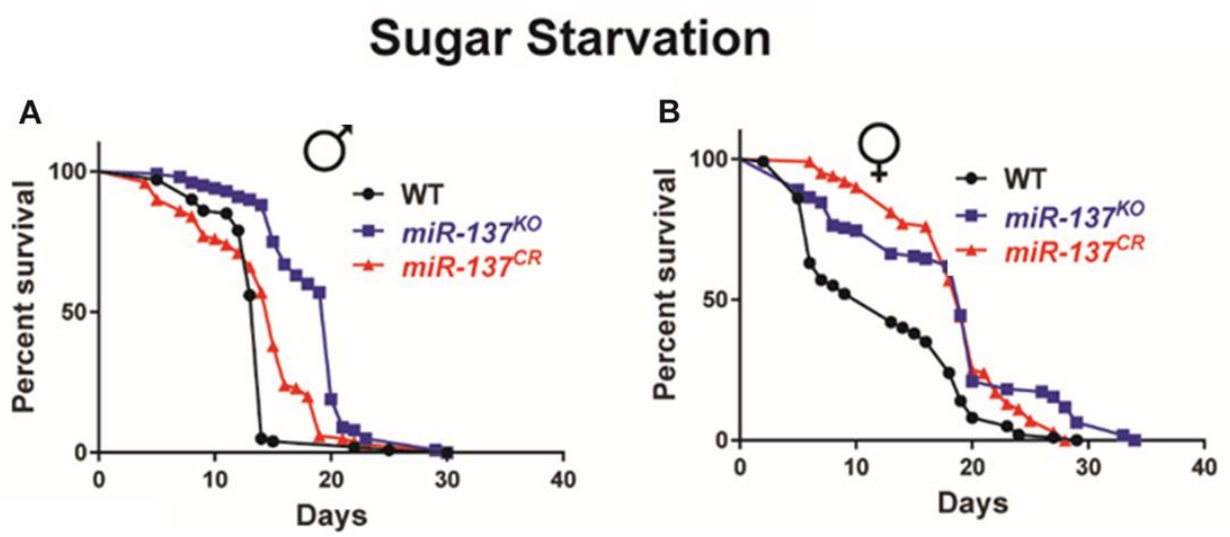

Figure 21. Loss of *miR-137* results in increased resistance to sugar starvation. Representative survival curves are shown for populations (N=100) of male ♂ (***A***) and female♀ (***B***) wild-type (WT; black), *miR-137*^{KO} (blue), and *miR-137*^{CR} (red), as indicated, under sugar starvation conditions (see Materials and Methods). *miR-137*^{KO} and *miR-137*^{CR} lines displayed significantly extended lifespans compared to WT, as analyzed by Log-rank test (P<0.0001).

Lastly, we tested the response to total starvation. Populations of newly-eclosed wild-type and *miR-137*^{CR} and *miR137*^{KO} mutants were collected, raised in a mixed population of males and females, and aged to 7 days. Then flies were raised on a media with complete food deprivation. Hydration was provided by water in the 1% agar media. 10 replicate vials (10 flies per vial) for each sex and two trial of each population of 100 were used to test starvation resistance. Total starvation survival curves for *miR-137*^{CR} (red line) and *miR-137*^{KO} (blue line) exhibited extended survival compared to

control populations (w^{1118} in black line) (Log-rank test p<0.0001) (Fig. 22A). Median survival of male *miR-137*^{CR} and *miR-137*^{KO} were 84 hrs and 72 hrs, respectively, and median survival of wild-type was 36 hrs. *miR-137*^{CR} and *miR-137*^{KO} females also exhibited an increase in survival compared to control populations (Log-rank test p<0.0001) (Fig. 22B). Median survival of female *miR-137*^{CR} and *miR-137*^{KO}, were 108 hrs and 84 hrs, respectively, and median survival of wild-type was 36 hrs.

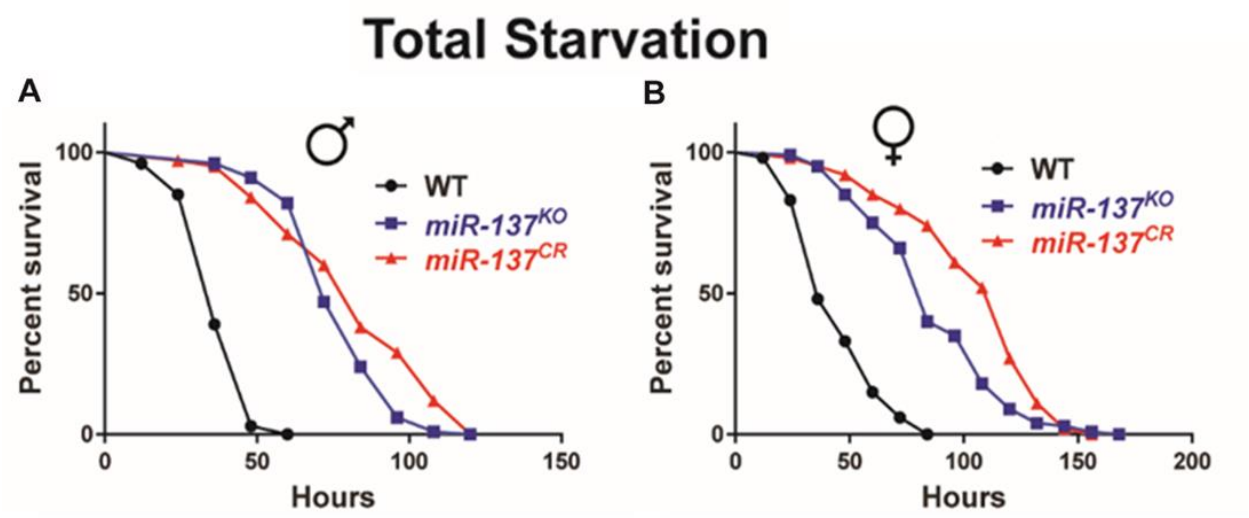

Figure 22. Loss of *miR-137* results in increased resistance to total starvation. Representative survival curves are shown for populations (N=100) of male ♂ (***A***) and female♀ (***B***) wild-type (WT; black), *miR-137*^{KO} (blue), and *miR-137*^{CR} (red), as indicated, under total starvation conditions (see Materials and Methods). *miR-137*^{KO} and *miR-137*^{CR} lines displayed significantly extended lifespans compared to WT, as analyzed by Log-rank test (P<0.0001).

To further ensure that the starvation resistance phenotype wasn't due to genetic background, we also tested the *miR-137*$^{CR/KO}$ trans-heterozygotes response to total starvation. To do that, we crossed *miR-137*^{KO} to *miR-137*^{CR}. Progeny were collected, raised in a mixed population of males and females, and aged to 7 days. Flies were then raised on media for total starvation. 10 replicate vials (10 flies per vial), and two trial of

each population of 100 males were used to test starvation resistance. Total starvation survival curves for *miR-137*^{CR} (red line) and *miR-137*^{KO} (blue line), and *miR-137*$^{CR/KO}$ (dark red line) exhibited extended survival compared to control populations (*w*^{1118} in black line) (Log-rank test p<0.0001) (Fig. 23). Median survival of male *miR-137*^{CR} and *miR-137*^{KO} were 84 hrs and 72 hrs, respectively, *miR-137*$^{CR/KO\ was}$ 96 hrs, and wild-type was 36 hrs. The comparable phenotype of *miR-137*$^{CR/KO}$ trans-heterozygotes and *miR-137*^{CR} and *miR-137*^{KO} homozygotes, suggests that the starvation resistance phenotype is indeed due to *miR-137* in *Drosophila melanogaster*.

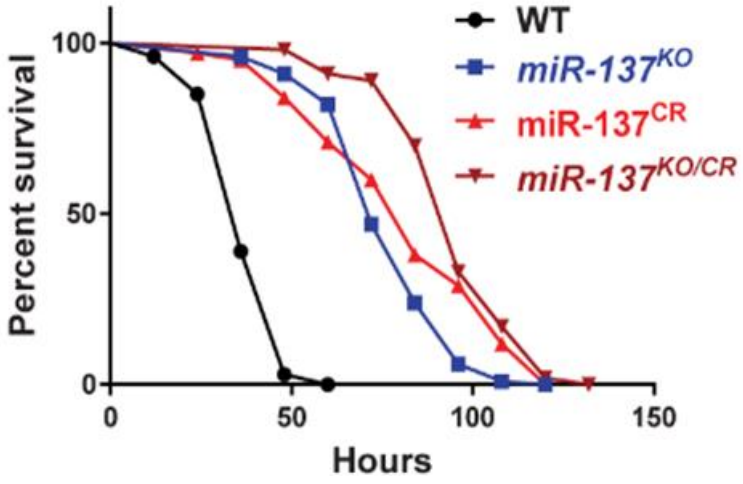

Figure 23. *miR-137*$^{CR/KO}$ trans-heterozygotes exhibited increased resistance to starvation. Representative survival curves are shown for male trans-heterozygote *miR-137*$^{CR/KO}$ (dark red), and *miR-137*^{CR} (red) and *miR-137*^{KO} (blue) homozygote lines, and WT (black) under total starvation conditions. Trans-heterozygote *miR-137*$^{CR/KO}$, similar to *miR-137*^{KO} and *miR-137*^{CR} homozygotes, showed significantly prolonged survival compared to WT (N=100, Log-rank test; P<0.0001).

In all cases, *miR-137*^{CR} and *miR-137*^{KO} males and females exhibited extended survival compared to control populations. In addition, total starvation resulted in the most robust phenotype, with *miR-137* mutants exhibiting a median survival twice that of wild-type flies (median survival of *miR-137*^{CR} and *miR-137*^{KO}, 84 hrs and 72 hrs, respectively;

median survival of wild-type, 36 hrs). As a result, continued studies were performed with males under conditions of total starvation, using both *miR-137*^{CR} and *miR-137*^{KO} homozygotes and/or *miR-137*$^{CR/KO}$ trans-heterozygotes, which similarly exhibited starvation resistance (median survival of 96 hrs).

4.2.2 *miR-137* Heterozygote Mutants Exhibit Semi-Dominant Starvation Resistance.

Because *miR-137* null mutants had an extreme starvation resistance phenotype, we wanted to examine if this phenotype is dominant, recessive, or semi-dominant. We also envisioned that some epistasis experiments (see chapter 5) would require tests with mutations on the same chromosome as *miR-137*, and it would be helpful to know if one copy of *miR-137*^{KO} or *miR-137*^{CR} would be starvation resistance. To test this, we crossed *miR-137*^{KO} and *miR-137*^{CR} to wild-type (*w*^{1118}). Progeny were collected, raised in a mixed population of males and females, and aged to 7 days to avoid any starvation resistance due to the reported persistence of the larval fat body in the young adult (Aguila et al., 2007; Rehman & Varghese, 2021a). Flies were then raised on a media for total starvation. 10 replicate vials (10 flies per vial) and two trials of each population of 100 males were used to test starvation resistance. We found that *miR-137*$^{CR/+}$ and *miR-137*$^{KO/+}$ heterozygotes exhibit a semi-dominant phenotype about halfway between wild-type and *miR-137* homozygotes, with median survival times of 48 hrs (Fig. 24).

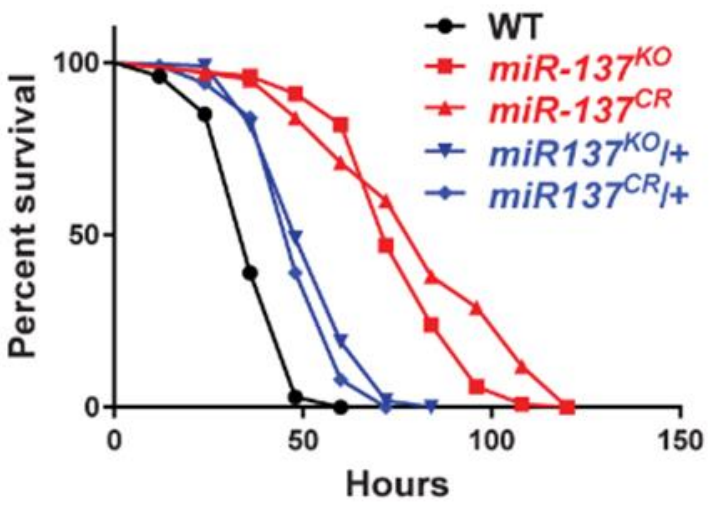

Figure 24. *miR-137* heterozygote mutants exhibit semi-dominant starvation resistance. Representative survival curves are shown for male *miR-137^{CR}* and *miR-137^{KO}* homozygote lines (red), WT (black), and *miR-137$^{CR/+}$* and *miR-137$^{KO/+}$* heterozygotes (blue lines, as indicated) under total starvation conditions. *miR-137$^{CR/+}$* and *miR-137$^{KO/+}$* heterozygotes show significant extension in lifespan under total starvation conditions, compared to WT (N=100, Log-rank test P<0.0001); survival curves from *miR-137^{KO}* and *miR-137^{CR}* homozygotes are shown for reference.

4.2.3 *miR-137* Overexpression in the Central Nervous System Results in An Increase in Starvation Sensitivity.

Next, we tested whether the overexpression of *miR-137* would have the opposite effect as the loss of *miR-137*. Since gain-of-function *miR-137* mutants in mammalian systems have been shown to display developmental defects (Smrt et al., 2010c), we set out to conditionally over-express *miR-137* post-development. We expressed *miR-137* in the CNS using *elav-Gal4>>UAS-miR-137*, a pan-neuronal *elav-Gal4* transgene to drive the expression of *miR-137* under the control of the relevant yeast upstream activating sequence (*UAS*), in combination with the ubiquitous expression of the temperature-sensitive Gal80^{ts} protein, which inhibits Gal4 activity at 18 °C, and permits Gal4 activity at 30 °C. We then raised *elav-Gal4, tub-Gal80^{ts}>>UAS-miR-137* flies at 18 °C to allow for

normal development, then shifted newly-eclosed flies to 30 °C to over-express *miR-137* post-development for 7 days. Over-expression of *miR-137* was confirmed by RT-qPCR and showed significant up-regulation in *miR-137* (Fig. 25A). We found that post-developmental overexpression of *miR-137* significantly reduced lifespan under starved conditions, with a median survival of 24 hrs, compared to genetic background controls with median survival times of 36 and 48 hrs (Fig. 25B).

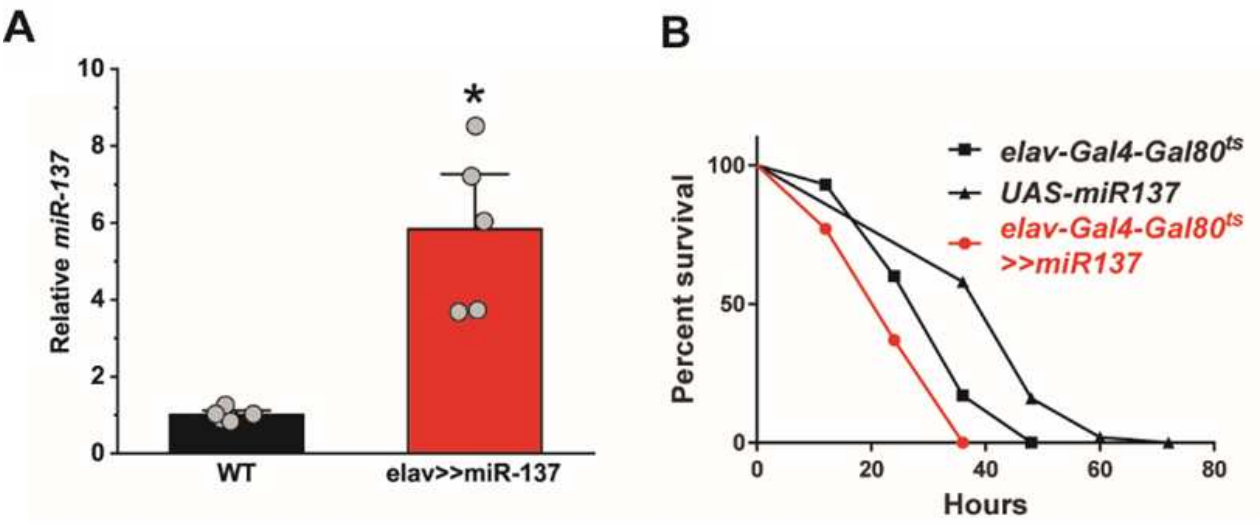

Figure 25. *miR-137* overexpression in the central nervous system results in an increase in starvation sensitivity. Conditional over-expression of *miR-137* was achieved using *elav-Gal4* driving *UAS-miR-137* in combination with *tub-Gal80^{ts}* (*elav-Gal4-Gal80^{ts}>>miR-137*); these flies were compared with parental lines, *UAS-miR-137* and *elav-Gal4; tub-Gal80^{ts}* (*elav-Gal4-Gal80*). Flies were raised at 18 °C for normal development, then shifted to 30 °C for 7 days to over-express *miR-137*. RT-qPCR confirming over-expression of *miR-137* in the *elav-Gal4-Gal80^{ts}>>miR*-137 line (***A***), and survival curves (***B***) of males under total starvation conditions are shown. The conditional overexpression of *miR-137* in the CNS after development significantly increased the sensitivity to starvation compared to the parental controls (Log-rank test, P<0.0001).

4.2.4 *miR-137* Expression in the Nervous System Rescues Starvation Resistance of *miR-137* Mutants.

Given that *miR-137* is enriched in the central nervous system (CNS), we tested whether the re-introduction of *miR-137* expression, specifically in the nervous system, was sufficient to reverse the starvation resistance of *miR-137* mutants. We expressed *miR-137* in the CNS of *miR-137* mutant backgrounds using *elav-Gal4>>UAS-miR-137*. We found that, indeed, pan-neuronal expression of *UAS-miR-137* in *miR-137^{CR}* or *miR-137^{KO}* backgrounds re-sensitized survival under starvation conditions (Fig. 26). These results indicate that it is primarily the expression of *miR-137* in the CNS that underlies the regulation of starvation resistance. Altogether, our results demonstrate that *miR-137* centrally regulates processes affecting organismal fitness under conditions of nutrient deprivation.

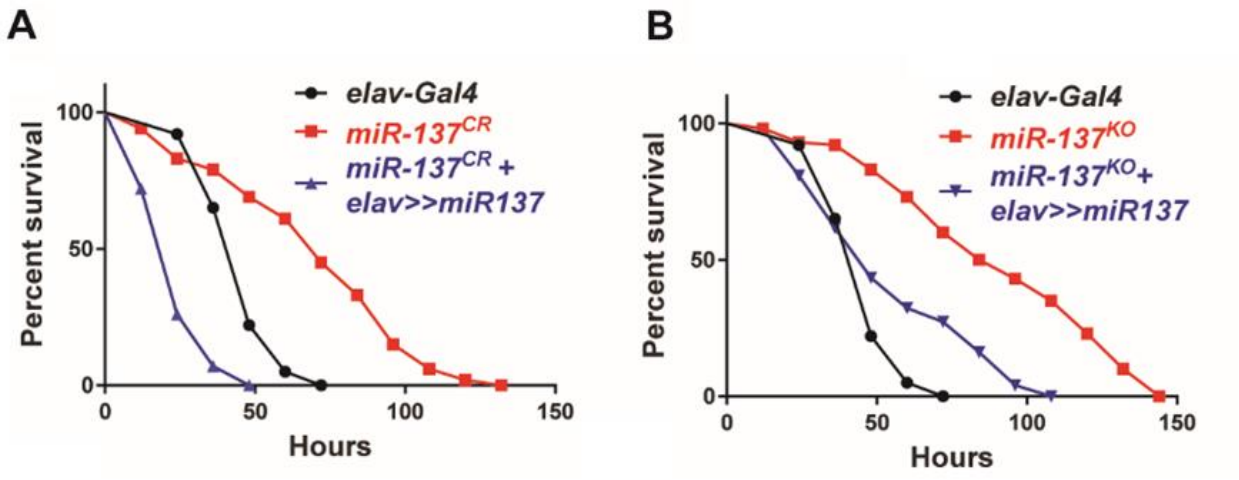

Figure 26. *miR-137* expression in the nervous system rescues starvation resistance of *mir-137* mutants. Male flies in which *elav-Gal4* transgene was used to drive *UAS-miR-137* expression in either a *miR-137^{CR}* (***A***) or *miR-137^{KO}* (***B***) mutant background (*miR-137^{CR}+elav>>miR-137* or *miR-137^{KO}+elav>>miR-137,* respectively) were compared with *elav-Gal4* and *miR-137* mutant parental lines, under conditions of total starvation. In both cases, *miR-137^{CR}+elav>>miR-137* and *miR-137^{KO}+elav>>miR-137* flies exhibit a

significant leftward shift in their survival sensitivity compared with *miR-137* mutant background lines (Log-rank test P<0.0001), indicating a rescue of starvation resistance with the reintroduction of *miR-137* expression driven by *elav-Gal4*.

4.3 *miR-137* Mutants Exhibit Increased Tolerance to Oxidative Stress.

In addition to the starvation resistant phenotype, we tested the response of *miR-137^{CR}* and *miR-137^{KO}* males to oxidative stress. Several studies have reported a positive correlation between starvation and oxidative resistance (Baldal et al., 2006a; Harshman & Haberer, 2000; Petti et al., 2011a). Physiological changes in gene expression in response to nutrient starvation strongly correlate with gene expression changes that occur in the oxidative stress response. For example, an increase in *d4E-BP*, a translation regulator, is essential for unfavorable conditions of starvation and oxidative resistance (Petti et al., 2011; Teleman et al., 2005a; Tettweiler et al., 2005).

In our experiments, we used paraquat to induce oxidative resistance. Paraquat is a highly toxic substance that has been shown to increase reactive oxygen species (ROS) and leads to oxidative stress in animals (Rzezniczak et al., 2011). 3-5 day old males were collected, divided into groups of 10 per vial, and fed 20% paraquat which was added to their regular diet. Flies were raised on standard fly food and not starved prior to oxidative exposure to avoid any unnecessary stress. 10 replicate vials (10 flies per vial) and two trials for each population of 100 males were used to test oxidative resistance, and survival was scored every 12 hrs. *miR-137^{CR}* and *miR-137^{KO}* showed increased viability on paraquat than the wild-type (*w^{1118}*) flies, with median survival twice that of wild-type flies. Median survival of *miR-137^{CR}* and *miR-137^{KO}* were 204 hrs, and 234 hrs, respectively, and median survival of wild-type was 108 hrs (Fig 27).

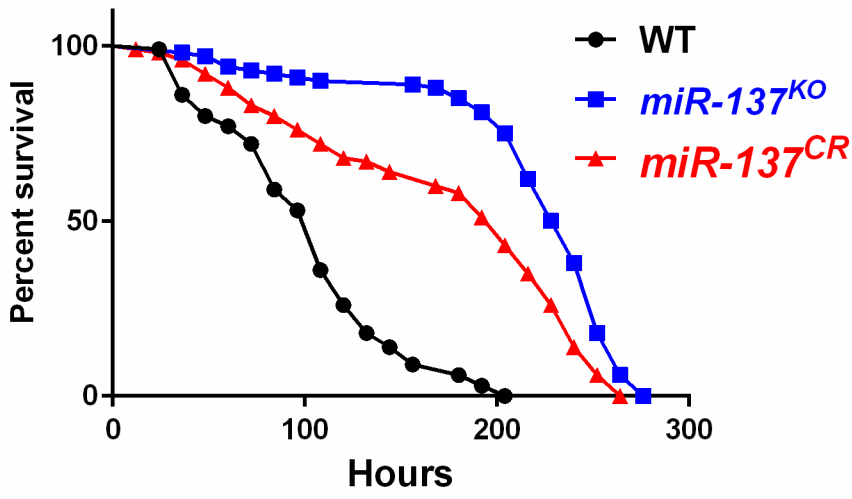

Figure 27. Loss of *miR-137* results in increased resistance to oxidative stress. Representative survival curves shown for populations (N=100) of male wild-type (WT; black), *miR-137*^{KO} (blue), and *miR-137*^{CR} (red), were exposed to 20% paraquat (see Materials and Methods). *miR-137*^{KO} and *miR-137*^{CR} lines displayed significantly extended lifespans compared to WT, as analyzed by Log-rank test ($P<0.0001$).

4.4 *miR-137* Mutants Exhibit Metabolic Dysfunction.

Stress triggers hormonal changes that coordinate numerous genetic, behavioral, physiological, and metabolic reactions that contribute to the ability to tolerate stress. In flies and fish, starvation resistance generally develops a reduced metabolic rate, greater energy conservation, and a larger body (Auer et al., 2018; Baldal et al., 2006b; E. B. Brown et al., 2019; Clark & Fucito, 1998). These results suggest that metabolic function and behavior contribute to starvation resistance seen in the flies. This led us to investigate the mechanism underlying the starvation resistance in *miR-137* mutants.

4.4.1 Loss of *miR-137* Impacts Body Weight/Size.

Energy homeostasis involves the complexity of balancing energy storage, energy expenditure, as well as nutrient consumption. Some studies have shown that extended survival is enabled by increased energy stores (Park et al., 2018). The starvation resistance of *miR-137* null mutants suggests an alteration in energy homeostasis. To test if the starvation resistance mediated by *miR-137* might be supported by enhanced energy storage, we first compared the size and body weight of *miR-137^{CR}, miR-137^{KO}, and miR-137$^{CR/KO}$* mutants to wild-type (*w^{1118}*). We measured the dry flyweight of batches of 15 male flies of wild-type and *miR-137* mutants were flash-frozen in the liquid nitrogen and weighed on an ultrasensitive balance. A total of 100-150 flies per genotype were measured. We found that *miR-137^{CR}, miR-137^{KO}, and miR-137$^{CR/KO}$* mutant flies exhibit a 23.8%, 28.1%, and 43% enhancement in body weight, respectively (Fig. 28). Thus, the lack of *miR-137* results in an obese phenotype. Studies showed that increased body size/weight is a fitness-related feature that promotes stress resistance (E. B. Brown et al., 2019). Our results suggest that increased body weight may contribute to the starvation stress resistance seen in *miR-137* mutants.

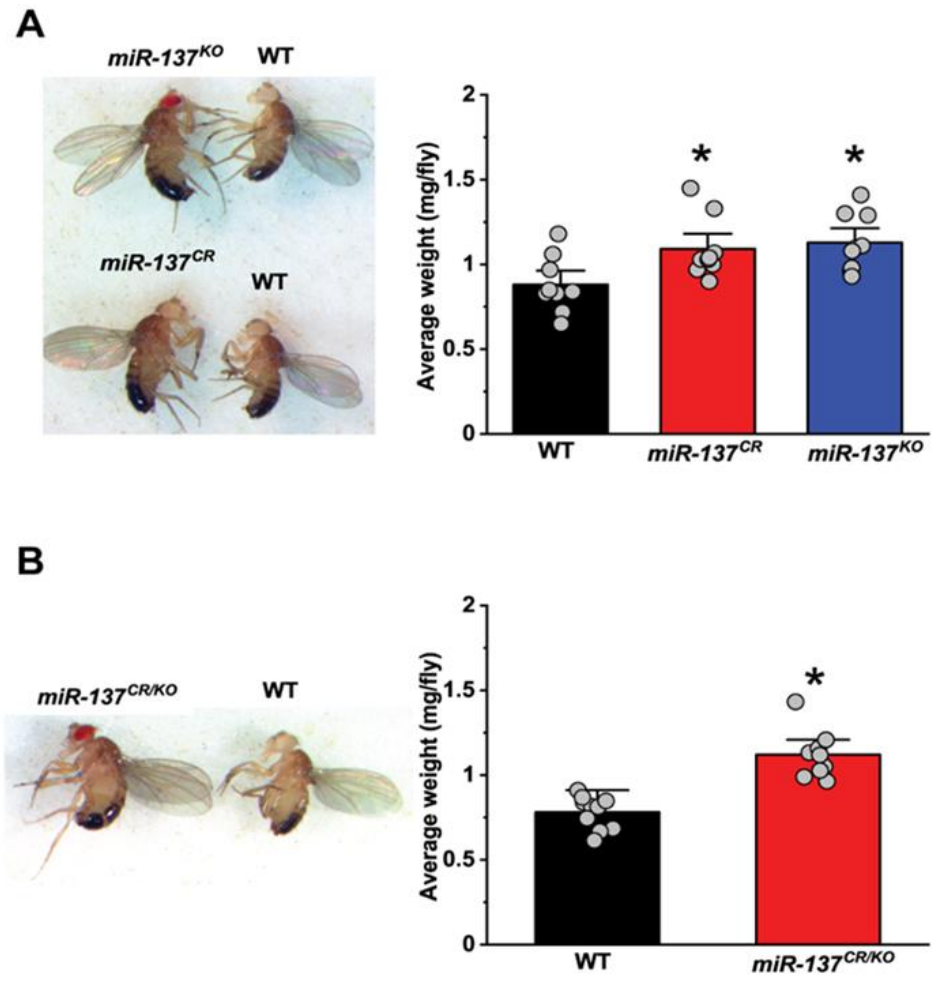

Figure 28. *miR-137* impact body weight/size. Males of wild-type (WT), *miR-137*^{CR}, and *miR-137*^{KO} (***A***). Males wild-type (WT) and *miR-137*$^{CR/KO}$ (***B***). Flies were aged for 7 days in a mixed population on a standard fly food diet, then tested for average body weight. *miR-137*^{CR}*, miR-137*^{KO}*,* and *miR-137*$^{CR/KO}$ mutant flies indeed exhibit a 23.8%, 28.1%, 43% enhancement in body weight, respectively, compared to WT. Shown are representative flies (***Left***). * Indicates significant differences (P<0.05) between the *miR-37*$^{CR/KO}$ and WT, or indicated conditions; data analyzed Student t-test. Error bars indicate SEM.

4.4.2 *miR-137* Mutants Exhibit an Increase in Energy Storage.

Survival during periods of nutrient deprivation is highly dependent on the capacity to retrieve energy from stored reservoirs to provide energy for cells (Baker & Thummel, 2007). In *Drosophila*, energy is stored mainly in the form of lipids and glycogen in the fat

body, which is a tissue functionally analogous to mammalian adipose and hepatic tissues (Baker & Thummel, 2007; Kühnlein, 2012). It has been reported that the amount of stored nutrients support survival under nutrient deprivation (Bharucha et al., 2008; Goenaga et al., 2013). As indicators of energy availability and storage, we examined triglyceride, glucose, and protein levels in individual samples of 5 whole male flies that were aged for 7 days on standard fly media (fed).

Under standard feeding conditions, triglyceride and cholesterol are broken down and absorbed by the intestine (Kozan et al., 2023). Cells either utilize these lipids or store them in fat body tissue. Triglyceride concentration was determined by incubating the samples with the triglyceride reagent, that will cleave triglyceride with lipoprotein lipase to release free glycerol and fatty acids. The triglyceride concentration in the samples is calculated based on the triglyceride standard curve. We found that *miR-137*$^{CR/KO}$ mutants displayed a significant elevation of 71.19% in the concentration of triglyceride content compared to *w1118* (Fig 29 A).

We also measured glucose levels as an indicator of readily available energy. Although trehalose is the major larval hemolymph sugar in adult flies, circulating trehalose and glucose both provide a source of energy through glycolysis (Tennessen et al., 2014). Glucose concentration was measured in the whole fly homogenate samples by a colorimetric-based enzymatic assay that measured the free glucose levels in the flies. The glucose concentration in the samples was calculated based on the glucose standard curve. We found that *miR-137*$^{CR/KO}$ mutants displayed a significant increase of 34.2% in the concentration of glucose compared to *w*^{1118} (Fig 29 B).

In addition to lipids and glucose, proteins can also be catabolized to yield energy. Although protein is not the preferable form of energy storage, under conditions of long starvation, protein has been shown to serve as a source of energy (Chatterjee & Perrimon, 2021; Marron et al., 2003a). Protein concentration was determined by incubating the samples with the BCA protein assay. The protein concentration in the samples was calculated based on the protein standard curve. Our results showed that *miR-137*$^{CR/KO}$ mutants displayed a significant elevation of 21% in the concentration of protein content compared to *w*^{1118} (Fig 29 C).

These results suggest that *miR-137* plays an important role in metabolic homeostasis, such that mutant flies store more energy in reserves, consequently supporting extended survival under nutrient restriction.

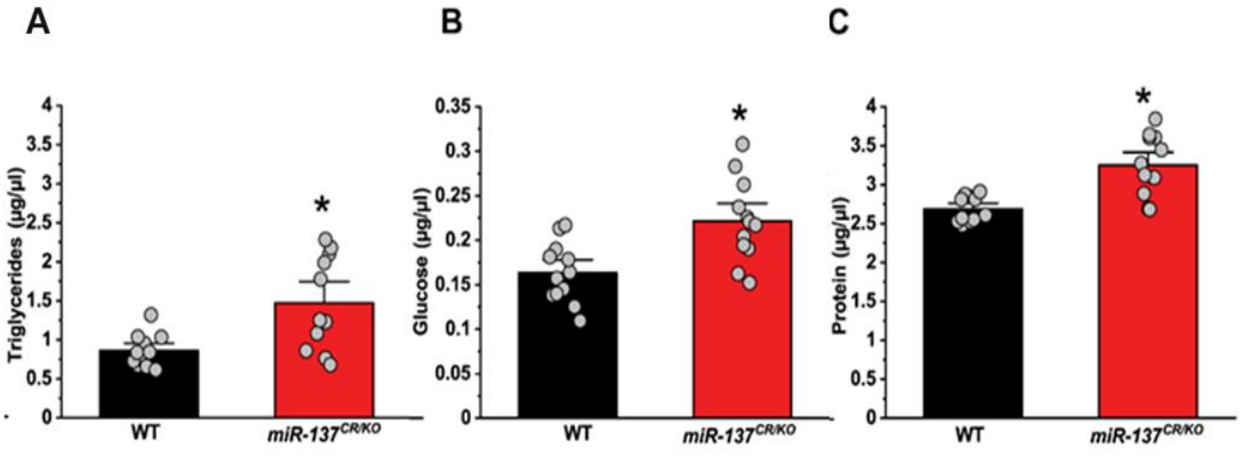

Figure 29. *miR-137* mutants exhibit altered energy storage. Wild-type (WT) and *miR-137*$^{CR/KO}$ male flies were aged for 7 days in a mixed population on a standard fly food diet, then tested for: ***A***, triglyceride content; **B**, glucose content; ***C***, protein content. Results from representative experiments *miR-137*$^{CR/KO}$ mutants displayed a significant elevation of 71.19%, 34.2%, 21% in the concentration of triglyceride, glucose, and protein contents, respectively, compared to *w*^{1118}. * Indicates significant differences ($P<0.05$) between the *miR-137*$^{CR/KO}$ and WT or indicated conditions; data analyzed Student t-test. Error bars indicate SEM.

4.4.3 *miR-137* Mutants Exhibit a Decrease in Food Intake.

Feeding behavior in *Drosophila* is a process that depends on motivation and sensory detection (Pool & Scott, 2014). The physiological drop in the fly's energy stores releases hunger signals that drive feeding motivation (Pool & Scott, 2014). After satiation, negative feedback in the CNS occurs to terminate the feeding and decrease the response to the food stimulation (Edgecomb et al., 1994). Studies have shown that animals respond to starvation by reducing their feeding and increasing their sleep to survive prolonged starvation (Masek et al., 2014). We examined whether *miR-137* mutants exhibit any difference in food consumption or motivated feeding behavior. We tested *miR-137^{CR}, miR-137^{KO}*, and wild-type flies. We aged flies for 7 days on standard fly food, then either kept them fed on standard food or starved them for 18 hrs before transferring them to 1% agar media containing 5% sucrose and 2.5% erioglaucine, an acid aminotriphenylmethane dye with a blue color that has been used to track the feeding of flies (Park et al., 2018). After 15 minutes, flies were homogenized and tested for the intensity of blue dye content as a measure of food consumption. We found that wild-type flies exhibited a dramatic increase in feeding following starvation (Fig. 30A), as expected from previous reports (Park et al., 2018), while *miR-137^{CR}* and *miR-137^{KO}* mutants displayed significantly less feeding than wild-type. To minimize the genetic background variation between *miR-137^{CR} and miR-137^{KO},* we also tested *miR-137$^{CR/KO}$* mutants. These *miR-137$^{CR/KO}$* flies also exhibited a near-complete lack of starvation-induced feeding (Fig. 30B). Together, our results suggest that the loss of *miR-137* results in reduced motivation to feed even after starvation.

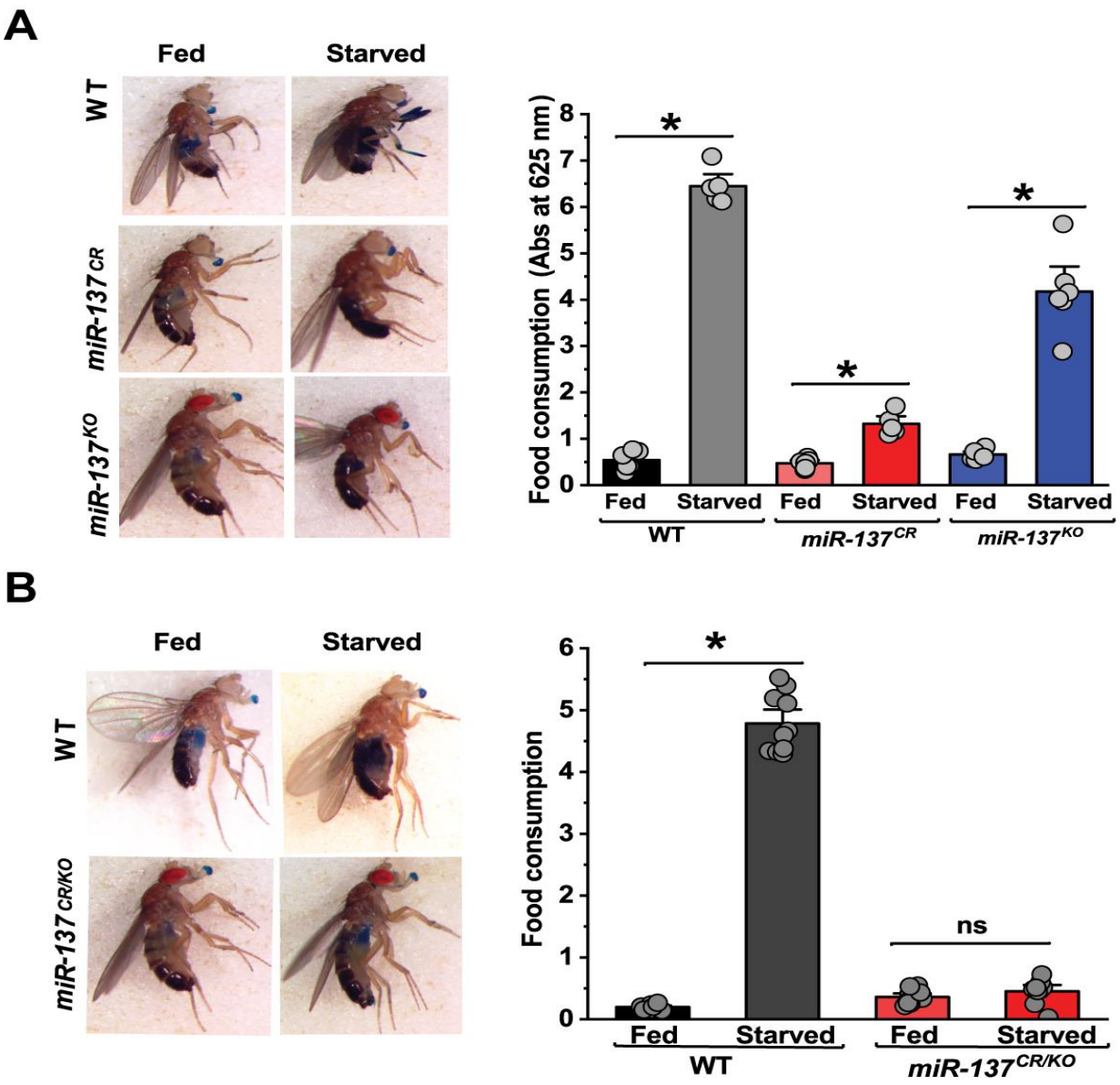

Figure 30. *miR-137* mutants exhibit altered energy homeostasis. 7-day old WT *miR-137^{CR}*, *miR-137^{KO}* (***A***), and *miR-137$^{CR/KO}$* (***B***) flies were Fed or Starved for 18 hrs prior to exposure to food containing a blue-dye (see Materials and Methods) for 15 minutes. Shown are representative flies with blue coloring seen in their abdomens (***Left***) and quantification (Absorbance read at 625 nm) of fly homogenates. * Indicates significant differences (P<0.05) between the *miR-137^{CR}*, *miR-137^{KO}*, *miR-137$^{CR/KO}$* and WT indicated conditions; data analyzed Student t-test. Error bars indicate SEM.

4.5 Conclusion.

In conclusion, male and female *miR-137* mutants showed increased resistance to starvation and oxidative stress. Mutant survival was almost double that of control flies under starvation and oxidative stress. *miR-137* mutants consumed less food than the controls after prolonged starvation, suggesting that these animals are less motivated to feed. In addition, *miR-137* mutants exhibit increased energy storage in the form of lipids, glucose, and protein, consistent with the increase in body weight. All of these phenotypes correlate with the extended survival of *miR-137* mutants under conditions of nutrient deprivation. According to these findings, *miR-137* plays a role in regulating metabolic adaptation during nutrient deprivation.

CHAPTER 5: STARVATION RESISTANCE OF miR-137 MUTANTS REQUIRES THE INSULIN SIGNALING PATHWAY.

5.1 Overview.

Genetic epistasis is a technique to characterize the relationship of two mutants that have a single phenotype, and specifically, to determine if they affect the same signaling pathway (Huang., 2006). The viability of loss-of-function mutants, like *miR-137,* make them amenable for genetic epistasis analysis. We hypothesized that the role of *miR-137* in energy homeostasis is likely to involve either the glucagon-like Adipokinetic hormone (Akh) and/or insulin signaling pathway, since both play critical roles in coordinating nutrient availability with metabolism across species. To explore if there is a pattern of epistatic interaction between *miR-137* and genes associated with the insulin or AKH signaling pathways, we constructed double mutant lines with genes associated with either of the pathways. These mutants have previously been reported to exhibit a similar phenotype to *miR-137*. If double-mutants exhibit an “additive” phenotype with starvation resistance increased beyond either single mutant, this would suggest that *miR-137* and a given component act in different pathways. However, if double-mutants exhibit starvation resistance similar to the single *miR-137* mutants, this would suggest that *miR-137* and a given component act in the same pathway. Here, we describe genetic epistasis experiments to determine in which metabolic pathways *miR-137* is required for starvation resistance.

5.2 Epistasis Analysis of *miR-137* And the Glucagon-Like Adipokinetic Hormone (AKH).

A polypeptide with a glucagon-like function (AKH) and its receptor AKHR are essential for normal behavioral and physiological responses to starvation. AKH is released during starvation conditions to signal the breakdown of glycogen stores and promote survival. *Akh*^{1} is a null mutant that carries a deletion in the AKH gene. The disruption in AKH signaling in *Akh*^{1} produces a slightly heavy fly with a lower metabolic rate and extended survival under starvation conditions (Lee & Park., 2004). The increased resistance to starvation in *Akh*^{1} is also accompanied by the absence of starvation-induced hyperactivity and increased energy reserves (Lee & Park., 2004). Since our results suggest that *miR-137* mutants also exhibit increase in energy reserves, and a lack of starvation-induced hyperactivity (data not shown; courtesy of Lea Giacchetta) we wanted to identify if AKH and *miR-137* act in the same pathways.

We tested the involvement of the AKH pathway in the starvation resistance response by generating *Akh*^{1} and *miR-137* double-mutant flies and comparing the starvation-resistant phenotype to that of each single mutant. We first tested single null mutants for *miR-137* and *Akh*^{1} for survival under starvation conditions. We found that each exhibited prolonged survival under starvation conditions with a median survival of 72 hrs for *miR-137*^{CR}, 84 hrs for *miR-137*^{KO} and *Akh*^{1} (Fig 31). We then generated double-mutants in which *miR-137*^{CR} or *miR-137*^{KO} mutations were combined with *Akh*^{1}. If double-mutants exhibit an “additive” phenotype with starvation resistance increased beyond either single mutant, this would suggest that *miR-137* and AKH act in different pathways, however, if double-mutants exhibit starvation resistance similar to the single *miR-137*

mutants, this would suggest that *miR-137* and AKH act in the same pathway. We found that the lifespan of either *miR-137*^{CR} and *miR-137*^{KO} mutations combined with the *Akh*^{1} mutation exhibited starvation resistance that was significantly enhanced beyond that of either single mutant (*miR-137*^{KO}+ *Akh*^{1} was 96 hrs, and *miR-137*^{CR} + *Akh*^{1} was 96 hrs) (Fig. 31). These results suggest that the function of *miR-137* in energy homeostasis is independent of the AKH pathway.

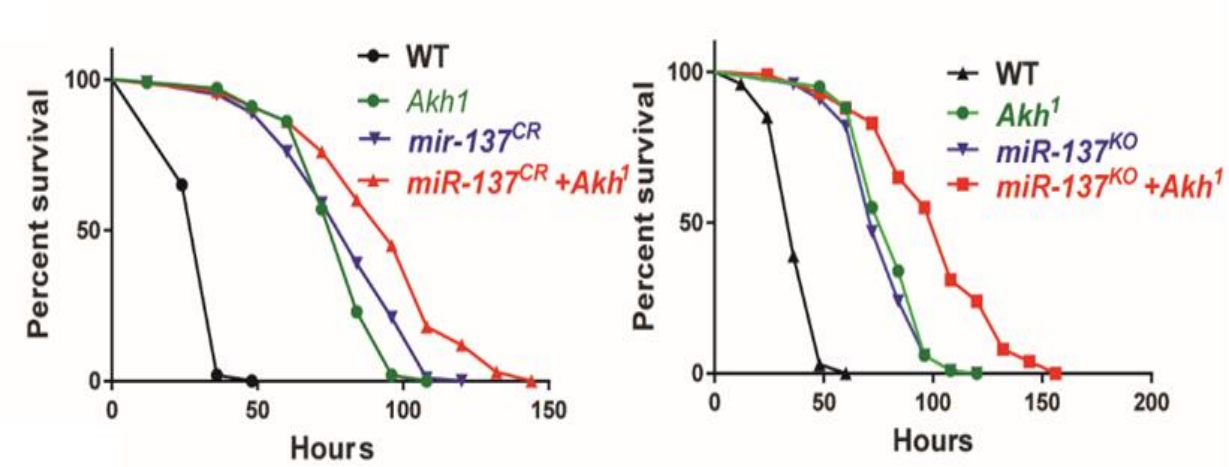

Figure 31. Genetic epistasis analyses of *miR-137* and the glucagon-like Adipokinetic hormone (AKH). Survival curves of single mutations of the AKH pathway under conditions of total starvation (see Materials and Methods). Survival curves of *Akh*^{1}combined with either the *miR-137*^{CR} **(*Left*)** or *miR-137*^{KO} **(*Right*)** mutations are shown to evaluate genetic epistasis; *miR-137*^{CR} and *miR-137*^{KO} backgrounds are also shown for comparison in each graph. *Akh*^{1} mutants (green) exhibit a significantly extended lifespan, similar to *miR-137*^{CR} and *miR-137*^{KO} (blue), when compared to wild-type (WT). *miR-137*^{CR}; *Akh*^{1} (*miR-137*^{CR}+*Akh*^{1}) and *miR-137*^{KO}; *Akh*^{1} (*miR-137*^{KO}+*Akh*^{1}) double mutants (red lines) show a lifespan extended significantly beyond the single *miR-137*^{CR}, *miR-137*^{KO}, and *Akh*^{1} mutants. Representative survival curves are shown from a population of 100 males. Significance between survival curves, evaluated by the Log-rank test ($P<0.05$), as noted in the legend.

5.3 Epistasis Analysis of *miR-137* in the Insulin Signaling Pathway.

We next wanted to test for a requirement of the insulin signaling pathway in the *miR-137*-mediated starvation resistance phenotype by genetic epistasis. Insulin plays a

major role in energy homeostasis. Defects in insulin signaling cause diabetes, obesity, accumulation of fat, and many metabolic disorders (Rehman & Varghese, 2021a). Manipulation of IIS/TOR signaling has been reported to dramatically influence the metabolic processes in an organism and affecting lipid and glucose homeostasis (Kannan & Fridell, 2013; Semaniuk et al., 2021; Tatar et al., 2003).

We tested a null mutant for the single insulin receptor substrate protein (IRS), *chico*, for survival under starvation conditions. We found that *chico*^{1} mutants, which have been shown to disrupt insulin signaling (Clancy et al., 2001), exhibited prolonged survival under starvation conditions (Fig. 32). Since *chico*^{1} is on the second chromosome as is *miR-137*, we examined *chico*^{1}*/CyO* heterozygotes which exhibit a significant, albeit less extreme, starvation resistance (Fig. 32). We then generated trans-heterozygous double-mutants in which *miR-137*^{CR} or *miR-137*^{KO} mutations were carried over the *chico*^{1} mutation. If double-mutants exhibit an “additive” phenotype with starvation resistance increased beyond either single mutant, this would suggest that *miR-137* and *chico* act in different pathways, however, if double-mutants exhibit starvation resistance similar to the single *miR-137* mutants, this would suggest that *miR-137* and *chico* act in the same pathway. We found that the lifespan of *chico*^{1}*/miR-137*^{CR} and *chico*^{1}*/miR-137*^{KO} transheterozygote double-mutants exhibited no enhancement in starvation resistance beyond that of *chico*^{1}*/CyO*, *miR-137*^{CR}*/+*, or *miR-137*^{KO}*/+* heterozygote backgrounds (Fig. 32). Our results suggest a genetic interaction between *miR-137* and the insulin signaling pathway.

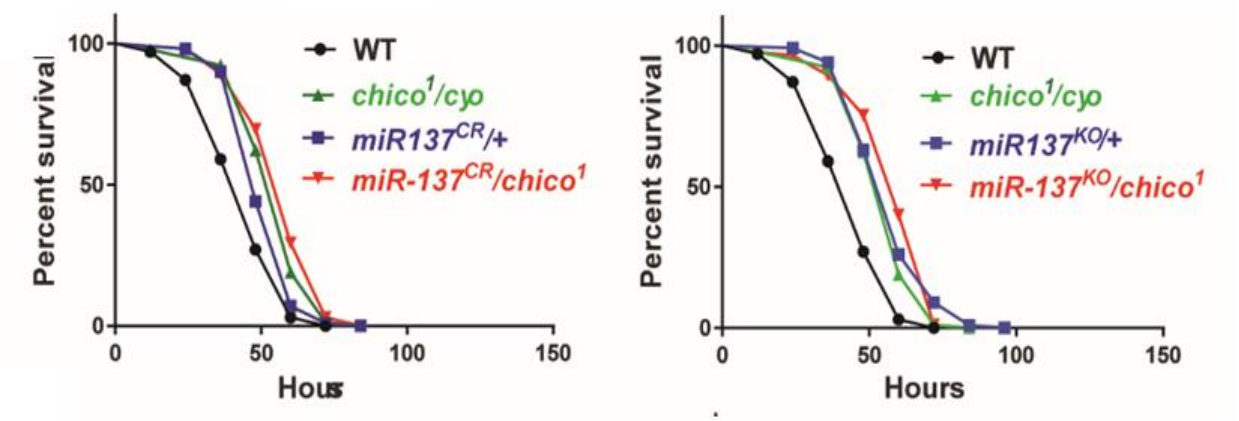

Figure 32. Genetic epistasis analyses indicate that starvation resistance of *miR-137* involves the insulin signaling pathway. Survival curves of single gene mutations are shown under conditions of total starvation (see Materials and Methods). Survival curves of mutations combined with either the *miR-137^{CR}* (***Left***) or *miR-137^{KO}* (***Right***) mutations are shown to evaluate genetic epistasis; *chico^{1}/CyO* heterozygotes (green), *miR-137^{CR}/+* and *miR-137^{KO}/+* heterozygotes (blue), and *miR-137^{CR}/chico^{1}* and *miR137^{KO}/chico^{1}* (red) all show similar (not significantly different) lifespans, but all significantly extended compared to WT. Representative survival curves are shown from a population of 100 males. Significance between survival curves, evaluated by the Log-rank test ($P<0.05$), as noted in the legend.

5.4 Epistasis analysis of *miR-137* and insulin signaling in the CNS.

We further tested if the *miR-137*-mediated starvation resistance phenotype is due to its interaction with insulin signaling specifically in the nervous system. We employed the UAS-GAL4 system to attain tissue-specific gene expression. We pan-neuronally expressed dominant-negative (DN) and/or RNAi transgenes that target the insulin receptor InR, the downstream effector phosphoinositide-3-kinase PI3K, or the downstream protein kinase B, AKT. To do this, we used *elav-Gal4* to drive *UAS-InR^{DN}*, *UAS-InR-RNAi*, *UAS-PI3K^{DN}*, or *UAS-AKT-RNAi*. Each of these lines exhibited starvation resistance compared to genetic background control lines (Fig. 33), demonstrating that disruption of insulin signaling in the CNS alone is sufficient to mimic the starvation

resistance phenotype of *miR-137* mutants. We then performed genetic epistasis experiments by combining each of these DN/RNAi lines with the *miR-137*^{CR} or *miR-137*^{KO} mutations and testing for starvation resistance. The rationale of these epistasis experiments was to investigate if the knockdown of InR, PI3K, or AKT in the CNS is relevant to starvation resistance of *miR-137* mutants. We found that the starvation resistance of each of these combined lines was not significantly enhanced compared with parental lines with disrupted insulin signaling alone (Fig. 33). These results suggest that the starvation resistance of *miR-137* involves the insulin signaling pathway in the CNS.

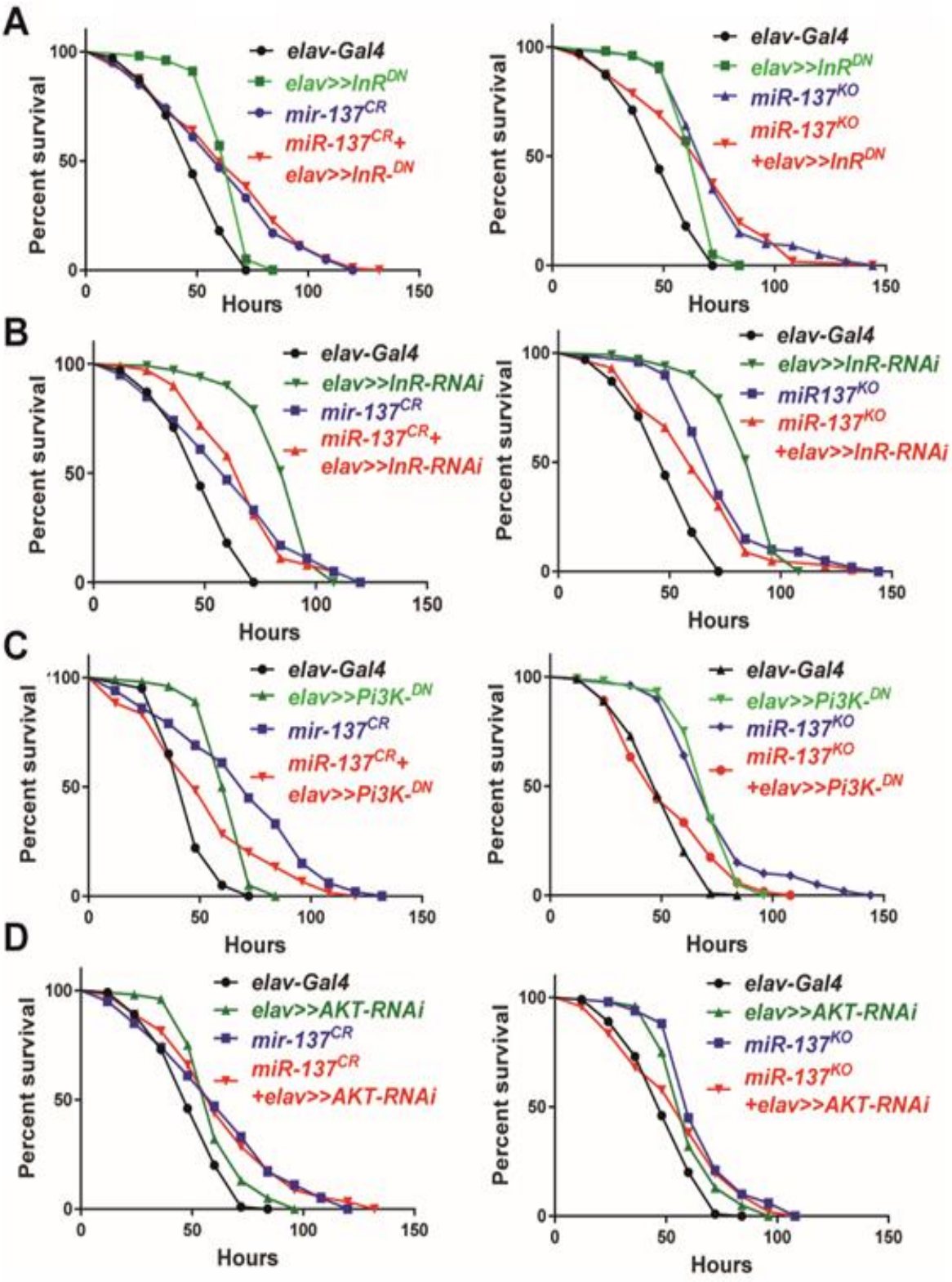
A
Percent survival
Hours
elav-Gal4
elav>>InR^DN
mir-137^CR
miR-137^CR+
elav>>InR-^DN
elav-Gal4
elav>>InR^DN
miR-137^KO
miR-137^KO
+elav>>InR^DN
B
elav-Gal4
elav>>InR-RNAi
mir-137^CR
miR-137^CR+
elav>>InR-RNAi
elav-Gal4
elav>>InR-RNAi
miR137^KO
miR-137^KO
+elav>>InR-RNAi
C
elav-Gal4
elav>>Pi3K-^DN
mir-137^CR
miR-137^CR+
elav>>Pi3K-^DN
elav-Gal4
elav>>Pi3K-^DN
miR-137^KO
miR-137^KO
+elav>>Pi3K-^DN
D
elav-Gal4
elav>>AKT-RNAi
mir-137^CR
miR-137^CR
+elav>>AKT-RNAi
elav-Gal4
elav>>AKT-RNAi
miR-137^KO
miR-137^KO
+elav>>AKT-RNAi

Figure 33. Genetic epistasis analyses indicate that starvation resistance of *miR-137* involves the insulin signaling pathway in the CNS. Survival curves of single mutations, or specific gene knockdowns, are shown for components of the insulin pathway (***A-D***) under conditions of total starvation (see Materials and Methods). Survival curves of these mutations/RNAi lines combined with either the *miR-137^{CR}* (***Left* column**) or *miR-137^{KO}* (***Right* column**) mutations are shown to evaluate genetic epistasis; *miR-137^{CR}* and *miR-137^{KO}* backgrounds are also shown for comparison in each graph. The parental *elav-Gal4* line is used as a control, and lines in which *elav-Gal4* is used to drive expression of an *UAS-* dominant-negative *InR^{DN}* subunit (***A***), an *UAS-InR-RNAi* (*InR-RNAi*) transgene (***B***), an *UAS-* dominant-negative *PI3K^{DN}* (*PI3K^{DN}*) transgene (***C***), an *UAS-AKT-RNAi* (*AKT-RNAi*) transgene (***D***) are shown for survival under total starvation conditions; *miR-137^{CR}* and *miR-137^{KO}* lines are shown again for reference. In all cases (***A-D***), the lines containing *miR-137^{CR}* (***Left***) or *miR-137^{KO}* (***Right***) combined with knockdown of components of the insulin signaling pathway in the nervous system all showed significant extension of lifespan (starvation resistance) compared to the *elav-Gal4* parental line, but no difference with *miR-137* mutations or knockdowns alone. Representative survival curves are shown from a population of 100 males. Significance between survival curves, evaluated by the Log-rank test ($P<0.05$), as noted in the legend.

5.5 Starvation Resistance of *miR-137* Mutants is Normalized by the Activation of the Insulin Signaling Pathway in the Nervous System.

We next tested if the *miR-137* starvation resistance phenotype could be reversed by activation of insulin signaling pathway. To do this, we used genetic tools to increase the activation of the insulin signaling pathway specifically in the nervous systems of *miR-137^{CR}* and *miR-137^{KO}* null mutants. We used *elav-Gal4* to induce expression of *UAS*-driven transgenes that would likely increase the insulin signaling. These transgenes encoded ligands of *Drosophila* insulin-like peptide, *dilp2* and *dilp5*, a constitutively active form of *InR* (*InR^{CA}*), *PI3K*, and *AKT*. Analysis of the survival curves showed that expression of any one of these was sufficient to restore normal starvation sensitivity to each of the *miR-137* null mutant lines (Fig. 34). Interestingly, expression of wild-type *InR* was not so clearly able to restore starvation sensitivity to *miR-137* mutants (Fig. 35), supporting the idea that it is increased activation of InR that is critical for this rescue.

These results indicate that activation of the insulin signaling pathway in the brains of *miR-137* mutants was sufficient to restore starvation sensitivity to these mutants.

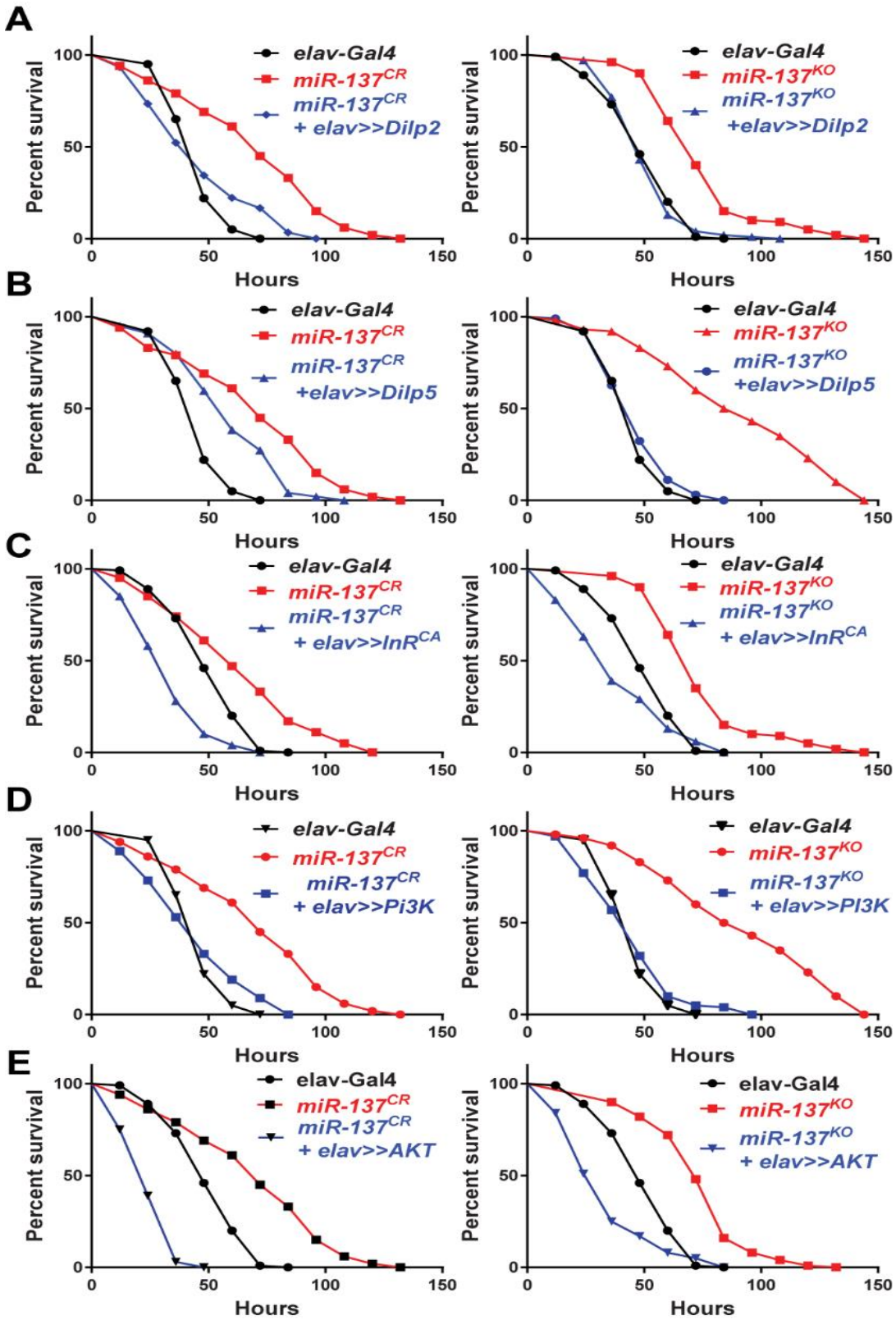
A
Percent survival
Hours
elav-Gal4
miR-137CR
miR-137CR
+ elav>>Dilp2
elav-Gal4
miR-137KO
miR-137KO
+elav>>Dilp2
B
elav-Gal4
miR-137CR
miR-137CR
+elav>>Dilp5
elav-Gal4
miR-137KO
miR-137KO
+elav>>Dilp5
C
elav-Gal4
miR-137CR
miR-137CR
+ elav>>InRCA
elav-Gal4
miR-137KO
miR-137KO
+ elav>>InRCA
D
elav-Gal4
miR-137CR
miR-137CR
+ elav>>Pi3K
elav-Gal4
miR-137KO
miR-137KO
+ elav>>PI3K
E
elav-Gal4
miR-137CR
miR-137CR
+ elav>>AKT
elav-Gal4
miR-137KO
miR-137KO
+ elav>>AKT

Figure 34. Starvation resistance of *miR-137* is reversed by activation of the insulin signaling pathway in CNS. Representative survival curves for genotypes over-expressing components of the insulin signaling pathway in the *miR-137^{CR}* (***Left column***) or *miR-137^{KO}* (***Right column***) backgrounds, under conditions of total starvation; survival curves for the parental *elav-Gal4* (black), *miR-137^{CR}* or *miR-137^{KO}* (red) lines are shown on each graph for comparison. *elav-Gal4* was used to drive pan-neuronal expression of insulin signaling components (blue), including ***A***, *UAS-Dilp2*; ***B***, *UAS-Dilp5*; ***C***, a constitutively active InR^{CA} subunit expressed from transgene, *UAS-InR^{CA}*; ***D***, *UAS-PI3K*; ***E***, *UAS-AKT*. In all cases, the survival curves of lines over-expressing insulin signaling components were shifted significantly to the left from those of *miR-137^{CR}* or *miR-137^{KO}* backgrounds, indicating the restoration of starvation sensitivity. Pairwise comparisons were evaluated by Log-rank tests, P<0.05.

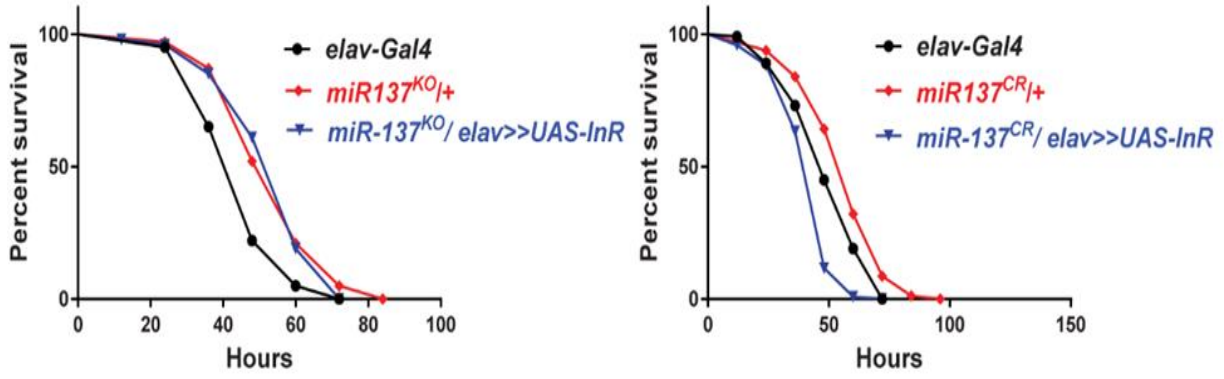

Figure 35. Expression of wild-type *InR* was not so clearly able to restore starvation sensitivity to *miR-137* mutants. Survival curves shown for lines pan-neuronally over-expressing of *UAS-InR* with one copy of *UAS-InR* in heterozygous *miR-137^{KO}/+* (***Left***) or *miR-137^{CR}/+* (***Right***) backgrounds (blue); parental *elav-Gal4* (black), *miR-137^{KO}/+* or *miR-137^{CR}/+* (red) backgrounds shown for comparison. In the *miR-137^{CR}/+* background, *elav>>InR* significantly shifted the survival curve to the left, restoring starvation sensitivity; in contrast, *miR-137^{KO}/elav>>InR* was not significantly different from *miR-137^{KO}/+*. Survival curves (N=100) from 7-day old males were evaluated by pairwise Log-rank tests; significance is as noted in legend.

5.6 Conclusion.

Genetic epistasis techniques are used to identify a functional interaction between genes within the same genetic pathway that results in a phenotype. In this study, single and double mutant lines were produced to characterize starvation resistance in *miR-137* mutants. Our comprehensive genetic epistasis analyses showed that the double mutants of *miR-137* and a mutation in the AKH pathway enhanced the starvation resistance beyond either single mutation, while the double mutants of *miR-137* and mutants affecting the insulin signaling pathway resulted in starvation resistance phenotypes similar to either single mutation. Moreover, we showed that the starvation resistance of *miR-137* was rescued by activation of the insulin signaling pathway, specifically in the CNS. These results provide strong evidence that a decrease in the insulin signaling pathway is responsible for the starvation resistance phenotype of the *miR-137* mutant.

CHAPTER 6: INSULIN SIGNALING IN THE BRAIN IS DOWN-REGULATED IN miR-137 NULL MUTANTS.

6.1 Overview.

Insulin signaling regulates cellular growth, reproduction, lifespan, metabolic homeostasis, and stress resistance (Clark & Fucito, 1998; Enell et al., 2010; Loewith et al., 2002; Teleman et al., 2005a). In the fed state, like mammalian systems, *Drosophila* insulin-like peptides (Dilps) are secreted in response to nutrients and accumulate in the insulin-producing cells (IPCs) during nutrient deprivation (Géminard et al., 2009). Dilps bind the single insulin receptor (InR), resulting in receptor subunit trans-autophosphorylation. The activation of InR leads to the activation of the tyrosine kinase activity of InR and promotes additional phosphorylation of InR and the insulin receptor substrate (chico). Phosphorylation and binding of chico to InR provides a scaffold for subsequent signaling molecules that lead to the activation of PI3K and AKT. AKT phosphorylates the transcriptional activator, FOXO, inhibiting its import into the nucleus; conversely, under nutrient scarcity, insulin signaling is reduced, and FOXO is able to activate downstream target genes, including *4E-BP* (Barthel et al., 2005; Teleman et al., 2005). Our results from the epistasis analysis (Chapter 5) suggest that the starvation resistance of *miR-137* mutants is due to insulin signaling dysfunction. In this chapter, we addressed whether *miR-137* mutants exhibit changes in insulin signaling components and signaling in the *Drosophila* brain.

6.2 The Effect of the Loss of *miR-137* on mRNA Levels of Insulin Signaling Components.

We showed that *miR-137* mutants exhibit altered metabolic homeostasis and starvation phenotypes related to dysfunction of insulin signaling. The next question we wanted to address is whether the expression of any insulin signaling components are altered in the heads of *miR-137* mutants. We decided to analyze the mRNA levels of two of the three *Dilps* that are expressed in the brain, *Dilp-2* and *Dilp-5*, *InR*, *FOXO,* and *4E-BP* by RT-qPCR. Wild-type and *miR-137*$^{CR/KO}$ mutant flies were aged to 7 days old on normal food before heads were collected, and total RNA was isolated. We found that mRNA levels of *InR*, and *4E-BP* mRNAs, two known targets of the *FOXO* transcription factor (Puig et al., 2003; Teleman et al., 2005a), *Dilp-5,* and *FOXO*, were all down-regulated in the *miR-137*$^{CR/KO}$ mutant heads compared to wild-type controls (Fig. 36B-D). In contrast, *Dilp-2* was found to be up-regulated in *miR-137*$^{CR/KO}$ mutants (Fig. 36A). We also found that levels of *InR* and *4E-BP* were also down-regulated in the whole fly (Fig 36 F-G). These results suggested that insulin signaling was somehow altered in the absence of *miR-137*.

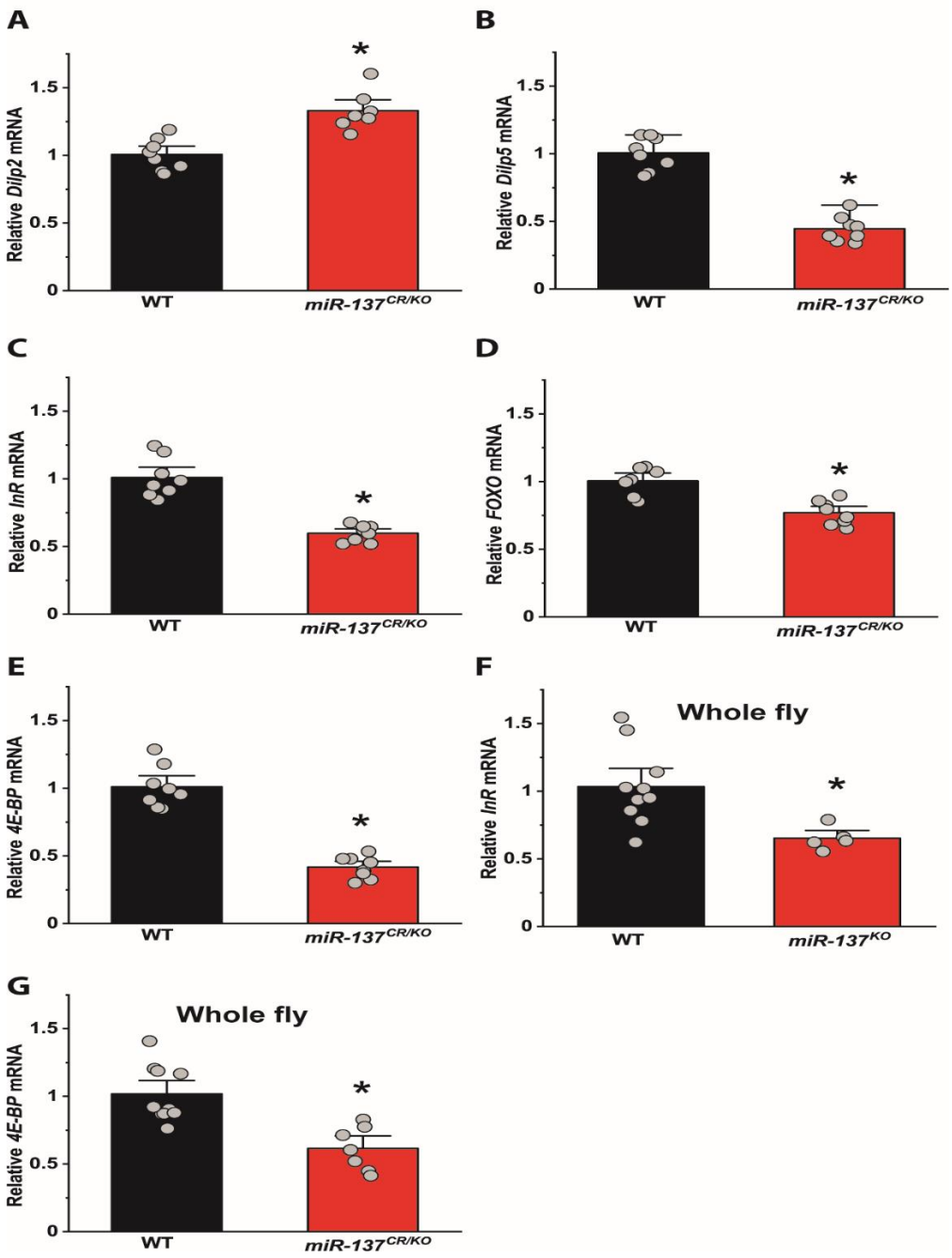

Figure 36. Insulin signaling is disrupted in *miR-137* mutants. *A-E*, Quantification of the relative expression of *Dilp2*, *Dilp5*, *InR*, *FOXO* and *4E-BP* by RT-qPCR from heads of 7-day old *miR137*$^{CR/KO}$ and wild-type (WT) males reared on standard food. ***F-G*** Quantification of the relative expression of *InR*, and *4E-BP* by RT-qPCR from whole fly of 7-day old *miR137*^{KO} and wild-type (WT) males reared on standard food. Data are represented as mean fold change +/- SEM (means are from N=7-8 independent RNA extractions and RT-qPCR); note that fold-changes are calculated in comparison to WT.

6.3 The Effect of the Loss of *miR-137* on Protein Levels of Insulin Signaling Components.

To gain further insight into how insulin signaling is changed in *miR-137* mutants, we set out to examine the activation of the insulin pathway more directly. To do this, we began by testing for levels of the activated/phosphorylated form of InR (in *Drosophila* Tyr1485; analogous to human Tyr1146 within the kinase activation loop), referred to as InR-P (Fernandez et al., 1995). Immunoblot analyses of protein extracts from heads and bodies of 7 days old flies that were raised on standard fly food showed that levels of InR-P were virtually abolished in *miR-137*^{CR} and *miR-137*^{KO} homozygotes and *miR-137*$^{CR/KO}$ trans-heterozygotes (Fig. 37A), indicating that insulin signaling is severely impaired in these mutant lines. Consistent with the semi-dominant starvation resistance phenotype we observed for *miR-137*$^{CR/+}$ and *miR-137*$^{KO/+}$ heterozygotes (Fig. 24), we observed a semi-dominant reduction in InR-P levels in *miR-137*$^{CR/+}$ and *miR-137*$^{KO/+}$ heterozygotes that was about halfway between levels observed in wild-type and *miR-137* null mutants (Fig. 37B). Additionally, we tested InR-P levels as result of *miR-137* overexpression. We used *elav-Gal4, tub-Gal80*^{ts} to drive the expression of *UAS-miR-137* post-development. Newly-eclosed flies were collected, divided into groups of 10 per vial, exposed to heat treatment at 30 °C for 7 days. Results showed that the overexpression of *miR-137* in the CNS showed normal levels of InR-P (Fig. 37C). Finally, we pan-neuronally expressed *UAS-miR-137* in the *miR-137*^{CR} background and tested whether we could rescue, or even partially rescue, levels of InR-P. We found that InR-P levels were elevated significantly, albeit to a small degree (Fig. 37D), suggesting that sub-wild-type levels of InR-P are responsive to *miR-137* expression.

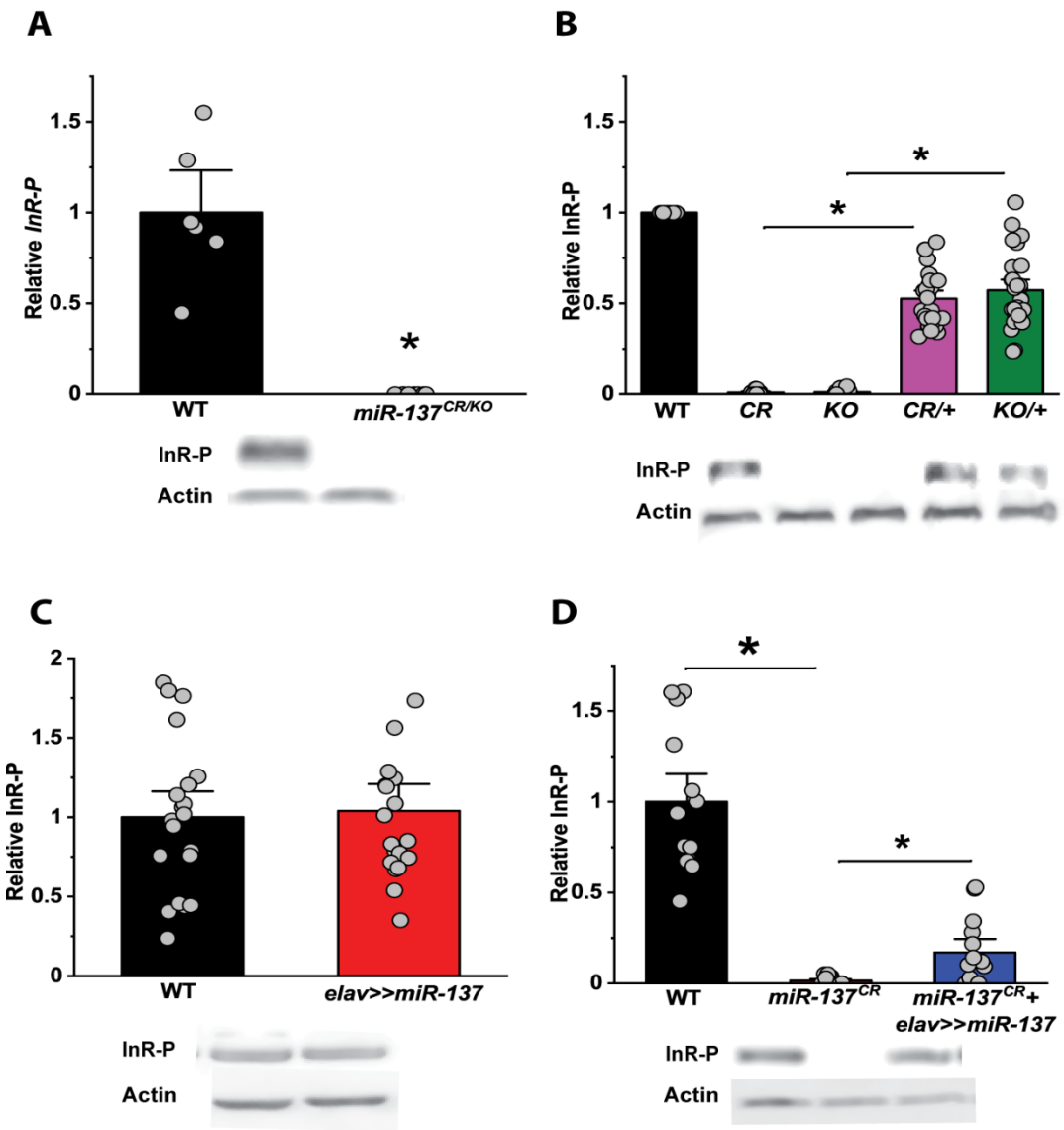

Figure 37. Sub-wild-type levels of InR-P are responsive to *miR-137* expression. *A-D*, Quantification and representative immunoblots of relative levels of InR-P from heads of 7-day old WT, *miR-137*$^{CR/KO}$ trans-heterozygotes, *miR-137*^{CR} (CR) and *miR-137*^{KO} (KO) homozygotes, as indicated. ***C***, Conditional over-expression of *miR-137* was achieved using *elav-Gal4* to drive *UAS-miR-137* in combination with *tub-Gal80*^{ts} (*elav-Gal4-Gal80*^{ts}*>>miR-137*); these flies were compared WT. Flies were raised at 18 °C for normal development, then shifted to 30 °C for 7 days to over-express *miR-137*. ***D***, Relative levels of InR-P also examined in a *miR-137*^{CR} background containing *UAS-miR-137* driven by *elav-Gal4* (*miR-137*^{CR} *+ elav>>miR-137*). Anti-InR-P levels are normalized to anti-actin, which was used as a loading control (N= 6-30 samples per genotype; 5 heads/sample); relative normalized levels are shown. *Significance indicated by *P<0.05*, Students t-test. Error bars indicate SEM.

To further investigate if insulin signaling was impaired in *miR-137* mutants, we tested total and activated/phosphorylated AKT levels. Immunoblot analyses of protein extracts from heads of 7 days old flies that were raised on standard fly food showed that levels of total AKT are not difference between *miR-137*$^{CR/KO}$ trans-heterozygotes and wild-type (Fig. 38A). Subsequently, we tested for levels of the phosphorylated form of AKT (in *Drosophila*, Ser505; analogous to human Ser473), referred to as AKT-P. We observed a significant reduction in activated AKT-P in *miR-137*$^{CR/KO}$ mutants (Fig. 38B). Since AKT can be activated by multiple signaling pathways, it is not surprising that the reduction in AKT-P is not as severe as we observed for InR-P.

Finally, we tested for levels of dFOXO, a down-stream target of the insulin signaling pathway that is involved in stress regulation. Immunoblot analyses of protein extracts from heads of 7 days old flies that were raised on standard fly food showed that despite the down-regulation of the AKT-P, the level of dFOXO also was down-regulated in *miR-137*$^{CR/KO}$ mutants (Fig. 38C). to sum up, these results suggest a general decrease in the activity of the insulin signaling pathway in the *miR-137* mutant.

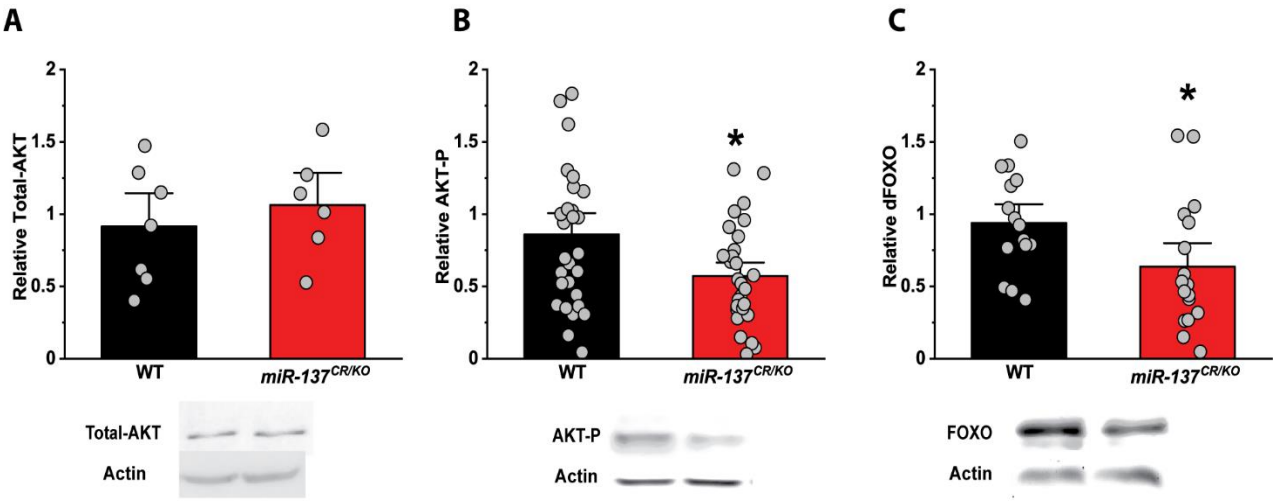

Figure 38. Insulin signaling is disrupted in *miR-137* mutants. Quantification and representative immunoblot of relative levels of AKT (***A***), AKT-P (***B***), and dFOXO (***C***) from heads of 7-day old WT and *miR-137*$^{CR/KO}$ trans-heterozygotes. Anti-AKT, Anti-AKT-P, and Anti-dFOXO levels are normalized to anti-actin, which was used as a loading control (N= 6-30 samples per genotype; 5 heads/sample); relative normalized levels are shown. *Significance indicated by *P<0.05*, Students t-test. Error bars indicate SEM.

6.4 *PTP61F* is a target *miR-137*.

The phenotype of miRNA mutants generally results from the up-regulation of one or multiple target genes. To search for predicted targets of *miR-137*, we used TargetScan (https://www.targetscan.org/), a well-established prediction algorithm that uses stringent seed pairing as a criteria across multiple genomes (Peterson et al., 2014; Ruby et al., 2006, 2007). We hypothesized that there must be a target(s) of *miR-137* that affects the activation/phosphorylation of the insulin receptor. Interestingly, predicted targets of *miR-137* by TargetScan, we found that one of the predicted targets of *miR-137* is the non-receptor protein tyrosine phosphatase *PTP61F*, the *Drosophila* homolog of mammalian *TC-PTP* and *PTP-1B*, which are known across species to negatively regulate insulin signaling by dephosphorylating InR (Tchankouo-Nguetcheu et al., 2014; Tiganis, 2013;

Willoughby et al., 2017b; C. L. Wu et al., 2011a). We further explored the possibility that *PTP61F* is a target of *miR-137 in vivo*.

6.4*.1 PTP61F* Overexpression Mimics *miR-137* Mutant Phenotypes

Since most miRNAs serve to dampen the expression of target mRNAs, we expect that if a particular miRNA is un-expressed, the protein that is normally regulated by that miRNA is likely to be over-expressed, while if the miRNA is over-expressed, levels of target(s) would expect to be reduced. We reasoned that if *PTP61F* is a target of *miR-137*, then *miR-137* null mutants would exhibit elevated levels of *PTP61F*, which would, in turn, result in hyper-dephosphorylation of InR. This scenario would be consistent with the low level of InR-P we observed in *miR-137* mutants (Fig. 37A).

First, we tested if overexpression of *PTP61F* would be sufficient to mimic the loss of InR-P and starvation resistance seen in *miR-137* mutants. Since *miR-137* is primarily expressed in the nervous system, we used *elav-Gal4* to drive overexpression of *UAS-PTP61F* in the nervous system and compared these flies to genetic background control lines. Indeed, we found that *elav-Gal4>>UAS-PTP61F* flies exhibited a near complete absence of InR-P (Fig. 39A), as well as an extended lifespan under conditions of nutrient deprivation (Fig. 39B). These results show that increased expression of *PTP61F* is sufficient to mimic the loss of insulin signaling and starvation resistance observed in *miR-137* null mutants.

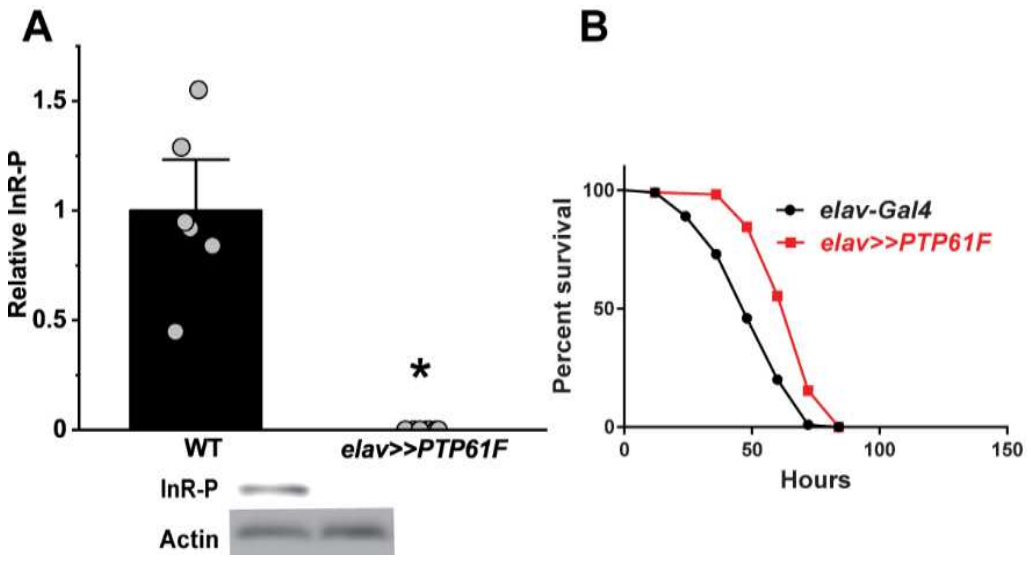

Figure 39. *PTP61F* overexpression mimics *miR-137* mutant phenotypes. Overexpression of *UAS-PTP61F* was driven pan-neuronally with the *elav-Gal4* transgene (*elav>>PTP61F*), resulting in the loss of relative InR-P levels (***A***) and significantly extended lifespan under total starvation conditions (***B***). For all immunoblot analyses, N= 6-9 samples were tested for each genotype (5 heads/sample); significance is indicated by *P<0.05, Students t-test, error bars represent SEM.

6.4.*2 PTP61F* Levels are Elevated in the Absence of *miR-137*.

To test more directly if *miR-137* regulates the expression of PTP61F *in vivo*, we set out to assay PTP61F in *miR-137* mutant flies. To detect endogenous levels of PTP61F, we used two independently generated fly lines in which an artificial exon, containing the coding sequence for GFP between splice acceptor and splice donor sequences (-SA-GFP-SD-) was inserted into an intron within the coding sequence of *PTP61F* such that GFP would be in-frame and fused to PTP61F (Venken et al., 2011). We verified that the resultant protein in these *GFP-PTP61F* flies was ~68 kD, consistent with the expression of a GFP-PTP61F fusion protein (PTP61F splice forms are predicted to have molecular weights ~48-62 kD). To test if the *GFP-PTP61F* is a target of *miR-137*

in vivo, we examined flies containing *GFP-PTP61F* and either of the *miR-137*^{CR} or *miR-137*^{KO} mutations. Immunoblot analyses of protein extracts from heads of 7 days old flies that were raised on standard fly food showed that levels of *GFP-PTP61F* were indeed significantly elevated in the absence of *miR-137* (Fig. 40A-B). To validate these results further, we tested the other line for *GFP-PTP61F*. As expected, we found that this line also exhibits up-regulation of *GFP-PTP61F* in the absence of *miR-137* (Fig. 40C). Together, these results suggest that *PTP61F* is a canonical target of *miR-137* that links *miR-137*-mediated effects on insulin signaling, metabolic homeostasis, and starvation resistance.

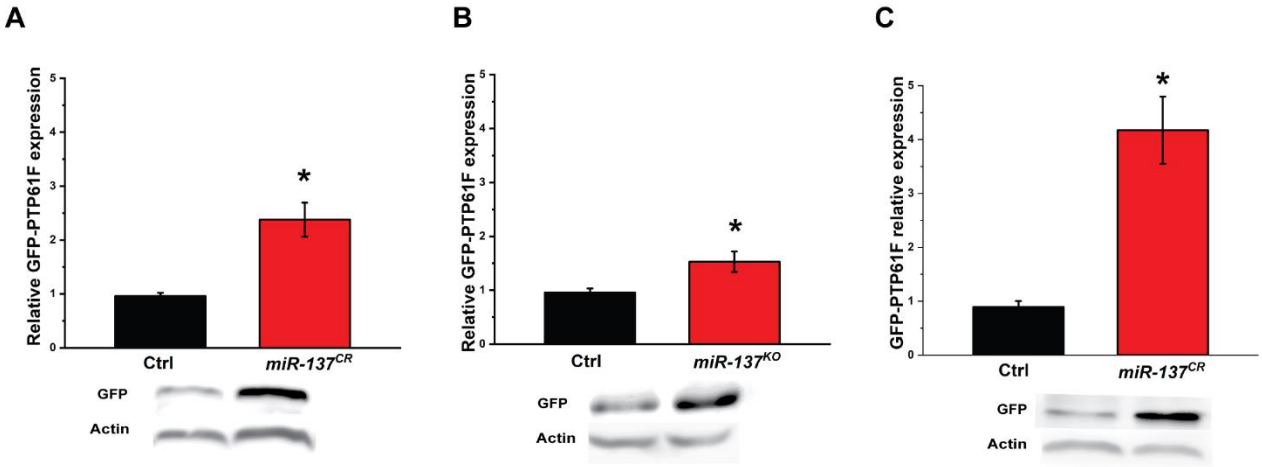

Figure 40. *PTP61F* is regulated by *miR-137 in vivo*. Two independent lines of endogenously GFP-tagged PTP61F (GFP-PTP61F-1 and GFPPTP61F-2) were tested without (Ctrl) and with the *miR-137*^{CR} (***A***), *miR-137*^{KO} (***B***), *miR-137*^{CR} (***C***). Quantification and representative immunoblot for relative anti-GFP levels normalized to anti-actin show that GFPPTP61F levels are increased in *miR-137*^{CR} and *miR-137*^{KO} mutants. For all immunoblot analyses, N= 6-31 samples were tested for each genotype (5 heads/sample); significance is indicated by *P<0.05, Students t-test, error bars represent SEM.

We also measured the relative mRNA of *PTP61F* in *miR-137*$^{CR/KO}$ mutants and wild-type. Wild-type and *miR-137*$^{CR/KO}$ mutant flies were aged to 7 days old on normal

food before heads were collected, and total RNA was isolated. Contrary to the elevation in GFP-PTP61F protein levels, we found that mRNA levels of *PTP61F* were down-regulated in the *miR-137*$^{CR/KO}$ mutant heads compared to wild-type controls (Fig. 41). One possibility is that *PTP61F* is differentially regulated by *miR-137* such that *miR-137* increases the stability of *PTP61F* mRNA but represses translation of *PTP61F*.

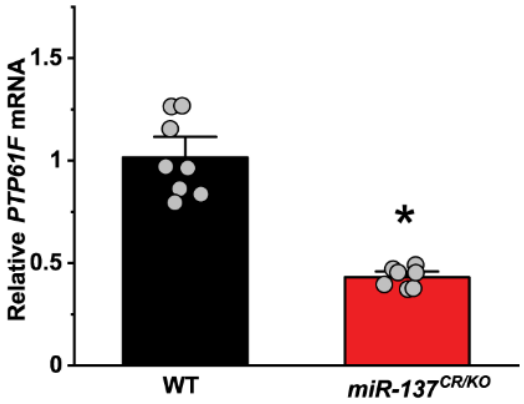

Figure 41. *PTP61F* mRNA is down-regulated in the *miR-137* mutants. RT-qPCR for PTP61F mRNA levels in WT and *miR-137*$^{CR/KO}$ trans-heterozygotes. Data are represented as mean fold-change +/- SEM (means are from N=7-8 independent RNA extractions and RT-qPCR); note that fold-changes are calculated in comparison to WT. *P<0.05, Students t-test, error bars represent SEM.

6.5 Testing for the Rescue of *miR-137* Mutant Phenotypes by Knockdown of *PTP61F*.

PTP61F has been identified to dephosphorylate the insulin receptor in *Drosophila* (C. L. Wu et al., 2011b). Previously, we showed that *miR-137* mutants have reduced insulin signaling characterized by a severe reduction in the phosphorylated InR (Fig. 37A), which may mediate the metabolic phenotypes shown in the *miR-137* mutant flies. Since we found up-regulation of *PTP61F* levels in *miR-137* mutants (Fig. 40), our next goal was to test whether the up-regulation of *PTP61F* in *miR-137* mutants could be mitigated by

RNAi knockdown of *PTP61F* in the CNS to restore a wild-type phenotype to *miR-137* mutants.

6.5.1 InR-P

We first tested if expression *PTP61F-RNAi* alone would result in a detectable increase in InR-P as expected. We used *elav-Gal4* to drive the expression of *UAS-PTP61F-RNAi* in the nervous system and compared these flies to wild-type controls. Immunoblots analysis was performed on protein extracts from heads of 7-day old flies that were raised on standard fly food. We were surprised, however, to find that *elav-Gal4>>PTP61F-RNAi* flies exhibited severely reduced levels of InR-P (Fig. 42A). To confirm that this was indeed due to the loss of *PTP61F*, we also examined *PTP61F*Δ null mutants. Similarly, we found severely reduced levels of InR-P (Fig. 42B). These results suggest that the InR-P regulation by *PTP61F* expression is likely to be complicated and may suggest that there is a compensatory up-regulation of another phosphatase when *PTP61F* levels are reduced.

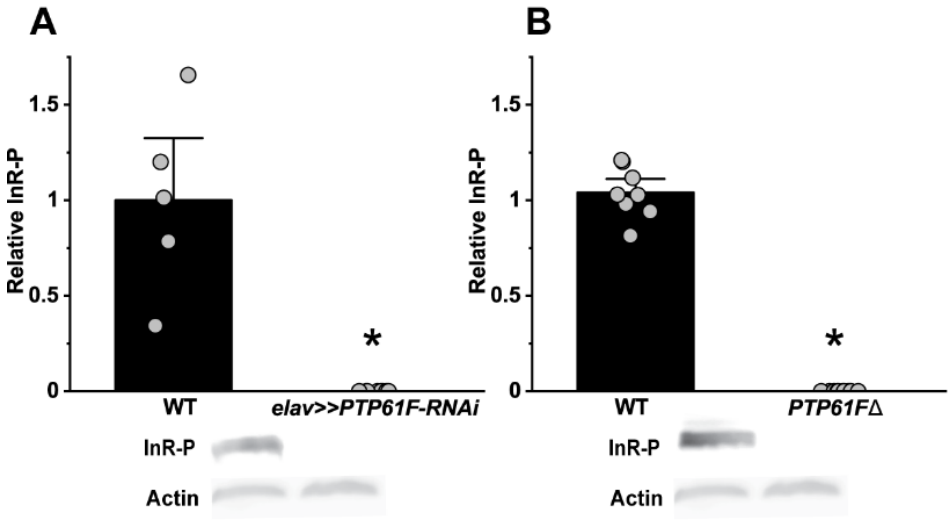

Figure 42. InR-P is down-regulated in the *PTP61F* mutants. Quantification and representative immunoblots for relative levels of InR-P in lines with PTP61F knock-down ***A,*** (*elav>>PTP61F-RNAi* heterozygotes), ***B,*** (*PTP61F*Δ homozygote), compared to wild-type (WT). Immunoblot analyses are as described in Materials and Methods (N= 5-16 samples for each genotype; 5 heads/samples). *P<0.05, Students t-test, error bars represent SEM.

Even with these unexpected results, we decided to test if *PTP61F-RNAi* knockdown in a *miR-137* mutant background would restore InR-P levels. We used *elav-Gal4* to drive the expression of *UAS-PTP61F-RNAi* in the nervous system in *miR-137* mutants and compared these flies to wild-type controls. Immunoblot analyses of protein extracts from heads of 7-day old flies that were raised on standard fly food showed that knocking down *PTP61F* in the nervous system successfully restored levels of InR-P in *miR-137* mutants (Fig 43B), suggesting that the loss of InR-P in *miR-137* mutants is indeed due to the overexpression of *PTP61F.*

6.5.2 Starvation Resistance and Body Weight.

We tested if *PTP61F* knockdown in *miR-137^{KO}* can normalize the enlarged body weight of *miR-137* mutants. We expressed *elav-Gal4>>PTP61F-RNAi* in the *miR-137^{KO}* background. Male progeny were collected and aged to 7 days. We found that *PTP61F* knockdown in *miR-137^{KO}* mutant was sufficient to restore normal body weight to *miR-137* mutants compared to wild-type and *miR-137* homozygote mutants (Fig 43A).

Lastly, we tested if *PTP61F* knockdown in the nervous system of *miR-137* mutants would restore starvation sensitivity to *miR-137* mutants. We used *elav-Gal4* to drive the expression of *UAS-PTP61F-RNAi* in the nervous system in *miR-137* mutants. Progeny were collected, raised in a mixed population of males and females, and aged to 7 days.

Then male flies were raised on media for total starvation. 8 replicate vials (10 flies per vial) and two trials of each population of 80 flies were used to test starvation resistance. We found that *elav-Gal4>>PTP61F-RNAi* in the *miR-137^{KO}* background was able to restore starvation sensitivity to the *miR-137* mutant (Fig 43C). Median survival of male *elav*; *miR-137^{KO}* was 90 hrs, *elav-Gal4>>PTP61F-RNAi* + *miR-137^{KO}* was 60 hrs, and *elav-Gal4* was 48 hrs.

To sum up, our results suggest that knocking down *PTP61F* in a *miR-137* mutant background successfully rescued InR-P levels, normalized body weight, and restored starvation sensitivity phenotypes in *miR-137* mutant flies.

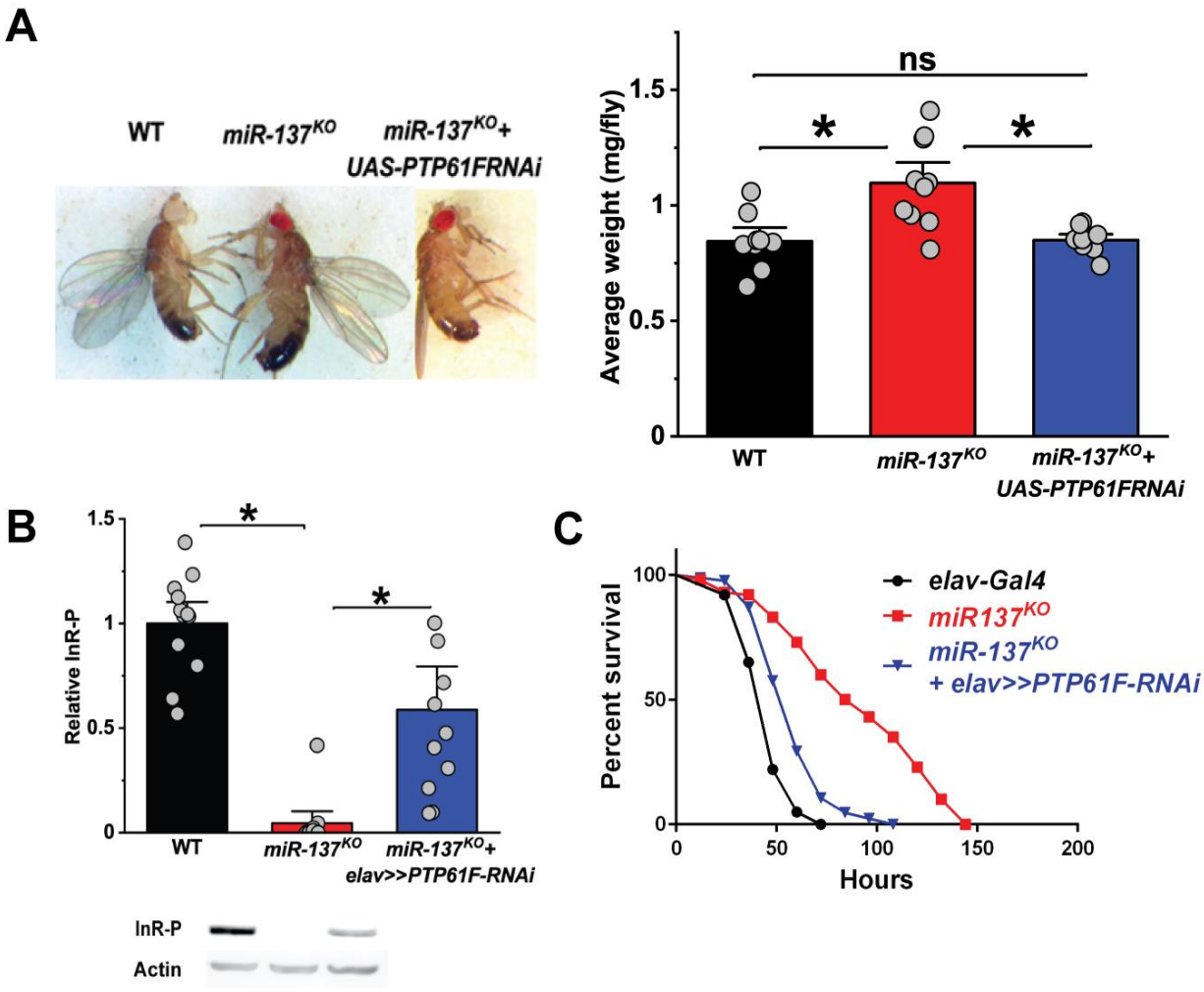

Figure 43. The knockdown of *PTP61F* in *miR-137* mutants successfully restored body weight, InR-P, and starvation sensitivity phenotypes. *A*, Male flies were aged for 7 days in a mixed population on a standard fly food diet tested for the average weight. *elav>>PTP61F*-RNAi+*miR-137*^{KO} restored the normal body weight in *miR-137*^{KO}. Shown are representative flies (***Left***), and quantification (***Right***). ***B,*** Quantification and representative immunoblots of relative levels of InR-P from heads of 7-day old WT, *miR-137*^{KO}, and *elav>>PTP61F*-RNAi+*miR-137*^{KO}, as indicated. Anti-InR-P levels are normalized to anti-actin, which was used as a loading control (N= 9 samples per genotype; 5 heads/sample). *Significance indicated by *P<0.05*, Students t-test. Data analyzed Student t-test. Error bars indicate SEM. ***C,*** Survival curves shown for lines (blue) pan-neuronally knockdown of *PTP61F-RNAi* in *miR-137*^{KO}, (red) *miR-137*^{KO}, and (black) *elav-Gal4* parental control. The survival curve of *elav>> PTP61F-RNAi* in *miR-137* mutant background was significantly shifted to the left compared to *miR-137*^{KO}, indicating the restoration of starvation sensitivity. Survival curves (N=80) from 7-day old males were evaluated by pairwise Log-rank tests.

6.6 Conclusion.

In the fed state, insulin is maintained at high levels, whereas insulin levels decrease during starvation. The decrease in the insulin signaling pathway promotes factors that enable the animal to promote a stress response and maintain metabolic homeostasis (Graham & Pick, 2017a; Gruntenko et al., 2016; Webb & Brunet, 2014). Our analysis of *miR137* mutants showed a decrease in the activity/phosphorylation of InR and AKT. In addition, *miR-137* mutants showed a decrease in *FOXO* transcript that is consistent with the down-regulation of its two targets, *InR* and 4E-*BP*, which may be indicative of an insulin resistance mechanism that may contribute to the obese phenotype of these flies. Dilps 2 and 5 have high homology to mammalian insulin are released from the IPCs in the brain (Puig et al., 2003; Tatar et al., n.d.). Changes in the level of Dilps may influence feeding and metabolism. For example, Dilp5 is known to bind and activate the InR for the purpose of lowering glucose levels (Chatterjee & Perrimon, 2021), and a decrease in Dilp5 causes the flies to consume more carbohydrates and protein (Pool & Scott, 2014). Despite all the changes in the expression levels of Dilps2/5, InR, FOXO, and 4E-BP in *miR-137* mutants, the most profound effect was a striking reduction in the activation of InR-P. We showed that *miR-137* mutants have an elevated level of an endogenously tagged PTP61F protein that may underlie the loss of phosphorylated InR and increased starvation resistance seen in *miR-137* mutants. In addition, knocking down *PTP61F* in the nervous system was sufficient to restore levels of InR-P, normal body weight, and starvation sensitivity in *miR-137* mutants. In summary, our studies show that the genomic loss of *miR137* is associated with a starvation-resistant phenotype and a decrease in insulin signaling that is likely due to its negative regulation of PTP61F.

CHAPTER 7: DISCUSSION

7.1 Summary.

Studies over the last decade have revealed that miRNAs play significant roles in regulating many cellular processes under stress conditions (Kloosterman & Plasterk, 2006; Leung & Sharp, 2010). miRNAs are small non-coding RNAs responsible for gene regulation at the posttranscriptional level by pairing to the 3' UTR. The miRNA *miR-137* is responsible for a critical aspect of cell proliferation and development (Mahmoudi & Cairns, 2017). We chose *Drosophila melanogaster* to study *miR-137* because it is genetically tractable and has well-characterized behaviors and physiology. *miR-137* is well conserved from *Drosophila* to humans and shares conservation of the seed sequence as well as the mature miRNA sequence (Kloosterman & Plasterk, 2006). Schizophrenia is a disease that is highly associated with SNPs in the *miR-137* locus (Pacheco et al., 2019). Changes in the level of *miR-137* cause early-onset neurodegeneration in the brain (De Sena Cortabitarte et al., 2018; Mahmoudi & Cairns, 2017; Thomas et al., 2017; Yin et al., 2014a).

Our study showed that *miR-137* is highly expressed in *Drosophila* heads with stable expression across different ages and with different environmental stressors. In addition, we showed that *miR-137* plays a regulatory role during several stress responses. Mutation in *miR-137* results in long-lived flies under starvation conditions. Genetic epistasis experiments using different mutants lines for components in the insulin signaling pathway showed that *miR-137* acts through the insulin signaling pathway in the CNS. We were also able to rescue the starvation resistance phenotype of *miR-137* mutants by reintroducing *miR-137* expression in the CNS. We also showed that *miR-137*

null mutants exhibit near undetectable levels of the activated/phosphorylated InR (InR-P), suggesting that these mutants are likely insulin resistant. *miR-137* showed an increase in energy stores and abnormal feeding behavior, which might be due to the mis-regulation of insulin signaling in the brain. Consistent with the starvation resistance, *miR-137* mutants also showed increased oxidative stress resistance when exposed to paraquat. Thus, *miR-137* mediates resistance to stress and our studies shed light on how *miR-137* mediates the regulation of InR and insulin signaling in the organism.

7.2 Fundamental Role of *miR-137* in Adaptation to Nutrient Deprivation

Stress can be defined as the environmental changes that force the cell to deviate from the normal state and activate pathways to promote cell survival. Food is not always available in nature. Food shortage is one of the most common causes of stress facing animals in the natural environment. Animals employ various adaptive mechanisms to survive stressful periods of food shortage and promote survival. The molecular basis behind heritable starvation resistance is not well understood. In *Drosophila melanogaster*, miRNA knockout mutants are a powerful genetic tool for understanding miRNA's complex roles in virous functions and behaviors. In this study, we found that *miR-137* mutant flies exhibited enhanced physiological plasticity, giving them greater resistance to severe starvation. We found that *miR-137* mutants exhibited increased accumulation of lipids, glucose, and protein content, which is often associated with starvation and oxidative resistance (Bubliy & Loeschcke, 2005; Marron et al., 2003b; Rion & Kawecki, 2007). Studies have shown that starvation resistance also often coexists with slowed development (Bubliy & Loeschcke, 2005; Rion & Kawecki, 2007). During our study, we noticed a delay in development in *miR-137* mutants. One possibility is that in *miR-*

137 mutants the starvation resistance could be due to a delay in development during the larval stage that leads to prolonged feeding, increased accumulation of energy stores, and increased body size that persists into the adult stage. Future studies should investigate whether the development time for *miR-137* is indeed prolonged.

miR-137 mutants also exhibit decreased energy expenditure as seen in their decreased locomotor and feeding behavior, and this may also contribute to prolonged starvation resistance. Hyperactivity causes the depletion of fat stores by accelerating the metabolic rate (Al-Anzi et al., 2009). Loss of *miR-137* causes impaired mobility in the flies (Y. W. Chen et al., 2014). Results from our lab showed that both *miR-137*^{CR} and *miR-137*^{KO} mutants exhibited significantly reduced locomotor performance whether they were fed or starved for 18 hrs prior to testing (data not shown; courtesy of Lea Giacchetta). These results suggest that *miR-137* has lower activity, which is one way to reduce energy expenditure. On the other hand, *miR-137* mutant flies do not consume food as do wild-type after 18 hrs of starvation. The increased fat levels may be communicated by insulin signaling to the brain to suppressing food intake (Al-Anzi et al., 2009; Park et al., 2018). Our results suggest that *miR-137* mutant flies have sufficient energy that decreases their consumption and motivation to feed even after long starvation. However, further studies may address whether the regulatory mechanisms of feeding hormones in the brain of *miR-137* mutant flies are altered.

Another possibility is that starvation resistance is associated with a slow metabolic rate (Rion & Kawecki, 2007). Studies showed that increased starvation resistance increases sleep and reduces feeding in adult flies (E. B. Brown et al., 2019). *miR-137* locus is genetically associated with sleep duration in mammals by regulating the

neuropeptide hypocretin/orexin (Holm et al., 2022). In mice, sleep deprivation reduces the level of *miR-137* (Holm et al., 2022). Future studies may investigate sleep phenotypes in *miR-137* mutant flies to further understand how *miR-137* may link sleep and metabolism.

In summary, our results suggest that *miR-137* mutants have reduced energy usage, perhaps supporting their enhanced energy stores. The combination of increased energy stores, body size, and decreased activity fits nicely with the increase in lifespan during starvation.

7.3 *miR-137* as a New Regulator of Insulin Signaling in the Brain.

Fitness and survival depend on an organism's balance of energy storage, metabolism, adaptation to changes in nutrient availability, as well as energy expenditure. Multiple nutrient sensing, metabolic and growth signaling pathways contribute to these homeostatic processes, including the insulin signaling pathway. The insulin signaling pathway is a well-conserved nutrient-sensing pathway throughout the animal kingdom. It depends on multiple phosphorylation steps starting from activation of the insulin receptor (InR), leading to PI3K activation and AKT phosphorylation. AKT phosphorylation can directly repress the FOXO transcription factor from translocating into the nucleus (Barthel et al., 2005; Liu & Lehmann, 2006; Puig et al., 2003). The other possible pathway that regulates lipid and protein synthesis levels is mediated via the PI3K/AKT/TOR signaling pathway. TOR pathway acts on two downstream translation regulators: inhibition of the eukaryotic initiation factor 4E-binding protein (4E-BP) and activation of S6 kinase (S6K). Both the insulin signaling pathway and TOR pathways contribute to energy balance and regulate the stress response (Hay & Sonenberg, 2004; Partridge et al., 2011). By using

miRNA-target prediction algorithms, multiple targets in the insulin signaling pathway are predicted to be regulated by *miR-137*. These targets include InR, AKT, S6K, AdipR and PTP61F. These predictions suggest that *miR-137* influences regulatory pathways that affect metabolic stress and insulin signaling.

In this study, we introduce *miR-137* as a new regulator of insulin signaling in the brain. We show that *miR-137* null mutants exhibit near undetectable levels of the activated/phosphorylated InR (InR-P), suggesting that these mutants are likely insulin resistant. While the chronic deactivation of InR likely feedsback to produce other secondary effects, the disruption in insulin signaling in *miR-137* mutants most likely underlies their increased body weight, altered metabolism, and starvation resistance. Indeed, genetic disruption of insulin signaling in both *Drosophila* and mammals has been shown to result in changes in body weight (Withers, D. J. et al., 1998; Broughton, S. J. et al., 1999), and elevated levels of glucose, trehalose, glycogen and triglycerides (Broughton, 2005.; Rulifson et al., 2002). Interestingly, the localization of insulin resistance can have different effects on body weight. Systemic insulin resistance has been shown to result in obesity across species (reviewed in (Kitamura et al., 2003)); this is observed, for example, in null mutants of the insulin receptor substrate *chico*, which results in obesity (Withers, D. J. et al., 1998; Broughton, S. J. et al., 1999). Ablation of IPCs, the neurons that secret Dilps in the brain, also results in obesity (Withers, D. J. et al., 1998; Broughton, S. J. et al., 1999). In contrast, insulin resistance restricted to the *Drosophila* fat body, which is functionally homologous to the mammalian liver and white adipose tissue (S. J. Broughton et al., 2005; Kühnlein, 2012), has been shown to result in leanness (Teleman et al., 2005b). Future studies will need to test for insulin resistance

in *miR-137* mutants more directly, perhaps by examining whether *miR-137* mutants do indeed exhibit a resistance to insulin signaling even when Dilps are over-abundantly available.

7.4 The Extended Lifespan of *miR-137* Mutants Under Conditions of Nutrient Deprivation is also Likely to be a Consequence of Lowered Levels of InR-P.

Our studies show that mutation in *miR-137* results in long-lived flies under starvation conditions, while the over-expression on *miR-137* restores the starvation sensitivity. Mutations that decrease insulin/PI3K/Akt/FOXO signaling exhibit increased resistance to starvation across species (Barthel et al., 2005; Clancy et al., 2001; Semaniuk, Piskovatska, et al., 2021; Tettweiler et al., 2005b). Ablation of IPCs that completely disrupts insulin signaling in the brain similarly results in an increased lifespan under starved conditions (Broughton, 2005). Conversely, enhanced insulin signaling, for example, in transgenic lines expressing a constitutively active InR (InR^{CA}) results in an increase in starvation sensitivity (Fig. 34). Starvation resistance in *miR-137* mutants is likely to be bolstered by their enhanced energy stores, since accumulation of lipid stores has been shown to be correlated with resistance to starvation (Borash & Ho, 2001; Marron et al., 2003b).

7.5 What are the mechanism(s) underlying the reduced levels of InR-P in *miR-137* mutants?

Using the algorithm TargetScanFly7.2 (https://www.targetscan.org/fly_72/) to gain insight into predicted targets of *miR-137* in *Drosophila*, we identified the candidate *PTP61F*, which has been shown to dephosphorylate InR in *Drosophila* (C. L. Wu et al.,

2011b). Since miRNA regulation most commonly results in target mRNA destabilization and/or translational repression (Bartel, 2018; Fabian & Sonenberg, 2012), we expected that the loss of *miR-137* would lead to enhanced expression of *PTP61F*, which could explain the near absence of InR-P. We present evidence that over-expression of *PTP61F* results in a phenotype that mimics the loss of *miR-137*, and that an endogenously tagged *GFP-PTP61F* is up-regulated in *miR-137* null mutants. Interestingly, when we used TargetScanMouse8.0 (https://www.targetscan.org/mmu_80/) and TargetScanHuman8.0 (https://www.targetscan.org/vert_80/), we found that both mouse and human *miR-137* are similarly predicted to target a mammalian ortholog of PTP61F, TC-PTP, which is encoded by the *PTPN2* gene; this phosphatase has also been shown to dephosphorylate the mammalian InR (Haj et al., 2005; Salmeen et al., 2000), suggesting that regulation of insulin signaling by *miR-137* is likely to be conserved across species.

The regulation of *PTP61F* expression, however, is likely to be complicated, as indicated by our results that RNAi knock-down, or a total loss of *PTP61F*, also results in a loss of InR-P, suggesting that there may be compensatory up-regulation of another phosphatase when *PTP61F* levels are reduced. Another curiosity we observed was that mRNA levels of *PTP61F* seem to be down-regulated in *miR-137* mutants (Fig. 41), contrary to the elevation in GFP-PTP61F protein levels we observed. One possibility is that *PTP61F* is differentially regulated by *miR-137* such that *miR-137* increases the stability of *PTP61F* mRNA but represses translation of *PTP61F*. Such a model has not previously been explored, but if true, would offer multifaceted regulation by *miR-137* that could come into play in different cell types, at developmental times, or under different environmental conditions. Results may also be difficult to interpret since *miR-137* has

multiple targets in intersecting pathways. For example, *miR-137* has been associated with growth and target of rapamycin (TOR) signaling (Gui et al., 2021; Thomas et al., 2017), and mammalian *AKT2* has been identified as a *miR-137* target (L. Wu et al., 2015). Future studies will need to address how the effect of *miR-137* is integrated across these different signaling pathways.

7.6 Does mis-regulation of *miR-137* in neuropsychiatric disorders contribute to metabolic co-morbidities associated with these disorders?

Multiple studies have found *miR-137* to be strongly linked to schizophrenia with genome-wide significance (E. He et al., 2018; Yin et al., 2014a). In addition to neuropsychiatric symptoms, individuals with schizophrenia have a ~10-15 year reduction in life expectancy (Saha et al., 2007; Weye et al., 2020), and this high mortality rate is largely due to the high prevalence of obesity, Type 2 diabetes, elevated cholesterol and triglycerides, high blood pressure, heart disease, high blood glucose, and irregularities in insulin signaling (Grundy et al., 2005; Saha et al., 2007). Although there are many studies that have examined metabolic syndrome associated with schizophrenia patients under anti-psychotic treatment, there is recent and substantial evidence that drug-naïve patients also exhibit metabolic disturbances (Grundy et al., 2005; Weye et al., 2020) and that anti-psychotics only worsen these metabolic symptoms (Deng et al., 2010; *Icns_15_5-6_30*, n.d.). Interestingly, impairment in insulin signaling in the brain has been suggested to underlie the metabolic dysfunction in drug-naïve schizophrenia patients (Dash et al., 2015; *Hypothalamic K(ATP) Channels Control Hepatic Glucose Production.*, n.d.). *miR-137* is also associated with Bipolar Disorder (Duan et al., 2014), and individuals with Bipolar Disorder have the highest incidence of obesity and metabolic disorders (~45%)

(Grover et al., 2014), resulting in a reduced life expectancy (Grover et al., 2014; Moreira et al., 2019), similar to schizophrenia patients. Thus, understanding how *miR-137* regulates insulin signaling may also help explain the metabolic co-morbidities that arise in schizophrenia patients. and Bipolar Disorder, and perhaps reveal new avenues of treatment.

7.7 Conclusion.

This project has successfully identified a novel role of *miR-137* in regulating the insulin signaling pathway in *Drosophila melanogaster.* We also identified a novel role of *miR-137* in regulating *PTP61F/PTP-1B in vivo*. We believe that *miR-137* regulation of the *PTP61F* mediates the severe reduction in activity/phosphorylation of InR. In addition, this thesis identified phenotypes associated with loss of *miR-137* in *Drosophila* including starvation resistance, increased body weight/size, hyperlipidemia, hyperglycemia and decreased feeding motivation. In conclusion, this study provides new insight into the potential role of *miR-137* in regulating complex physiological and behavioral phenotypes in adult *Drosophila* associated with metabolic homeostasis through the insulin signaling pathway. Hopefully, our findings will help guide our understanding of metabolic disorders associated with insulin signaling.

BIBLIOGRAPHY

Agarwal, V., Subtelny, A. O., Thiru, P., Ulitsky, I., & Bartel, D. P. (2018). Predicting microRNA targeting efficacy in Drosophila. *Genome Biology*, *19*(1). https://doi.org/10.1186/s13059-018-1504-3

Aguila, J. R., Suszko, J., Gibbs, A. G., & Hoshizaki, D. K. (2007). The role of larval fat cells in adult Drosophila melanogaster. *Journal of Experimental Biology*, *210*(6), 956–963. https://doi.org/10.1242/jeb.001586

Ahmad, M., He, L., & Perrimon, N. (2020). Regulation of insulin and adipokinetic hormone/glucagon production in flies. In *Wiley Interdisciplinary Reviews: Developmental Biology* (Vol. 9, Issue 2). John Wiley and Sons Inc. https://doi.org/10.1002/wdev.360

Akomolafe, A., Beiser, A., Meigs, J. B., Au, R., Green, R. C., Farrer, L. A., Wolf, P. A., & Seshadri, S. (n.d.). *Diabetes Mellitus and Risk of Developing Alzheimer Disease Results From the Framingham Study*. https://jamanetwork.com/

Al-Anzi, B., Sapin, V., Waters, C., Zinn, K., Wyman, R. J., & Benzer, S. (2009). Obesity-Blocking Neurons in Drosophila. *Neuron*, *63*(3), 329–341. https://doi.org/10.1016/j.neuron.2009.07.021

Alessi, D. R., Andjelkovic1, M., Caudwell, B., Cron1, P., Morrice, N., Cohen, P., Hemmings1', B. A., & Miescher, F. (1996). Mechanism of activation of protein kinase B by insulin and IGF-1: insulin signalling/phosphatidylinositol 3-kinase/protein kinase B/protein phosphorylation. In *The EMBO Journal* (Vol. 15, Issue 23).

Ambros, V. (1989). A Hierarchy of Regulatory Genes Controls a Larva-to-Adult Developmental Switch in C. elegans. In *Cell* (Vol. 57).

Arakawa, Y., Yokoyama, K., Tasaki, S., Kato, J., Nakashima, K., Takeyama, M., Nakatani, A., & Suzuki, M. (2019). Transgenic mice overexpressing miR-137 in the brain show schizophrenia-associated behavioral deficits and transcriptome profiles. *PLoS ONE*, *14*(7). https://doi.org/10.1371/journal.pone.0220389

Arcidiacono, B., Iiritano, S., Nocera, A., Possidente, K., Nevolo, M. T., Ventura, V., Foti, D., Chiefari, E., & Brunetti, A. (2012). Insulin resistance and cancer risk: An overview of the pathogenetic mechanisms. In *Experimental Diabetes Research* (Vol. 2012). https://doi.org/10.1155/2012/789174

Auer, S. K., Salin, K., Anderson, G. J., & Metcalfe, N. B. (2018). Individuals exhibit consistent differences in their metabolic rates across changing thermal conditions. *Comparative Biochemistry and Physiology -Part A : Molecular and Integrative Physiology*, *217*, 1–6. https://doi.org/10.1016/j.cbpa.2017.11.021

Baenas, N., & Wagner, A. E. (2022). Drosophila Melanogaster as a Model Organism for Obesity and Type-2 Diabetes Mellitus by Applying High-Sugar and High-Fat Diets. *Biomolecules*, *12*(2). https://doi.org/10.3390/biom12020307

Bai, H., Kang, P., & Tatar, M. (2012). Drosophila insulin-like peptide-6 (dilp6) expression from fat body extends lifespan and represses secretion of Drosophila insulin-like peptide-2 from the brain. *Aging Cell*, *11*(6), 978–985. https://doi.org/10.1111/acel.12000

Baker, K. D., & Thummel, C. S. (2007). Diabetic larvae and obese flies-emerging studies of metabolism in Drosophila. In *Cell Metab* (Vol. 6, Issue 4).

Baldal, E. A., Brakefield, P. M., & Zwaan, B. J. (2006a). MULTITRAIT EVOLUTION IN LINES OF DROSOPHILA MELANOGASTER SELECTED FOR INCREASED STARVATION RESISTANCE: THE ROLE OF METABOLIC RATE AND IMPLICATIONS FOR THE EVOLUTION OF LONGEVITY . *Evolution*, *60*(7), 1435–1444. https://doi.org/10.1111/j.0014-3820.2006.tb01222.x

Baldal, E. A., Brakefield, P. M., & Zwaan, B. J. (2006b). MULTITRAIT EVOLUTION IN LINES OF DROSOPHILA MELANOGASTER SELECTED FOR INCREASED STARVATION RESISTANCE: THE ROLE OF METABOLIC RATE AND IMPLICATIONS FOR THE EVOLUTION OF LONGEVITY . *Evolution*, *60*(7), 1435–1444. https://doi.org/10.1111/j.0014-3820.2006.tb01222.x

Band, C. J., Posner, B. I., Dumas, V., & Contreres, J.-O. (1997). Early Signaling Events Triggered by Peroxovanadium [bpV(phen)] Are Insulin Receptor Kinase (IRK)-Dependent: Specificity of Inhibition of IRK-Associated Protein Tyrosine Phosphatase(s) by bpV(phen). In *Mo-lecular Endocrinology* (Vol. 11). https://academic.oup.com/mend/article/11/13/1899/2754068

Barbagallo, B., & Garrity, P. A. (2015). Temperature sensation in Drosophila. In *Current Opinion in Neurobiology* (Vol. 34, pp. 8–13). Elsevier Ltd. https://doi.org/10.1016/j.conb.2015.01.002

Bartel, D. P. (2018). Metazoan MicroRNAs. In *Cell* (Vol. 173, Issue 1, pp. 20–51). Cell Press. https://doi.org/10.1016/j.cell.2018.03.006

Barthel, A., Schmoll, D., & Unterman, T. G. (2005). FoxO proteins in insulin action and metabolism. In *Trends in Endocrinology and Metabolism* (Vol. 16, Issue 4, pp. 183–189). Elsevier Inc. https://doi.org/10.1016/j.tem.2005.03.010

Baserga, R. (1999). *The IGF-I Receptor in Cancer Research 1*. http://www.idealibrary.com

Beghi, E., Giussani, G., Abd-Allah, F., Abdela, J., Abdelalim, A., Abraha, H. N., Adib, M. G., Agrawal, S., Alahdab, F., Awasthi, A., Ayele, Y., Barboza, M. A., Belachew, A. B., Biadgo, B., Bijani, A., Bitew, H., Carvalho, F., Chaiah, Y., Daryani, A., … Murray, C. J. L. (2019). Global, regional, and national burden of epilepsy, 1990–

2016: a systematic analysis for the Global Burden of Disease Study 2016. *The Lancet Neurology*, *18*(4), 357–375. https://doi.org/10.1016/S1474-4422(18)30454-X

Bellemer, A. (2015). Thermotaxis, circadian rhythms, and TRP channels in Drosophila. In *Temperature* (Vol. 2, Issue 2, pp. 227–243). Routledge. https://doi.org/10.1080/23328940.2015.1004972

Bharucha, K. N., Tarr, P., & Zipursky, S. L. (2008). A glucagon-like endocrine pathway in Drosophila modulates both lipid and carbohydrate homeostasis. *Journal of Experimental Biology*, *211*(19), 3103–3110. https://doi.org/10.1242/jeb.016451

Bier, A., Giladi, N., Kronfeld, N., Lee, H. K., Cazacu, S., Finniss, S., Xiang, C., Poisson, L., Decarvalho, A. C., Slavin, S., Jacoby, E., Yalon, M., Toren, A., Mikkelsen, T., & Brodie, C. (2013). MicroRNA-137 is downregulated in glioblastoma and inhibits the stemness of glioma stem cells by targeting RTVP-1. In *Oncotarget* (Vol. 4). www.impactjournals.com/oncotarget

Blüher, M., Kahn, B. B., & Ronald Kahn, C. (1977). Extended Longevity in Mice Lacking the Insulin Receptor in Adipose Tissue. In *Curr. Opin. Neurobiol* (Vol. 138). Humana. www.sciencemag.org/cgi/content/full/299/5606/568/

Borash, D. J., & Ho, G. T. (2001). Patterns of selection: stress resistance and energy storage in density-dependent populations of Drosophila melanogaster. In *Journal of Insect Physiology* (Vol. 47). www.elsevier.com/locate/jinsphys

Boucher, J., Tseng, Y. H., & Kahn, C. R. (2010). Insulin and insulin-like growth factor-1 receptors act as ligand-specific amplitude modulators of a common pathway regulating gene transcription. *Journal of Biological Chemistry*, *285*(22), 17235–17245. https://doi.org/10.1074/jbc.M110.118620

Britton, J. S., Lockwood, W. K., Li, L., Cohen, S. M., & Edgar, B. A. (2002). Drosophila's Insulin/PI3-Kinase Pathway Coordinates Cellular Metabolism with Nutritional Conditions generating a variety of second messengers. The critical second messenger produced by the class I A PI3-kinases is generated when phosphatidylinositol-4,5-P 2 (PIP 2 ; mostly found in lipid membranes) is phosphorylated in 1 Molecular and Cellular Biology Program and the third position, producing phosphatidylinositol-3,4,5-2 Division of Basic Sciences P 3 (PIP 3 ; Rameh and Cantley. In *Developmental Cell* (Vol. 2).

Brogiolo, W., Stocker, H., Ikeya, T., Rintelen, F., Fernandez, R., & Hafen, E. (2001). *An evolutionarily conserved function of the Drosophila insulin receptor and insulin-like peptides in growth control*.

Broughton, S., Alic, N., Slack, C., Bass, T., Ikeya, T., Vinti, G., Tommasi, A. M., Driege, Y., Hafen, E., & Partridge, L. (2008). Reduction of DILP2 in Drosophila triages a metabolic phenotype from lifespan revealing redundancy and compensation among DILPs. *PLoS ONE*, *3*(11). https://doi.org/10.1371/journal.pone.0003721

Broughton, S. J., Piper, M. D. W., Ikeya, T., Bass, T. M., Jacobson, J., Driege, Y., Martinez, P., Hafen, E., Withers, D. J., Leevers, S. J., & Partridge, L. (2005). *Longer lifespan, altered metabolism, and stress resistance in Drosophila from ablation of cells making insulin-like ligands*. www.pnas.orgcgidoi10.1073pnas.0405775102

Brown, E. B., Slocumb, M. E., Szuperak, M., Kerbs, A., Gibbs, A. G., Kayser, M. S., & Keene, A. C. (2019). Starvation resistance is associated with developmentally specified changes in sleep, feeding and metabolic rate. *Journal of Experimental Biology*, *222*(3). https://doi.org/10.1242/jeb.191049

Brown, J. T., Chin, J., Leiser, S. C., Pangalos, M. N., & Randall, A. D. (2011). Altered intrinsic neuronal excitability and reduced Na+ currents in a mouse model of Alzheimer's disease. *Neurobiology of Aging*, *32*(11), 2109.e1-2109.e14. https://doi.org/10.1016/j.neurobiolaging.2011.05.025

Bubliy, O. A., & Loeschcke, V. (2005). Correlated responses to selection for stress resistance and longevity in a laboratory population of Drosophila melanogaster. *Journal of Evolutionary Biology*, *18*(4), 789–803. https://doi.org/10.1111/j.1420-9101.2005.00928.x

Buch, S., Melcher, C., Bauer, M., Katzenberger, J., & Pankratz, M. J. (2008). Opposing Effects of Dietary Protein and Sugar Regulate a Transcriptional Target of Drosophila Insulin-like Peptide Signaling. *Cell Metabolism*, *7*(4), 321–332. https://doi.org/10.1016/j.cmet.2008.02.012

Buszard, B. J., Johnson, T. K., Meng, T.-C., Burke, R., Warr, C. G., & Tiganis, T. (2013). The Nucleus- and Endoplasmic Reticulum-Targeted Forms of Protein Tyrosine Phosphatase 61F Regulate Drosophila Growth, Life Span, and Fecundity. *Molecular and Cellular Biology*, *33*(7), 1345–1356. https://doi.org/10.1128/mcb.01411-12

Cao, L., Wang, Z., & Wan, W. (2018). Suppressor of cytokine signaling 3: Emerging role linking central insulin resistance and Alzheimer's disease. In *Frontiers in Neuroscience* (Vol. 12, Issue JUN). Frontiers Media S.A. https://doi.org/10.3389/fnins.2018.00417

Chalfie, M., Robert Horvitz, H., & Sulston, J. E. (1981). Mutations That Lead to Reiterations in the Cell Lineages of C. elegans. In *Cell* (Vol. 24).

Chatterjee, N., & Perrimon, N. (2021). What fuels the fly: Energy metabolism in Drosophila and its application to the study of obesity and diabetes. In *Sci. Adv* (Vol. 7). https://www.science.org

Chauhan, V., Anis, A., & Chauhan, A. (2021). Effects of Starvation on the Levels of Triglycerides, Diacylglycerol, and Activity of Lipase in Male and Female Drosophila Melanogaster. *Journal of Lipids*, *2021*, 1–7. https://doi.org/10.1155/2021/5583114

Chen, C. Y., Chen, J., He, L., & Stiles, B. L. (2018). PTEN: Tumor suppressor and metabolic regulator. In *Frontiers in Endocrinology* (Vol. 9, Issue JUL). Frontiers Media S.A. https://doi.org/10.3389/fendo.2018.00338

Chen, Y. W., Song, S., Weng, R., Verma, P., Kugler, J. M., Buescher, M., Rouam, S., & Cohen, S. M. (2014). Systematic study of Drosophila MicroRNA functions using a collection of targeted knockout mutations. *Developmental Cell*, *31*(6), 784–800. https://doi.org/10.1016/j.devcel.2014.11.029

Cheng, Y., Wang, Z. M., Tan, W., Wang, X., Li, Y., Bai, B., Li, Y., Zhang, S. F., Yan, H. L., Chen, Z. L., Liu, C. M., Mi, T. W., Xia, S., Zhou, Z., Liu, A., Tang, G. Bin, Liu, C., Dai, Z. J., Wang, Y. Y., … Jin, P. (2018). Partial loss of psychiatric risk gene Mir137 in mice causes repetitive behavior and impairs sociability and learning via increased Pde10a. *Nature Neuroscience*. https://doi.org/10.1038/s41593-018-0261-7

Chien, S., Reiter, L. T., Bier, E., & Gribskov, M. (2002). Homophila: human disease gene cognates in Drosophila. In *Nucleic Acids Research* (Vol. 30, Issue 1). http://homophila.sdsc.edu.

Chippindale, A. K., Chu, T. J. F., & Rose, M. R. (1996a). COMPLEX TRADE-OFFS AND THE EVOLUTION OF STARVATION RESISTANCE IN DROSOPHILA MELANOGASTER. In *Evolution* (Vol. 50, Issue 2). https://academic.oup.com/evolut/article/50/2/753/6870710

Chippindale, A. K., Chu, T. J. F., & Rose, M. R. (1996b). COMPLEX TRADE-OFFS AND THE EVOLUTION OF STARVATION RESISTANCE IN DROSOPHILA MELANOGASTER. In *Evolution* (Vol. 50, Issue 2). https://academic.oup.com/evolut/article/50/2/753/6870710

Clancy, D. J., Gems, D., Harshman, L. G., Oldham, S., Stocker, H., Hafen, E., Leevers, S. J., & Partridge, L. (2001). Extension of life-span by loss of CHICO, a Drosophila insulin receptor substrate protein. *Science*, *292*(5514), 104–106. https://doi.org/10.1126/science.1057991

Clark, A. G., & Fucito, C. D. (1998). Stress tolerance and metabolic response to stress in Drosophila melanogaster. In *Heredity* (Vol. 81).

Crowley, J. J., Collins, A. L., Lee, R. J., Nonneman, R. J., Farrell, M. S., Ancalade, N., Mugford, J. W., Agster, K. L., Nikolova, V. D., Moy, S. S., & Sullivan, P. F. (2015). Disruption of the MicroRNA 137 primary transcript results in early embryonic lethality in mice. In *Biological Psychiatry* (Vol. 77, Issue 2, pp. e5–e7). Elsevier USA. https://doi.org/10.1016/j.biopsych.2014.05.022

Dash, S., Xiao, C., Morgantini, C., Koulajian, K., & Lewis, G. F. (2015). Intranasal insulin suppresses endogenous glucose production in humans compared with placebo in

the presence of similar venous insulin concentrations. *Diabetes*, *64*(3), 766–774. https://doi.org/10.2337/db14-0685

De Sena Cortabitarte, A., Berkel, S., Cristian, F. B., Fischer, C., & Rappold, G. A. (2018). A direct regulatory link between microRNA-137 and SHANK2: Implications for neuropsychiatric disorders. *Journal of Neurodevelopmental Disorders*, *10*(1). https://doi.org/10.1186/s11689-018-9233-1

Deng, C., Weston-Green, K., & Huang, X. F. (2010). The role of histaminergic H1 and H3 receptors in food intake: A mechanism for atypical antipsychotic-induced weight gain? In *Progress in Neuro-Psychopharmacology and Biological Psychiatry* (Vol. 34, Issue 1, pp. 1–4). https://doi.org/10.1016/j.pnpbp.2009.11.009

Depetris, R. S., Hu, J., Gimpelevich, I., Holt, L. J., Daly, R. J., & Hubbard, S. R. (2005). Structural basis for inhibition of the insulin receptor by the adaptor protein Grb14. *Molecular Cell*, *20*(2), 325–333. https://doi.org/10.1016/j.molcel.2005.09.001

Devanna, P., & Vernes, S. C. (2014). A direct molecular link between the autism candidate gene RORa and the schizophrenia candidate MIR137. *Scientific Reports*, *4*. https://doi.org/10.1038/srep03994

Dillon, M. E., Wang, G., Garrity, P. A., & Huey, R. B. (2009). Thermal preference in Drosophila. In *Journal of Thermal Biology* (Vol. 34, Issue 3, pp. 109–119). https://doi.org/10.1016/j.jtherbio.2008.11.007

Dimmeler, S., & Nicotera, P. (2013). MicroRNAs in age-related diseases. In *EMBO Molecular Medicine* (Vol. 5, Issue 2, pp. 180–190). https://doi.org/10.1002/emmm.201201986

Ding, X., Iyer, R., Novotny, C., Metzger, D., Zhou, H. H., Smith, G. I., Yoshino, M., Yoshino, J., Klein, S., Swaminath, G., Talukdar, S., & Zhou, Y. (2020). Inhibition of Grb14, a negative modulator of insulin signaling, improves glucose homeostasis without causing cardiac dysfunction. *Scientific Reports*, *10*(1), 3417. https://doi.org/10.1038/s41598-020-60290-1

Duan, J., Shi, J., Fiorentino, A., Leites, C., Chen, X., Moy, W., Chen, J., Alexandrov, B. S., Usheva, A., He, D., Freda, J., O'Brien, N. L., McQuillin, A., Sanders, A. R., Gershon, E. S., Delisi, L. E., Bishop, A. R., Gurling, H. M. D., Pato, M. T., … Gejman, P. V. (2014). A rare functional noncoding variant at the GWAS-Implicated MIR137/MIR2682 locus might confer risk to schizophrenia and bipolar disorder. *American Journal of Human Genetics*, *95*(6), 744–753. https://doi.org/10.1016/j.ajhg.2014.11.001

Dunham, I., Kundaje, A., Aldred, S. F., Collins, P. J., Davis, C. A., Doyle, F., Epstein, C. B., Frietze, S., Harrow, J., Kaul, R., Khatun, J., Lajoie, B. R., Landt, S. G., Lee, B. K., Pauli, F., Rosenbloom, K. R., Sabo, P., Safi, A., Sanyal, A., … Lochovsky, L.

(2012). An integrated encyclopedia of DNA elements in the human genome. *Nature*, *489*(7414), 57–74. https://doi.org/10.1038/nature11247

Durmaz, E., Rajpurohit, S., Betancourt, N., Fabian, D. K., Kapun, M., Schmidt, P., & Flatt, T. (2019). A clinal polymorphism in the insulin signaling transcription factor foxo contributes to life-history adaptation in Drosophila*. *Evolution*, *73*(9), 1774–1792. https://doi.org/10.1111/evo.13759

Eckert, A., Hauptmann, S., Scherping, I., Meinhardt, J., Rhein, V., Dröse, S., Brandt, U., Fändrich, M., Müller, W. E., & Götz, J. (2008). Oligomeric and fibrillar species of β-amyloid (Aβ42) both impair mitochondrial function in P301L tau transgenic mice. *Journal of Molecular Medicine*, *86*(11), 1255–1267. https://doi.org/10.1007/s00109-008-0391-6

Edgecomb, R. S., Harth, C. E., & Schneiderman, A. M. (1994). REGULATION OF FEEDING BEHAVIOR IN ADULT DROSOPHILA MELANOGASTER VARIES WITH FEEDING REGIME AND NUTRITIONAL STATE. In *J. exp. Biol* (Vol. 197).

Enell, L. E., Kapan, N., Söderberg, J. A. E., Kahsai, L., & Nässe, D. R. (2010). Insulin signaling, lifespan and stress resistance are modulated by metabotropic GABA receptors on insulin producing cells in the brain of Drosophila. *PLoS ONE*, *5*(12). https://doi.org/10.1371/journal.pone.0015780

Epiney, D. G., Salameh, C., Cassidy, D., Zhou, L. T., Kruithof, J., Milutinović, R., Andreani, T. S., Schirmer, A. E., & Bolterstein, E. (2021). Characterization of stress responses in a drosophila model of werner syndrome. *Biomolecules*, *11*(12). https://doi.org/10.3390/biom11121868

Ez-Ventoso, C., Vora, M., & Driscoll, M. (2008). Sequence Relationships among C. elegans, D. melanogaster and Human microRNAs Highlight the Extensive Conservation of microRNAs in Biology. *PLoS ONE*, *3*(7), 2818. https://doi.org/10.1371/journal.pone.0002818

Fabian, M. R., & Sonenberg, N. (2012). The mechanics of miRNA-mediated gene silencing: A look under the hood of miRISC. In *Nature Structural and Molecular Biology* (Vol. 19, Issue 6, pp. 586–593). https://doi.org/10.1038/nsmb.2296

Fast, I., Hewel, C., Wester, L., Schumacher, J., Gebert, D., Zischler, H., Berger, C., & Rosenkranz, D. (2017a). *Temperature-responsive miRNAs in Drosophila orchestrate adaptation to different ambient temperatures*. https://doi.org/10.1261/rna.061119

Fast, I., Hewel, C., Wester, L., Schumacher, J., Gebert, D., Zischler, H., Berger, C., & Rosenkranz, D. (2017b). *Temperature-responsive miRNAs in Drosophila orchestrate adaptation to different ambient temperatures*. https://doi.org/10.1261/rna.061119

Fernandez, R., Tabarini, D., Azpiazu, N., Frasch, M., & Schlessinger, J. (1995). The Drosophila insulin receptor homolog: A gene essential for embryonic development encodes two receptor isoforms with different signaling potential. *EMBO Journal*, *14*(14), 3373–3384. https://doi.org/10.1002/j.1460-2075.1995.tb07343.x

Fernandez-Almonacid, R., & Rosen, O. M. (1987). Structure and Ligand Specificity of the Drosophila melanogaster Insulin Receptor. In *MOLECULAR AND CELLULAR BIOLOGY* (Vol. 7, Issue 8).

Finelli, A., Kelkar, A., Song, H. J., Yang, H., & Konsolaki, M. (2004). A model for studying Alzheimer's Aβ42-induced toxicity in Drosophila melanogaster. *Molecular and Cellular Neuroscience*, *26*(3), 365–375. https://doi.org/10.1016/j.mcn.2004.03.001

Fischer, F. P., Karge, R. A., Weber, Y. G., Koch, H., Wolking, S., & Voigt, A. (2023). Drosophila melanogaster as a versatile model organism to study genetic epilepsies: An overview. In *Frontiers in Molecular Neuroscience* (Vol. 16). Frontiers Media S.A. https://doi.org/10.3389/fnmol.2023.1116000

Flightless-I Controls Fat Storage in Drosophila. (n.d.).

Fricke, C., Green, D., Smith, D., Dalmay, T., & Chapman, T. (2014). MicroRNAs influence reproductive responses by females to male sex peptide in drosophila melanogaster. *Genetics*, *198*(4), 1603–1619. https://doi.org/10.1534/genetics.114.167320

Fu, X. D. (2014). Non-coding RNA: A new frontier in regulatory biology. In *National Science Review* (Vol. 1, Issue 2, pp. 190–204). Oxford University Press. https://doi.org/10.1093/nsr/nwu008

Galic, S., Klingler-Hoffmann, M., Fodero-Tavoletti, M. T., Puryer, M. A., Meng, T.-C., Tonks, N. K., & Tiganis, T. (2003). Regulation of Insulin Receptor Signaling by the Protein Tyrosine Phosphatase TCPTP. *Molecular and Cellular Biology*, *23*(6), 2096–2108. https://doi.org/10.1128/mcb.23.6.2096-2108.2003

Géminard, C., Rulifson, E. J., & Léopold, P. (2009). Remote Control of Insulin Secretion by Fat Cells in Drosophila. *Cell Metabolism*, *10*(3), 199–207. https://doi.org/10.1016/j.cmet.2009.08.002

Genetic analysis of insulin signaling. (n.d.).

Georgescu, M. M. (2010a). Pten tumor suppressor network in PI3K-Akt pathway control. In *Genes and Cancer* (Vol. 1, Issue 12, pp. 1170–1177). https://doi.org/10.1177/1947601911407325

Georgescu, M. M. (2010b). Pten tumor suppressor network in PI3K-Akt pathway control. In *Genes and Cancer* (Vol. 1, Issue 12, pp. 1170–1177). https://doi.org/10.1177/1947601911407325

Ghildiyal, M., & Zamore, P. D. (2009). Small silencing RNAs: An expanding universe. In *Nature Reviews Genetics* (Vol. 10, Issue 2, pp. 94–108). https://doi.org/10.1038/nrg2504

Glenner, G. G., & Wong, C. W. (1984). *BIOCHEMICAL AND BIOPHYSICAL RESEARCH COMMUNICATIONS Pages 885-890 AND CHARACTERIZATION OF A NOVEL CEREBROVASCULAR AMYLOID PROTEIN* (Vol. 120, Issue 3).

Goenaga, J., Fanara, J. J., & Hasson, E. (2013). Latitudinal Variation in Starvation Resistance is Explained by Lipid Content in Natural Populations of Drosophila melanogaster. *Evolutionary Biology*, *40*(4), 601–612. https://doi.org/10.1007/s11692-013-9235-6

González, A., & Hall, M. N. (2017). Nutrient sensing and TOR signaling in yeast and mammals . *The EMBO Journal*, *36*(4), 397–408. https://doi.org/10.15252/embj.201696010

Gosline, S. J. C., Gurtan, A. M., JnBaptiste, C. K., Bosson, A., Milani, P., Dalin, S., Matthews, B. J., Yap, Y. S., Sharp, P. A., & Fraenkel, E. (2016). Elucidating MicroRNA Regulatory Networks Using Transcriptional, Post-transcriptional, and Histone Modification Measurements. *Cell Reports*, *14*(2), 310–319. https://doi.org/10.1016/j.celrep.2015.12.031

Graham, P., & Pick, L. (2017a). Drosophila as a Model for Diabetes and Diseases of Insulin Resistance. In *Current Topics in Developmental Biology* (Vol. 121, pp. 397–419). Academic Press Inc. https://doi.org/10.1016/bs.ctdb.2016.07.011

Graham, P., & Pick, L. (2017b). Drosophila as a Model for Diabetes and Diseases of Insulin Resistance. In *Current Topics in Developmental Biology* (Vol. 121, pp. 397–419). Academic Press Inc. https://doi.org/10.1016/bs.ctdb.2016.07.011

Gratz, S. J., Harrison, M. M., Wildonger, J., & O'connor-Giles, K. M. (2015). Precise genome editing of drosophila with CRISPR RNA- guided cas9. *Methods in Molecular Biology*, *1311*, 335–348. https://doi.org/10.1007/978-1-4939-2687-9_22

Gratz, S. J., Rubinstein, C. D., Harrison, M. M., Wildonger, J., & O'Connor-Giles, K. M. (2015). CRISPR-Cas9 genome editing in Drosophila. *Current Protocols in Molecular Biology*, *2015*, 31.2.1-31.2.20. https://doi.org/10.1002/0471142727.mb3102s111

Greenspan, R. J., Finn, J. A., & Hall, J. C. (1980). Acetylcholinesterase mutants in drosophila and their effects on the structure and function of the cental nervous system. *Journal of Comparative Neurology*, *189*(4), 741–774. https://doi.org/10.1002/cne.901890409

Grö Nke, S., Nter Mü Ller, G., Hirsch, J., Fellert, S., Andreou, A., Haase, T., Jä Ckle, H., & Kü Hnlein, R. P. (n.d.). *Dual Lipolytic Control of Body Fat Storage and Mobilization in Drosophila*. https://doi.org/10.1371/journal.pbio.0050137.g001

Grover, S., Nebhinani, N., Chakrabarti, S., Avasthi, A., Kulhara, P., Basu, D., Mattoo, S. K., & Malhotra, S. (2014). Comparative study of prevalence of metabolic syndrome in bipolar disorder and schizophrenia from North India. *Nordic Journal of Psychiatry*, *68*(1), 72–77. https://doi.org/10.3109/08039488.2012.754052

Grundy, S. M., Cleeman, J. I., Daniels, S. R., Donato, K. A., Eckel, R. H., Franklin, B. A., Gordon, D. J., Krauss, R. M., Savage, P. J., Smith, S. C., Spertus, J. A., & Costa, F. (2005). Diagnosis and management of the metabolic syndrome: An American Heart Association/National Heart, Lung, and Blood Institute scientific statement. In *Circulation* (Vol. 112, Issue 17, pp. 2735–2752). https://doi.org/10.1161/CIRCULATIONAHA.105.169404

Gruntenko, N. E., Adonyeva, N. V., Burdina, E. V., Karpova, E. K., Andreenkova, O. V., Gladkikh, D. V., Ilinsky, Y. Y., & Rauschenbach, I. Y. (2016). The impact of FOXO on dopamine and octopamine metabolism in Drosophila under normal and heat stress conditions. *Biology Open*, *5*(11), 1706–1711. https://doi.org/10.1242/bio.022038

Gu, S., & Kay, M. A. (2010). *How do miRNAs mediate translational repression?* (Vol. 1). http://www.silencejournal.com/content/

Gual, P., le Marchand-Brustel, Y., & Tanti, J. F. (2005). Positive and negative regulation of insulin signaling through IRS-1 phosphorylation. *Biochimie*, *87*(1 SPEC. ISS.), 99–109. https://doi.org/10.1016/j.biochi.2004.10.019

Guella, I., Sequeira, A., Rollins, B., Morgan, L., Torri, F., van Erp, T. G. M., Myers, R. M., Barchas, J. D., Schatzberg, A. F., Watson, S. J., Akil, H., Bunney, W. E., Potkin, S. G., Macciardi, F., & Vawter, M. P. (2013). Analysis of miR-137 expression and rs1625579 in dorsolateral prefrontal cortex. *Journal of Psychiatric Research*, *47*(9), 1215–1221. https://doi.org/10.1016/j.jpsychires.2013.05.021

Gui, Y., Wang, L., & Huang, Z. (2021). MiR-137 inhibits cervical cancer progression via down-modulating Notch1 and inhibiting the PI3K/AKT/mTOR signaling pathway. *Translational Cancer Research*, *10*(8), 3748–3756. https://doi.org/10.21037/tcr-21-1049

Guo, L., Zhang, Q., Ma, X., Wang, J., & Liang, T. (2017). MiRNA and mRNA expression analysis reveals potential sex-biased miRNA expression. *Scientific Reports*, *7*. https://doi.org/10.1038/srep39812

Ha, M., Pang, M., Agarwal, V., & Chen, Z. J. (2008). Interspecies regulation of microRNAs and their targets. In *Biochimica et Biophysica Acta - Gene Regulatory Mechanisms* (Vol. 1779, Issue 11, pp. 735–742). https://doi.org/10.1016/j.bbagrm.2008.03.004

Hahm, E. T., Nagaraja, R. Y., Waro, G., & Tsunoda, S. (2018). Cholinergic Homeostatic Synaptic Plasticity Drives the Progression of Aβ-Induced Changes in Neural Activity. *Cell Reports*, *24*(2), 342–354. https://doi.org/10.1016/j.celrep.2018.06.029

Haj, F. G., Zabolotny, J. M., Kim, Y. B., Kahn, B. B., & Neel, B. G. (2005). Liver-specific protein-tyrosine phosphatase 1B (PTP1B) re-expression alters glucose homeostasis of PTP1B-/- mice. *Journal of Biological Chemistry*, *280*(15), 15038–15046. https://doi.org/10.1074/jbc.M413240200

Hall, C., Yu, H., & Choi, E. (2020). Insulin receptor endocytosis in the pathophysiology of insulin resistance. In *Experimental and Molecular Medicine* (Vol. 52, Issue 6, pp. 911–920). Springer Nature. https://doi.org/10.1038/s12276-020-0456-3

Hammond, S. M. (2015a). An overview of microRNAs. In *Advanced Drug Delivery Reviews* (Vol. 87, pp. 3–14). Elsevier B.V. https://doi.org/10.1016/j.addr.2015.05.001

Hammond, S. M. (2015b). An overview of microRNAs. In *Advanced Drug Delivery Reviews* (Vol. 87, pp. 3–14). Elsevier B.V. https://doi.org/10.1016/j.addr.2015.05.001

Hardy, C. M., Burke, M. K., Everett, L. J., Han, M. v., Lantz, K. M., & Gibbs, A. G. (2018). Genome-Wide Analysis of Starvation-Selected Drosophila melanogaster-A Genetic Model of Obesity. *Molecular Biology and Evolution*, *35*(1), 50–65. https://doi.org/10.1093/molbev/msx254

Harshman, L. G., & Haberer, B. A. (2000). Oxidative Stress Resistance: A Robust Correlated Response to Selection in Extended Longevity Lines of Drosophila melanogaster ? In *Journal of Gerontology: BIOLOGICAL SCIENCES Copyright* (Vol. 55, Issue 9). https://academic.oup.com/biomedgerontology/article/55/9/B415/2948047

Harshman, L. G., Hoffmann, A. A., & Clark, A. G. (1999a). Selection for starvation resistance in Drosophila melanogaster: Physiological correlates, enzyme activities and multiple stress responses. *Journal of Evolutionary Biology*, *12*(2), 370–379. https://doi.org/10.1046/j.1420-9101.1999.00024.x

Harshman, L. G., Hoffmann, A. A., & Clark, A. G. (1999b). Selection for starvation resistance in Drosophila melanogaster: Physiological correlates, enzyme activities and multiple stress responses. *Journal of Evolutionary Biology*, *12*(2), 370–379. https://doi.org/10.1046/j.1420-9101.1999.00024.x

Hatzihristidis, T., Desai, N., Hutchins, A. P., Meng, T. C., Tremblay, M. L., & Miranda-Saavedra, D. (2015). A Drosophila-centric view of protein tyrosine phosphatases. In *FEBS Letters* (Vol. 589, Issue 9, pp. 951–966). Elsevier B.V. https://doi.org/10.1016/j.febslet.2015.03.005

Hazell, S. P., & Bale, J. S. (2011). Low temperature thresholds: Are chill coma and CTmin synonymous? In *Journal of Insect Physiology* (Vol. 57, Issue 8, pp. 1085–1089). https://doi.org/10.1016/j.jinsphys.2011.04.004

He, E., Lozano, M. A. G., Stringer, S., Watanabe, K., Sakamoto, K., Oudsten, F. den, Koopmans, F., Giamberardino, S. N., Hammerschlag, A., Niels Cornelisse, L., Li, K. W., van Weering, J., Posthuma, D., Smit, A. B., Sullivan, P. F., & Verhage, M. (2018). MIR137 schizophrenia-associated locus controls synaptic function by regulating synaptogenesis, synapse maturation and synaptic transmission. *Human Molecular Genetics*, *27*(11), 1879–1891. https://doi.org/10.1093/hmg/ddy089

He, Q., Du, J., Wei, L., & Zhao, Z. (2020). AKH-FOXO pathway regulates starvation-induced sleep loss through remodeling of the small ventral lateral neuron dorsal projections. *PLoS Genetics*, *16*(10). https://doi.org/10.1371/journal.pgen.1009181

Henshall, D. C., Hamer, H. M., Pasterkamp, J., Goldstein, D. B., Kjems, J., Prehn, J. H. M., Schorge, S., Lamottke, K., & Rosenow, F. (2016). *Rapid Review MicroRNAs in epilepsy: pathophysiology and clinical utility* (Vol. 15). http://www.mirbase.org/

Hernandez-Sanchez, C., Blakesley, V., Kalebic, T., Helman, L., & LeRoith, D. (1995). The role of the tyrosine kinase domain of the insulin-like growth factor- I receptor in intracellular signaling, cellular proliferation, and tumorigenesis. *Journal of Biological Chemistry*, *270*(49), 29176–29181. https://doi.org/10.1074/jbc.270.49.29176

Hietakangas, V., & Cohen, S. M. (2009). Regulation of tissue growth through nutrient sensing. In *Annual Review of Genetics* (Vol. 43, pp. 389–410). https://doi.org/10.1146/annurev-genet-102108-134815

Holm, A., Possovre, M.-L., Bandarabadi, M., Moseholm, K. F., Justinussen, J. L., Bozic, I., Lemcke, R., Arribat, Y., Amati, F., Silahtaroglu, A., Juventin, M., Adamantidis, A., Tafti, M., Kornum, B. R., & by Joseph Takahashi, E. (2022). *The evolutionarily conserved miRNA-137 targets the neuropeptide hypocretin/orexin and modulates the wake to sleep ratio*. https://doi.org/10.1073/pnas

Holt, L. J., & Siddle, K. (2005). Grb10 and Grb14: enigmatic regulators of insulin action-and more? In *Biochem. J* (Vol. 388).

Howard, M. A., & Baraban, S. C. (2017). *Catastrophic Epilepsies of Childhood*. https://doi.org/10.1146/annurev-neuro-072116

Howell, K. R., & Law, A. J. (2020). Neurodevelopmental concepts of schizophrenia in the genome-wide association era: AKT/mTOR signaling as a pathological mediator of genetic and environmental programming during development. *Schizophrenia Research*, *217*, 95–104. https://doi.org/10.1016/j.schres.2019.08.036

Hu, Z., & Li, Z. (2017). miRNAs in synapse development and synaptic plasticity. In *Current Opinion in Neurobiology* (Vol. 45, pp. 24–31). Elsevier Ltd. https://doi.org/10.1016/j.conb.2017.02.014

Huang, J., & Manning, B. D. (2009). A complex interplay between Akt, TSC2 and the two mTOR complexes. In *Biochemical Society Transactions* (Vol. 37, Issue 1, pp. 217–222). https://doi.org/10.1042/BST0370217

Huang, L. (2006). Genetic dissection of developmental pathways. *WormBook*. https://doi.org/10.1895/wormbook.1.88.1

Huang, R., Song, T., Su, H., Lai, Z., Qin, W., Tian, Y., Dong, X., & Wang, L. (2020). High-fat diet enhances starvation-induced hyperactivity via sensitizing hunger-sensing neurons in drosophila. *ELife*, *9*. https://doi.org/10.7554/eLife.53103

Huang, Y., Wan, Z., Wang, Z., & Zhou, B. (2019). Insulin signaling in Drosophila melanogaster mediates Aβ toxicity. *Communications Biology*, *2*(1). https://doi.org/10.1038/s42003-018-0253-x

Huey, R. B., Suess, J., Hamilton, H., & Gilchrist, G. W. (2004). Starvation resistance in Drosophila melanogaster: Testing for a possible “cannibalism” bias. *Functional Ecology*, *18*(6), 952–954. https://doi.org/10.1111/j.0269-8463.2004.00915.x

Hypothalamic K(ATP) channels control hepatic glucose production. (n.d.).

Ibáñez-Ventoso, C., Vora, M., & Driscoll, M. (2008). Sequence relationships among C. elegans, D. melanogaster and human microRNAs highlight the extensive conservation of microRNAs in biology. *PLoS ONE*, *3*(7). https://doi.org/10.1371/journal.pone.0002818

icns_15_5-6_30. (n.d.).

Iijima, K., Chiang, H. C., Hearn, S. A., Hakker, I., Gatt, A., Shenton, C., Granger, L., Leung, A., Iijima-Ando, K., & Zhong, Y. (2008). Aβ42 mutants with different aggregation profiles induce distinct pathologies in Drosophila. *PLoS ONE*, *3*(2). https://doi.org/10.1371/journal.pone.0001703

Iijima, K., Liu, H.-P., Chiang, A.-S., Hearn, S. A., Konsolaki, M., & Zhong, Y. (2004). *Dissecting the pathological effects of human A40 and A42 in Drosophila: A potential model for Alzheimer’s disease*. www.pnas.orgcgidoi10.1073pnas.0400895101

Ion channels Opposite thermosensor in fruitfly and mouse. (2003). www.ico.org/frameset/coffset.htm

Jacinto, E., Facchinetti, V., Liu, D., Soto, N., Wei, S., Jung, S. Y., Huang, Q., Qin, J., & Su, B. (2006). SIN1/MIP1 Maintains rictor-mTOR Complex Integrity and Regulates Akt Phosphorylation and Substrate Specificity. *Cell*, *127*(1), 125–137. https://doi.org/10.1016/j.cell.2006.08.033

Jacob, A. I., Horovitz-Fried, M., Aga-Mizrachi, S., Brutman-Barazani, T., Okhrimenko, H., Zick, Y., Brodie, C., & Sampson, S. R. (2010). The regulatory domain of protein

kinase C delta positively regulates insulin receptor signaling. *Journal of Molecular Endocrinology*, *44*(3), 155–169. https://doi.org/10.1677/JME-09-0119

Jiang, Y., Liu, J., Chen, L., Jin, Y., Zhang, G., Lin, Z., Du, S., Fu, Z., Chen, T., Qin, Y., & Sun, X. (2019a). Serum secreted miR-137-containing exosomes affects oxidative stress of neurons by regulating OXR1 in Parkinson's disease. *Brain Research*, *1722*. https://doi.org/10.1016/j.brainres.2019.146331

Jiang, Y., Liu, J., Chen, L., Jin, Y., Zhang, G., Lin, Z., Du, S., Fu, Z., Chen, T., Qin, Y., & Sun, X. (2019b). Serum secreted miR-137-containing exosomes affects oxidative stress of neurons by regulating OXR1 in Parkinson's disease. *Brain Research*, *1722*. https://doi.org/10.1016/j.brainres.2019.146331

Jiang, Y., Xu, B., Chen, J., Sui, Y., Ren, L., Li, J., Zhang, H., Guo, L., & Sun, X. (2018). Micro-RNA-137 inhibits tau hyperphosphorylation in alzheimer's disease and targets the CACNA1C gene in transgenic mice and human neuroblastoma SH-SY5Y cells. *Medical Science Monitor*, *24*, 5635–5644. https://doi.org/10.12659/MSM.908765

Kadener, S., Menet, J. S., Sugino, K., Horwich, M. D., Weissbein, U., Nawathean, P., Vagin, V. v., Zamore, P. D., Nelson, S. B., & Rosbash, M. (2009). A role for microRNAs in the Drosophila circadian clock. *Genes and Development*, *23*(18), 2179–2191. https://doi.org/10.1101/gad.1819509

Kálmán, S., Garbett, K. A., Vereczkei, A., Shelton, R. C., Korade, Ž., & Mirnics, K. (2014). Metabolic stress-induced microRNA and mRNA expression profiles of human fibroblasts. *Experimental Cell Research*, *320*(2), 343–353. https://doi.org/10.1016/j.yexcr.2013.10.019

Kang, K., Panzano, V. C., Chang, E. C., Ni, L., Dainis, A. M., Jenkins, A. M., Regna, K., Muskavitch, M. A. T., & Garrity, P. A. (2012). Modulation of TRPA1 thermal sensitivity enables sensory discrimination in Drosophila. *Nature*, *481*(7379), 76–81. https://doi.org/10.1038/nature10715

Kannan, K., & Fridell, Y.-W. C. (2013). Functional implications of Drosophila insulin-like peptides in metabolism, aging, and dietary restriction. *Frontiers in Physiology*, *4*. https://doi.org/10.3389/fphys.2013.00288

Kapahi, P., & Zid, B. (2004). TOR pathway: linking nutrient sensing to life span. In *Science of aging knowledge environment : SAGE KE* (Vol. 2004, Issue 36). https://doi.org/10.1126/sageke.2004.36.pe34

Kashani, E., Hadizadeh, M., Chaleshi, V., Mirfakhraie, R., Young, C., Savabkar, S., Irani, S., Aghdaei, H. A., & Bonab, M. A. (2019). The differential DNA hypermethylation patterns of microRNA-137 and microRNA-342 locus in early colorectal lesions and tumours. *Biomolecules*, *9*(10). https://doi.org/10.3390/biom9100519

Kawecki, T. J., Erkosar, B., Dupuis, C., Hollis, B., Stillwell, R. C., & Kapun, M. (2021). The Genomic Architecture of Adaptation to Larval Malnutrition Points to a Trade-off with Adult Starvation Resistance in Drosophila. *Molecular Biology and Evolution*, *38*(7), 2732–2749. https://doi.org/10.1093/molbev/msab061

Kiltschewskij, D., & Cairns, M. J. (2019). Temporospatial guidance of activity-dependent gene expression by microRNA: Mechanisms and functional implications for neural plasticity. *Nucleic Acids Research*, *47*(2), 533–545. https://doi.org/10.1093/nar/gky1235

Kimura, K. D. ;, Tissenbaum, H. A. ;, Liu, Y. ;, & Ruvkun, G. (1997). daf-2, an insulin receptor-like gene that regulates longevity and diapause in Caenorhabditis elegans. In *Science* (Vol. 277).

Kinser, H. E., & Pincus, Z. (2020). MicroRNAs as modulators of longevity and the aging process. In *Human Genetics* (Vol. 139, Issue 3, pp. 291–308). Springer. https://doi.org/10.1007/s00439-019-02046-0

Kitamura, T., Kahn, C. R., & Accili, D. (2003). Insulin Receptor Knockout Mice. In *Annual Review of Physiology* (Vol. 65, pp. 313–332). https://doi.org/10.1146/annurev.physiol.65.092101.142540

Klepsatel, P., Wildridge, D., & Gáliková, M. (2019). Temperature induces changes in Drosophila energy stores. *Scientific Reports*, *9*(1). https://doi.org/10.1038/s41598-019-41754-5

Klinge, C. M. (2009). Estrogen Regulation of MicroRNA Expression. In *Current Genomics* (Vol. 10). http://www.nursa.org/index.cfm

Klinge, C. M. (2015). miRNAs regulated by estrogens, tamoxifen, and endocrine disruptors and their downstream gene targets. In *Molecular and Cellular Endocrinology* (Vol. 418, pp. 273–297). Elsevier Ireland Ltd. https://doi.org/10.1016/j.mce.2015.01.035

Kou, X., Chen, D., & Chen, N. (2020). The Regulation of microRNAs in Alzheimer's Disease. In *Frontiers in Neurology* (Vol. 11). Frontiers Media S.A. https://doi.org/10.3389/fneur.2020.00288

Kozan, D. W., Derrick, J. T., Ludington, W. B., & Farber, S. A. (2023). From worms to humans: Understanding intestinal lipid metabolism via model organisms. *Biochimica et Biophysica Acta - Molecular and Cell Biology of Lipids*, *1868*(4). https://doi.org/10.1016/j.bbalip.2023.159290

Krebs, D. L., Uren, R. T., Metcalf, D., Rakar, S., Zhang, J.-G., Starr, R., de Souza, D. P., Hanzinikolas, K., Eyles, J., Connolly, L. M., Simpson, R. J., Nicola, N. A., Nicholson, S. E., Baca, M., Hilton, D. J., & Alexander, W. S. (2002). SOCS-6 Binds to Insulin Receptor Substrate 4, and Mice Lacking the SOCS-6 Gene Exhibit Mild

Growth Retardation. *Molecular and Cellular Biology*, *22*(13), 4567–4578. https://doi.org/10.1128/mcb.22.13.4567-4578.2002

Kuebler, D., & Tanouye, M. A. (2000). *Modifications of Seizure Susceptibility in Drosophila*.

Kuehbacher, A., Urbich, C., Zeiher, A. M., & Dimmeler, S. (2007). Role of Dicer and Drosha for endothelial microRNA expression and angiogenesis. *Circulation Research*, *101*(1), 59–68. https://doi.org/10.1161/CIRCRESAHA.107.153916

Kühnlein, R. P. (2012). Thematic review series: Lipid droplet synthesis and metabolism: From Yeast to man. Lipid droplet-based storage fat metabolism in Drosophila. In *Journal of Lipid Research* (Vol. 53, Issue 8, pp. 1430–1436). https://doi.org/10.1194/jlr.R024299

Lagos-Quintana, M., Rauhut, R., Yalcin, A., Meyer, J., Lendeckel, W., & Tuschl, T. (2002). Identification of Tissue-Specific MicroRNAs from Mouse ated proteins from RNA degradation. These putative proteins may as well mediate the translational suppres-sion. The miRNA precursor processing reaction requires Department of Cellular Biochemistry Dicer RNase III and Argonaute family members [12-14]; Dicer and Argonaute proteins are also involved in. In *Current Biology* (Vol. 12).

Landgraf, P., Rusu, M., Sheridan, R., Sewer, A., Iovino, N., Aravin, A., Pfeffer, S., Rice, A., Kamphorst, A. O., Landthaler, M., Lin, C., Socci, N. D., Hermida, L., Fulci, V., Chiaretti, S., Foà, R., Schliwka, J., Fuchs, U., Novosel, A., … Tuschl, T. (2007). A Mammalian microRNA Expression Atlas Based on Small RNA Library Sequencing. *Cell*, *129*(7), 1401–1414. https://doi.org/10.1016/j.cell.2007.04.040

Langevin, S. M., Stone, R. A., Bunker, C. H., Grandis, J. R., Sobol, R. W., & Taioli, E. (2010). MicroRNA-137 promoter methylation in oral rinses from patients with squamous cell carcinoma of the head and neck is associated with gender and body mass index. *Carcinogenesis*, *31*(5), 864–870. https://doi.org/10.1093/carcin/bgq051

Lee, G., & Park, J. H. (n.d.). *Hemolymph Sugar Homeostasis and Starvation-Induced Hyperactivity Affected by Genetic Manipulations of the Adipokinetic Hormone-Encoding Gene in Drosophila melanogaster*. https://academic.oup.com/genetics/article/167/1/311/6050677

Lee, K. P., & Jang, T. (2014). Exploring the nutritional basis of starvation resistance in Drosophila melanogaster. *Functional Ecology*, *28*(5), 1144–1155. https://doi.org/10.1111/1365-2435.12247

Lee, R. C., Feinbaum, R. L., & Ambrost, V. (1993). The C. elegans Heterochronic Gene lin-4 Encodes Small RNAs with Antisense Complementarity to &II-14. In *Cell* (Vol. 75).

Lee, S., & Dong, H. H. (2017). FoxO integration of insulin signaling with glucose and lipid metabolism. In *Journal of Endocrinology* (Vol. 233, Issue 2, pp. R67–R79). BioScientifica Ltd. https://doi.org/10.1530/JOE-17-0002

Lee, Y., Ahn, C., Han, J., Choi, H., Kim, J., Yim, J., Lee, J., Provost, P., Rå Dmark, O., Kim, S., & Kim, V. N. (2003). *The nuclear RNase III Drosha initiates microRNA processing*. www.nature.com/nature

Lee, Y. H., Giraud, J., Davis, R. J., & White, M. F. (2003). c-Jun N-terminal kinase (JNK) mediates feedback inhibition of the insulin signaling cascade. *Journal of Biological Chemistry*, *278*(5), 2896–2902. https://doi.org/10.1074/jbc.M208359200

Leister, D., Herrmann, J. M., Angel Fernández-Moreno, M., Farr, C. L., Kaguni, L. S., & Garesse, R. (n.d.). Drosophila melanogaster as a Model System to Study Mitochondrial Biology. In *From: Methods in Molecular Biology* (Vol. 372). Mitochondria: Practical Protocols. http://www.sdbonline.org/

Leung, A. K. L., & Sharp, P. A. (2007). microRNAs: A Safeguard against Turmoil? In *Cell* (Vol. 130, Issue 4, pp. 581–585). Elsevier B.V. https://doi.org/10.1016/j.cell.2007.08.010

Leung, A. K. L., & Sharp, P. A. (2010a). MicroRNA Functions in Stress Responses. In *Molecular Cell* (Vol. 40, Issue 2, pp. 205–215). https://doi.org/10.1016/j.molcel.2010.09.027

Leung, A. K. L., & Sharp, P. A. (2010b). MicroRNA Functions in Stress Responses. In *Molecular Cell* (Vol. 40, Issue 2, pp. 205–215). https://doi.org/10.1016/j.molcel.2010.09.027

Lewis, B. P., Burge, C. B., & Bartel, D. P. (2005). Conserved seed pairing, often flanked by adenosines, indicates that thousands of human genes are microRNA targets. In *Cell* (Vol. 120, Issue 1, pp. 15–20). Cell Press. https://doi.org/10.1016/j.cell.2004.12.035

Li, J., & Liu, C. (2019). Coding or noncoding, the converging concepts of RNAs. In *Frontiers in Genetics* (Vol. 10, Issue MAY). Frontiers Media S.A. https://doi.org/10.3389/fgene.2019.00496

Li, L., He, Z., Zhu, C., Chen, S., Yang, Z., Xu, J., Bi, N., Yu, C., & Sun, C. (2020). MiR-137 promotes anoikis through modulating the AKT signaling pathways in Pancreatic Cancer. *Journal of Cancer*, *11*(21), 6277–6285. https://doi.org/10.7150/jca.44037

Li, Y. Z., di Cristofano, A., & Woo, M. (2020). Metabolic role of PTEN in insulin signaling and resistance. *Cold Spring Harbor Perspectives in Medicine*, *10*(8), 1–17. https://doi.org/10.1101/cshperspect.a036137

Lin, C.-C., Liu, L.-Z., Addison, J. B., Wonderlin, W. F., Ivanov, A. V., & Ruppert, J. M. (2011). A KLF4–miRNA-206 Autoregulatory Feedback Loop Can Promote or Inhibit Protein Translation Depending upon Cell Context. *Molecular and Cellular Biology*, *31*(12), 2513–2527. https://doi.org/10.1128/mcb.01189-10

Liu, N., Landreh, M., Cao, K., Abe, M., Hendriks, G. J., Kennerdell, J. R., Zhu, Y., Wang, L. S., & Bonini, N. M. (2012). The microRNA miR-34 modulates ageing and neurodegeneration in Drosophila. *Nature*, *482*(7386), 519–523. https://doi.org/10.1038/nature10810

Liu, N., Okamura, K., Tyler, D. M., Phillips, M. D., Chung, W. J., & Lai, E. C. (2008). The evolution and functional diversification of animal microRNA genes. In *Cell Research* (Vol. 18, Issue 10, pp. 985–996). https://doi.org/10.1038/cr.2008.278

Liu, P., Guo, Y., Xu, W., Song, S., Li, X., Wang, X., Lu, J., Guo, X., Richardson, H. E., & Ma, X. (2022). Ptp61F integrates Hippo, TOR, and actomyosin pathways to control three-dimensional organ size. *Cell Reports*, *41*(7). https://doi.org/10.1016/j.celrep.2022.111640

Liu, W. W., & Wilson, R. I. (2013). Glutamate is an inhibitory neurotransmitter in the Drosophila olfactory system. *Proceedings of the National Academy of Sciences of the United States of America*, *110*(25), 10294–10299. https://doi.org/10.1073/pnas.1220560110

Liu, Y., & Lehmann, M. (2006). FOXO-independent suppression of programmed cell death by the PI3K/Akt signaling pathway in Drosophila. *Development Genes and Evolution*, *216*(9), 531–535. https://doi.org/10.1007/s00427-006-0063-x

Lizcano, J. M., & Alessi, D. R. (n.d.). *The insulin signalling pathway*.

Loewith, R., Jacinto, E., Wullschleger, S., Lorberg, A., Crespo, J. L., bora Bonenfant, D., Oppliger, W., Jenoe, P., & Hall, M. N. (2002). Two TOR Complexes, Only One of which Is Rapamycin Sensitive, Have Distinct Roles in Cell Growth Control mycin-treated or TOR-depleted yeast cells display sev-eral physiological properties characteristic of starved or otherwise stressed cells, including an altered cell. In *Molecular Cell* (Vol. 10). Schmelzle and Hall. http://dove.embl-

Lopaczynski, W., Terry, C., & Nissley, P. (2000). Autophosphorylation of the insulin-like growth factor I receptor cytoplasmic domain. *Biochemical and Biophysical Research Communications*, *279*(3), 955–960. https://doi.org/10.1006/bbrc.2000.4046

Lu, J., & Clark, A. G. (2012). Impact of microRNA regulation on variation in human gene expression. *Genome Research*, *22*(7), 1243–1254. https://doi.org/10.1101/gr.132514.111

Lugli, G., Larson, J., Martone, M. E., Jones, Y., & Smalheiser, N. R. (2005). Dicer and eIF2c are enriched at postsynaptic densities in adult mouse brain and are modified

by neuronal activity in a calpain-dependent manner. *Journal of Neurochemistry*, *94*(4), 896–905. https://doi.org/10.1111/j.1471-4159.2005.03224.x

Luo, J., Becnel, J., Nichols, C. D., & Nässel, D. R. (2012). Insulin-producing cells in the brain of adult Drosophila are regulated by the serotonin 5-HT 1A receptor. *Cellular and Molecular Life Sciences*, *69*(3), 471–484. https://doi.org/10.1007/s00018-011-0789-0

MacMillan, H. A., Knee, J. M., Dennis, A. B., Udaka, H., Marshall, K. E., Merritt, T. J. S., & Sinclair, B. J. (2016). Cold acclimation wholly reorganizes the Drosophila melanogaster transcriptome and metabolome. *Scientific Reports*, *6*. https://doi.org/10.1038/srep28999

MacMillan, H. A., & Sinclair, B. J. (2011). Mechanisms underlying insect chill-coma. In *Journal of Insect Physiology* (Vol. 57, Issue 1, pp. 12–20). https://doi.org/10.1016/j.jinsphys.2010.10.004

Mahmoudi, E., & Cairns, M. J. (2017). MiR-137: An important player in neural development and neoplastic transformation. In *Molecular Psychiatry* (Vol. 22, Issue 1, pp. 44–55). Nature Publishing Group. https://doi.org/10.1038/mp.2016.150

Malsam, J., Satoh, A., Pelletier, L., & Warren, G. (2005). Golgin tethers define subpopulations of COPI vesicles. *Science*, *307*(5712), 1095–1098. https://doi.org/10.1126/science.1108061

Manning, B. D. (2004). Balancing Akt with S6K: Implications for both metabolic diseases and tumorigenesis. In *Journal of Cell Biology* (Vol. 167, Issue 3, pp. 399–403). https://doi.org/10.1083/jcb.200408161

Manoach, D. S., & Stickgold, R. (2015). Sleep, memory and schizophrenia. In *Sleep Medicine* (Vol. 16, Issue 5, pp. 553–554). Elsevier. https://doi.org/10.1016/j.sleep.2015.01.009

Marron, M. T., Markow, T. A., Kain, K. J., & Gibbs, A. G. (2003a). Effects of starvation and desiccation on energy metabolism in desert and mesic Drosophila. *Journal of Insect Physiology*, *49*(3), 261–270. https://doi.org/10.1016/S0022-1910(02)00287-1

Marron, M. T., Markow, T. A., Kain, K. J., & Gibbs, A. G. (2003b). Effects of starvation and desiccation on energy metabolism in desert and mesic Drosophila. *Journal of Insect Physiology*, *49*(3), 261–270. https://doi.org/10.1016/S0022-1910(02)00287-1

Masek, P., Reynolds, L. A., Bollinger, W. L., Moody, C., Mehta, A., Murakami, K., Yoshizawa, M., Gibbs, A. G., & Keene, A. C. (2014). Altered regulation of sleep and feeding contributes to starvation resistance in Drosophila melanogaster. *Journal of Experimental Biology*, *217*(17), 2123–2132. https://doi.org/10.1242/jeb.103309

Mazzelli, M., Maj, C., Mariani, N., Mora, C., Begni, V., Pariante, C. M., Riva, M. A., Cattaneo, A., & Cattane, N. (2020). The Long-Term Effects of Early Life Stress on

the Modulation of miR-19 Levels. *Frontiers in Psychiatry*, *11*. https://doi.org/10.3389/fpsyt.2020.00389

Meza-Sosa, K. F., Pedraza-Alva, G., & Pérez-Martínez, L. (2014). MicroRNAs: Key triggers of neuronal cell fate. *Frontiers in Cellular Neuroscience*, *8*(JUN). https://doi.org/10.3389/FNCEL.2014.00175/ABSTRACT

Miquel, J., Lundgren, P. R., Bensch, K. G., & Atlan, H. (1976). Printed in the Netherlands EFFECTS OF TEMPERATURE ON THE LIFE SPAN, VITALITY AND FINE STRUCTURE OF DROSOPHILA MELANOGASTER. In *Mechanisms of Ageing and Development* (Vol. 5).

Mirzoyan, Z., Sollazzo, M., Allocca, M., Valenza, A. M., Grifoni, D., & Bellosta, P. (2019). Drosophila melanogaster: A model organism to study cancer. In *Frontiers in Genetics* (Vol. 10). Frontiers Media S.A. https://doi.org/10.3389/fgene.2019.00051

Mochanová, M., Tomčala, A., Svobodová, Z., & Kodrík, D. (2018). Role of adipokinetic hormone during starvation in Drosophila. *Comparative Biochemistry and Physiology Part - B: Biochemistry and Molecular Biology*, *226*, 26–35. https://doi.org/10.1016/j.cbpb.2018.08.004

Mondol, V., & Pasquinelli, A. E. (2012). Let's Make It Happen. The Role of let-7 MicroRNA in Development. In *Current Topics in Developmental Biology* (Vol. 99, pp. 1–30). Academic Press Inc. https://doi.org/10.1016/B978-0-12-387038-4.00001-X

Moreira, F. P., Jansen, K., Cardoso, T. D. A., Mondin, T. C., Magalhães, P. V., Kapczinski, F., Souza, L. D. M., Da Silva, R. A., Oses, J. P., & Wiener, C. D. (2019). Metabolic syndrome and psychiatric disorders: A population-based study. *Revista Brasileira de Psiquiatria*, *41*(1), 38–43. https://doi.org/10.1590/1516-4446-2017-2328

Newell, N. R., Ray, S., Dalton, J. E., Fortier, J. C., Kao, J. Y., Chang, P. L., Nuzhdin, S. V., & Arbeitman, M. N. (2020). The drosophila post-mating response: Gene expression and behavioral changes reveal perdurance and variation in cross-tissue interactions. *G3: Genes, Genomes, Genetics*, *10*(3), 967–983. https://doi.org/10.1534/g3.119.400963

Ni, Y. G., Wang, N., Cao, D. J., Sachan, N., Morris, D. J., Gerard, R. D., Kuro-O §, M., Rothermel, B. A., Hill, J. A., & Reynolds, D. W. (2007). *FoxO transcription factors activate Akt and attenuate insulin signaling in heart by inhibiting protein phosphatases*. www.pnas.org/cgi/content/full/

Nichols, C. D., Becnel, J., & Pandey, U. B. (2012). Methods to Assay Drosophila Behavior. *Journal of Visualized Experiments*, *61*. https://doi.org/10.3791/3795

Nielsen, M. D., Luo, X., Biteau, B., Syverson, K., & Jasper, H. (2008). 14-3-3ε antagonizes FoxO to control growth, apoptosis and longevity in Drosophila. *Aging Cell*, *7*(5), 688–699. https://doi.org/10.1111/j.1474-9726.2008.00420.x

Nijhout, H. F., & McKenna, K. Z. (2018). The distinct roles of insulin signaling in polyphenic development. In *Current Opinion in Insect Science* (Vol. 25, pp. 58–64). Elsevier Inc. https://doi.org/10.1016/j.cois.2017.11.011

Ninova, M., Ronshaugen, M., & Griffiths-Jones, S. (2014). Conserved temporal patterns of microRNA expression in Drosophila support a developmental hourglass model. *Genome Biology and Evolution*, *6*(9), 2459–2467. https://doi.org/10.1093/gbe/evu183

Nowak, K., Seisenbacher, G., Hafen, E., & Stocker, H. (2013). Nutrient restriction enhances the proliferative potential of cells lacking the tumor suppressor PTEN in mitotic tissues. *ELife*, *2013*(2). https://doi.org/10.7554/eLife.00380

Nudelman, A. S., Dirocco, D. P., Lambert, T. J., Garelick, M. G., Le, J., Nathanson, N. M., & Storm, D. R. (2010). Neuronal activity rapidly induces transcription of the CREB-regulated microRNA-132, in vivo. *Hippocampus*, *20*(4), 492–498. https://doi.org/10.1002/hipo.20646

Nutrient-Dependent Expression of Insulin-like Peptides from Neuroendocrine Cells in the CNS Contributes to Growth Regulation in Drosophila median neurosecretory cells (m-NSCs) possessing axon. (n.d.).

O'Brien, J., Hayder, H., Zayed, Y., & Peng, C. (2018). Overview of microRNA biogenesis, mechanisms of actions, and circulation. In *Frontiers in Endocrinology* (Vol. 9, Issue AUG). Frontiers Media S.A. https://doi.org/10.3389/fendo.2018.00402

Olde Loohuis, N. F. M., Ba, W., Stoerchel, P. H., Kos, A., Jager, A., Schratt, G., Martens, G. J. M., van Bokhoven, H., Nadif Kasri, N., & Aschrafi, A. (2015a). MicroRNA-137 Controls AMPA-Receptor-Mediated Transmission and mGluR-Dependent LTD. *Cell Reports*, *11*(12), 1876–1884. https://doi.org/10.1016/j.celrep.2015.05.040

Olde Loohuis, N. F. M., Ba, W., Stoerchel, P. H., Kos, A., Jager, A., Schratt, G., Martens, G. J. M., van Bokhoven, H., Nadif Kasri, N., & Aschrafi, A. (2015b). MicroRNA-137 Controls AMPA-Receptor-Mediated Transmission and mGluR-Dependent LTD. *Cell Reports*, *11*(12), 1876–1884. https://doi.org/10.1016/j.celrep.2015.05.040

Olde Loohuis, N. F. M., Ba, W., Stoerchel, P. H., Kos, A., Jager, A., Schratt, G., Martens, G. J. M., van Bokhoven, H., Nadif Kasri, N., & Aschrafi, A. (2015c). MicroRNA-137 Controls AMPA-Receptor-Mediated Transmission and mGluR-Dependent LTD. *Cell Reports*, *11*(12), 1876–1884. https://doi.org/10.1016/j.celrep.2015.05.040

Oldham, S. (2011). Obesity and nutrient sensing TOR pathway in flies and vertebrates: Functional conservation of genetic mechanisms. In *Trends in Endocrinology and Metabolism* (Vol. 22, Issue 2, pp. 45–52). https://doi.org/10.1016/j.tem.2010.11.002

Olejniczak, M., Kotowska-Zimmer, A., & Krzyzosiak, W. (2018). Stress-induced changes in miRNA biogenesis and functioning. In *Cellular and Molecular Life Sciences* (Vol. 75, Issue 2, pp. 177–191). Birkhauser Verlag AG. https://doi.org/10.1007/s00018-017-2591-0

Oliver, P. L., Finelli, M. J., Edwards, B., Bitoun, E., Butts, D. L., Becker, E. B. E., Cheeseman, M. T., Davies, B., & Davies, K. E. (2011). Oxr1 is essential for protection against oxidative stress-induced neurodegeneration. *PLoS Genetics*, *7*(10). https://doi.org/10.1371/journal.pgen.1002338

Olson, L. F., Troty, C. L., Schaffer, W. M., Harrison, R. G., Biswas, D. J., Rapp, P. E., Holden, A. V, Babbyantz, A., Destenhe, A., Gokibeqec, A. L., Rigney, D. R., Mietus, J., Autman, E. M., Greenwald, S., &finkel, A., Kaneko, K., Cuyton, A. C., Coleman, T. C., Cowlay, A. W., … May, R. M. (1986). R455-R466 24 Pool, R. (19B9) Scicncr 243,25-2B 25 van Roasum. In *Pmt. Neff Acnd. Sci. USA* (Vol. 33). Manchester univemily Press 20 GoldberBec.

Orang, A. V., Safaralizadeh, R., & Kazemzadeh-Bavili, M. (2014). Mechanisms of miRNA-mediated gene regulation from common downregulation to mRNA-specific upregulation. In *International Journal of Genomics* (Vol. 2014). Hindawi Limited. https://doi.org/10.1155/2014/970607

Ørom, U. A., Nielsen, F. C., & Lund, A. H. (2008). MicroRNA-10a Binds the 5′UTR of Ribosomal Protein mRNAs and Enhances Their Translation. *Molecular Cell*, *30*(4), 460–471. https://doi.org/10.1016/j.molcel.2008.05.001

Pacheco, A., Berger, R., Freedman, R., & Law, A. J. (2019). A VNTR Regulates miR-137 Expression Through Novel Alternative Splicing and Contributes to Risk for Schizophrenia. *Scientific Reports*, *9*(1). https://doi.org/10.1038/s41598-019-48141-0

Padmanabhan, S., Mukhopadhyay, A., Narasimhan, S. D., Tesz, G., Czech, M. P., & Tissenbaum, H. A. (2009). A PP2A Regulatory Subunit Regulates C. elegans Insulin/IGF-1 Signaling by Modulating AKT-1 Phosphorylation. *Cell*, *136*(5), 939–951. https://doi.org/10.1016/j.cell.2009.01.025

Pallares-Cartes, C., Cakan-Akdogan, G., & Teleman, A. A. (2012). Tissue-Specific Coupling between Insulin/IGF and TORC1 Signaling via PRAS40 in Drosophila. *Developmental Cell*, *22*(1), 172–182. https://doi.org/10.1016/j.devcel.2011.10.029

Park, J. E., Lee, E. J., Kim, J. K., Song, Y., Choi, J. H., & Kang, M. J. (2018). Flightless-I controls fat storage in drosophila. *Molecules and Cells*, *41*(6), 603–611. https://doi.org/10.14348/molcells.2018.0120

Parkash, R., Ranga, P., & Aggarwal, D. D. (2014). Developmental acclimation to low or high humidity conditions affect starvation and heat resistance of Drosophila melanogaster. *Comparative Biochemistry and Physiology -Part A : Molecular and Integrative Physiology*, *175*(1), 46–56. https://doi.org/10.1016/j.cbpa.2014.05.006

Parker, L., Howlett, I. C., Rusan, Z. M., & Tanouye, M. A. (2011). Seizure and epilepsy: Studies of seizure disorders in drosophila. In *International Review of Neurobiology* (Vol. 99, pp. 1–21). Academic Press Inc. https://doi.org/10.1016/B978-0-12-387003-2.00001-X

Parker, L., Padilla, M., Du, Y., Dong, K., & Tanouye, M. A. (2011a). Drosophila as a model for epilepsy: bss is a gain-of-function mutation in the para sodium channel gene that leads to seizures. *Genetics*, *187*(2), 523–534. https://doi.org/10.1534/genetics.110.123299

Parker, L., Padilla, M., Du, Y., Dong, K., & Tanouye, M. A. (2011b). Drosophila as a model for epilepsy: bss is a gain-of-function mutation in the para sodium channel gene that leads to seizures. *Genetics*, *187*(2), 523–534. https://doi.org/10.1534/genetics.110.123299

Peng, Y., & Croce, C. M. (2016). The role of microRNAs in human cancer. In *Signal Transduction and Targeted Therapy* (Vol. 1). Springer Nature. https://doi.org/10.1038/sigtrans.2015.4

Perez-Reyes, Wei, Castellano, X., & Brown, A. &. (1998). letters to nature 900 Identification and mapping of human cDNAs homologous to Drosophila mutant genes through EST database searches A new algorithm for idealizing single ion channel data containing multiple unknown conductance levels. In *J. Pharmacol. Exp. Ther* (Vol. 391). www.hgmp.mrc.ac.uk/cgi-bin/contig/rhmapper.pl.

Peterson, S. M., Thompson, J. A., Ufkin, M. L., Sathyanarayana, P., Liaw, L., & Congdon, C. B. (2014). Common features of microRNA target prediction tools. In *Frontiers in Genetics* (Vol. 5, Issue FEB). Frontiers Research Foundation. https://doi.org/10.3389/fgene.2014.00023

Petti, A. A., Crutchfield, C. A., Rabinowitz, J. D., & Botstein, D. (2011a). Survival of starving yeast is correlated with oxidative stress response and nonrespiratory mitochondrial function. *Proceedings of the National Academy of Sciences of the United States of America*, *108*(45). https://doi.org/10.1073/pnas.1101494108

Petti, A. A., Crutchfield, C. A., Rabinowitz, J. D., & Botstein, D. (2011b). Survival of starving yeast is correlated with oxidative stress response and nonrespiratory mitochondrial function. *Proceedings of the National Academy of Sciences of the United States of America*, *108*(45). https://doi.org/10.1073/pnas.1101494108

Ping, Y., Hahm, E. T., Waro, G., Song, Q., Vo-Ba, D. A., Licursi, A., Bao, H., Ganoe, L., Finch, K., & Tsunoda, S. (2015). Linking Aβ42-Induced Hyperexcitability to

Neurodegeneration, Learning and Motor Deficits, and a Shorter Lifespan in an Alzheimer's Model. *PLoS Genetics*, *11*(3). https://doi.org/10.1371/journal.pgen.1005025

Pool, A. H., & Scott, K. (2014). Feeding regulation in Drosophila. In *Current Opinion in Neurobiology* (Vol. 29, pp. 57–63). Elsevier Ltd. https://doi.org/10.1016/j.conb.2014.05.008

Puig, O., Marr, M. T., Ruhf, M. L., & Tjian, R. (2003). Control of cell number by Drosophila FOXO: Downstream and feedback regulation of the insulin receptor pathway. *Genes and Development*, *17*(16), 2006–2020. https://doi.org/10.1101/gad.1098703

Qiu, S., Xiao, C., & Meldrum Robertson, R. (2017). Different age-dependent performance in Drosophila wild-type Canton-S and the white mutant w1118 flies. *Comparative Biochemistry and Physiology -Part A : Molecular and Integrative Physiology*, *206*, 17–23. https://doi.org/10.1016/j.cbpa.2017.01.003

Reduced Body Size in chico Mutants Is Due. (n.d.-a).

Reduced Body Size in chico Mutants Is Due. (n.d.-b).

Regazzetti, C., Peraldi, P., Grémeaux, T., Najem-Lendom, R., Ben-Sahra, I., Cormont, M., Bost, F., Marchand-Brustel, Y. le, Tanti, J. F., & Giorgetti-Peraldi, S. (2009). Hypoxia decreases insulin signaling pathways in adipocytes. *Diabetes*, *58*(1), 95–103. https://doi.org/10.2337/db08-0457

Rehman, N., & Varghese, J. (2021a). Larval nutrition influences adult fat stores and starvation resistance in Drosophila. *PLoS ONE*, *16*(2 February 2021). https://doi.org/10.1371/journal.pone.0247175

Rehman, N., & Varghese, J. (2021b). Larval nutrition influences adult fat stores and starvation resistance in Drosophila. *PLoS ONE*, *16*(2 February 2021). https://doi.org/10.1371/journal.pone.0247175

Reinhart et al., 2000. (n.d.).

Reiter, L. T., Potocki, L., Chien, S., Gribskov, M., & Bier, E. (2001). A systematic analysis of human disease-associated gene sequences in Drosophila melanogaster. *Genome Research*, *11*(6), 1114–1125. https://doi.org/10.1101/gr.169101

Remenyi, J., van den Bosch, M. W. M., Palygin, O., Mistry, R. B., McKenzie, C., Macdonald, A., Hutvagner, G., Arthur, J. S. C., Frenguelli, B. G., & Pankratov, Y. (2013). miR-132/212 Knockout Mice Reveal Roles for These miRNAs in Regulating Cortical Synaptic Transmission and Plasticity. *PLoS ONE*, *8*(4). https://doi.org/10.1371/journal.pone.0062509

Rion, S., & Kawecki, T. J. (2007). Evolutionary biology of starvation resistance: What we have learned from Drosophila. In *Journal of Evolutionary Biology* (Vol. 20, Issue 5, pp. 1655–1664). https://doi.org/10.1111/j.1420-9101.2007.01405.x

Ripke, S., Sanders, A. R., Kendler, K. S., Levinson, D. F., Sklar, P., Holmans, P. A., Lin, D. Y., Duan, J., Ophoff, R. A., Andreassen, O. A., Scolnick, E., Cichon, S., st. Clair, D., Corvin, A., Gurling, H., Werge, T., Rujescu, D., Blackwood, D. H. R., Pato, C. N., … Gejman, P. v. (2011). Genome-wide association study identifies five new schizophrenia loci. *Nature Genetics*, *43*(10), 969–978. https://doi.org/10.1038/ng.940

Roessingh, S., & Stanewsky, R. (2017). The drosophila TRPA1 channel and neuronal circuits controlling rhythmic behaviours and sleep in response to environmental temperature. In *International Journal of Molecular Sciences* (Vol. 18, Issue 10). MDPI AG. https://doi.org/10.3390/ijms18102028

Ruan, Y., Chen, C., Cao, Y., & Garofalo, R. S. (1995). The Drosophila insulin receptor contains a novel carboxyl-terminal extension likely to play an important role in signal transduction. *Journal of Biological Chemistry*, *270*(9), 4236–4243. https://doi.org/10.1074/jbc.270.9.4236

Ruby, J. G., Jan, C., Player, C., Axtell, M. J., Lee, W., Nusbaum, C., Ge, H., & Bartel, D. P. (2006). Large-Scale Sequencing Reveals 21U-RNAs and Additional MicroRNAs and Endogenous siRNAs in C. elegans. *Cell*, *127*(6), 1193–1207. https://doi.org/10.1016/j.cell.2006.10.040

Ruby, J. G., Stark, A., Johnston, W. K., Kellis, M., Bartel, D. P., & Lai, E. C. (2007). Evolution, biogenesis, expression, and target predictions of a substantially expanded set of Drosophila microRNAs. *Genome Research*, *17*(12), 1850–1864. https://doi.org/10.1101/gr.6597907

Rudrapatna, V. A., Cagan, R. L., & Das, T. K. (2012). Drosophila cancer models. In *Developmental Dynamics* (Vol. 241, Issue 1, pp. 107–118). https://doi.org/10.1002/dvdy.22771

Rulifson, E. J., Kim, S. K., & Nusse, R. (2002). Ablation of insulin-producing neurons in files: Growth and diabetic phenotypes. *Science*, *296*(5570), 1118–1120. https://doi.org/10.1126/science.1070058

Rzezniczak, T. Z., Douglas, L. A., Watterson, J. H., & Merritt, T. J. S. (2011). Paraquat administration in Drosophila for use in metabolic studies of oxidative stress. *Analytical Biochemistry*, *419*(2), 345–347. https://doi.org/10.1016/j.ab.2011.08.023

Saha, S., Chant, D., & Mcgrath, J. (2007). A Systematic Review of Mortality in Schizophrenia Is the Differential Mortality Gap Worsening Over Time? Population-based studies that re-ported primary data on deaths in people with schizo-phrenia. In *Arch Gen Psychiatry* (Vol. 64, Issue 10).

Sakamoto, K., & Crowley, J. J. (2018a). A comprehensive review of the genetic and biological evidence supports a role for MicroRNA-137 in the etiology of schizophrenia. In *American Journal of Medical Genetics, Part B: Neuropsychiatric Genetics* (Vol. 177, Issue 2, pp. 242–256). Blackwell Publishing Inc. https://doi.org/10.1002/ajmg.b.32554

Sakamoto, K., & Crowley, J. J. (2018b). A comprehensive review of the genetic and biological evidence supports a role for MicroRNA-137 in the etiology of schizophrenia. In *American Journal of Medical Genetics, Part B: Neuropsychiatric Genetics* (Vol. 177, Issue 2, pp. 242–256). Blackwell Publishing Inc. https://doi.org/10.1002/ajmg.b.32554

Salmeen, A., Andersen, J. N., Myers, M. P., Tonks, N. K., & Barford, D. (2000). Molecular Basis for the Dephosphorylation of the Activation Segment of the Insulin Receptor by Protein Tyrosine Phosphatase 1B quired for maximal activation (White et al., 1988). Follow-ing activation, additional autophosphorylation reactions occur in the juxtamembrane segment and the C-terminal tail of the subunit. IRK-catalyzed phosphorylation of proteins, such as IRS-1 and IRS-2, creates high-affinity. In *Molecular Cell* (Vol. 6).

Salvaterra2, P. M., & Mccaman, R. E. (1985). Choline Acetyltransferase and Acetylcholine Levels in Drosophila Melanogaster: A Study Using Two Temperature-sensitive Mutants'. In *The Journal of Neurosci ence* (Vol. 5, Issue 4).

Saul, M. C., Zhao, C., Driessen, T. M., Eisinger, B. E., & Gammie, S. C. (2016). MicroRNA expression is altered in lateral septum across reproductive stages. *Neuroscience*, *312*, 130–140. https://doi.org/10.1016/j.neuroscience.2015.11.019

Scanga, S. E., Ruel, L., Binari, R. C., Snow, B., Stambolic, V., Bouchard, D., Peters, M., Calvieri, B., Mak, T. W., Woodgett, J. R., & Manoukian, A. S. (n.d.). *The conserved PI3'K/PTEN/Akt signaling pathway regulates both cell size and survival in Drosophila*. www.nature.com/onc

Schanen, B. C., & Li, X. (2011). Transcriptional regulation of mammalian miRNA genes. In *Genomics* (Vol. 97, Issue 1, pp. 1–6). https://doi.org/10.1016/j.ygeno.2010.10.005

Schooneveld, H., Tesser, G. I., Veenstra, J. A., & Romberg-Privee, H. M. (1983). Cell and Tissue Research Adipokinetic hormone and AKH-like peptide demonstrated in the corpora cardiaca and nervous system of Locusta migratoria by immunocytochemistry. In *Cell Tissue Res* (Vol. 230).

Semaniuk, U., Piskovatska, V., Strilbytska, O., Strutynska, T., Burdyliuk, N., Vaiserman, A., Bubalo, V., Storey, K. B., & Lushchak, O. (2021). Drosophila insulin-like peptides: from expression to functions – a review. In *Entomologia Experimentalis et Applicata* (Vol. 169, Issue 2, pp. 195–208). Blackwell Publishing Ltd. https://doi.org/10.1111/eea.12981

Semaniuk, U., Strilbytska, O., Malinovska, K., Storey, K. B., Vaiserman, A., Lushchak, V., & Lushchak, O. (2021). Factors that regulate expression patterns of insulin-like peptides and their association with physiological and metabolic traits in Drosophila. In *Insect Biochemistry and Molecular Biology* (Vol. 135). Elsevier Ltd. https://doi.org/10.1016/j.ibmb.2021.103609

Semple, R. K., Savage, D. B., Cochran, E. K., Gorden, P., & O'Rahilly, S. (2011). Genetic syndromes of severe insulin resistance. In *Endocrine Reviews* (Vol. 32, Issue 4, pp. 498–514). https://doi.org/10.1210/er.2010-0020

Sharma, S., & Eghbali, M. (2014). Influence of sex differences on microRNA gene regulation in disease. In *Biology of Sex Differences* (Vol. 5, Issue 1). BioMed Central Ltd. https://doi.org/10.1186/2042-6410-5-3

Shi, B., Gao, W., & Wang, J. (2012). Sequence Fingerprints of MicroRNA Conservation. *PLoS ONE*, *7*(10). https://doi.org/10.1371/journal.pone.0048256

Siegert, S., Seo, J., Kwon, E. J., Rudenko, A., Cho, S., Wang, W., Flood, Z., Martorell, A. J., Ericsson, M., Mungenast, A. E., & Tsai, L. H. (2015a). The schizophrenia risk gene product miR-137 alters presynaptic plasticity. *Nature Neuroscience*, *18*(7), 1008–1016. https://doi.org/10.1038/nn.4023

Siegert, S., Seo, J., Kwon, E. J., Rudenko, A., Cho, S., Wang, W., Flood, Z., Martorell, A. J., Ericsson, M., Mungenast, A. E., & Tsai, L. H. (2015b). The schizophrenia risk gene product miR-137 alters presynaptic plasticity. *Nature Neuroscience*, *18*(7), 1008–1016. https://doi.org/10.1038/nn.4023

Silber, J., Lim, D. A., Petritsch, C., Persson, A. I., Maunakea, A. K., Yu, M., Vandenberg, S. R., Ginzinger, D. G., James, C. D., Costello, J. F., Bergers, G., Weiss, W. A., Alvarez-Buylla, A., & Hodgson, J. G. (2008). miR-124 and miR-137 inhibit proliferation of glioblastoma multiforme cells and induce differentiation of brain tumor stem cells. *BMC Medicine*, *6*. https://doi.org/10.1186/1741-7015-6-14

Sim, S. E., Bakes, J., & Kaang, B. K. (2014). Neuronal activity-dependent regulation of MicroRNAs. In *Molecules and cells* (Vol. 37, Issue 7, pp. 511–517). https://doi.org/10.14348/molcells.2014.0132

Siomi, H., & Siomi, M. C. (2009). On the road to reading the RNA-interference code. In *Nature* (Vol. 457, Issue 7228, pp. 396–404). https://doi.org/10.1038/nature07754

Slack, F. J., Basson, M., Liu, Z., Ambros, V., Robert Horvitz, H., Ruvkun, G., Way, K., South, S., & Francisco, C. 94080. (2000). The lin-14 gene regulates cell fate decisions during Massachusetts General Hospital the early larval stages by generating a temporal gradient of LIN-14 protein during the L1 stage (Ruvkun and Gi-(Reinhart et al., 2000) and the larval lethal phenotypes The suppression of a lethal 6 Present address: Department of Cell Biology and Molecular Genet-

phenotype provides a powerful selection for new hetero-We performed F1 and F2 screens for mutations that. In *Molecular Cell* (Vol. 5).

Smrt, R. D., Szulwach, K. E., Pfeiffer, R. L., Li, X., Guo, W., Pathania, M., Teng, Z. Q., Luo, Y., Peng, J., Bordey, A., Jin, P., & Zhao, X. (2010a). MicroRNA miR-137 regulates neuronal maturation by targeting ubiquitin ligase mind bomb-1. *Stem Cells (Dayton, Ohio)*, *28*(6), 1060–1070. https://doi.org/10.1002/stem.431

Smrt, R. D., Szulwach, K. E., Pfeiffer, R. L., Li, X., Guo, W., Pathania, M., Teng, Z. Q., Luo, Y., Peng, J., Bordey, A., Jin, P., & Zhao, X. (2010b). MicroRNA miR-137 regulates neuronal maturation by targeting ubiquitin ligase mind bomb-1. *Stem Cells (Dayton, Ohio)*, *28*(6), 1060–1070. https://doi.org/10.1002/stem.431

Smrt, R. D., Szulwach, K. E., Pfeiffer, R. L., Li, X., Guo, W., Pathania, M., Teng, Z. Q., Luo, Y., Peng, J., Bordey, A., Jin, P., & Zhao, X. (2010c). MicroRNA miR-137 regulates neuronal maturation by targeting ubiquitin ligase mind bomb-1. *Stem Cells (Dayton, Ohio)*, *28*(6), 1060–1070. https://doi.org/10.1002/stem.431

Soeda, Y., Tsuneki, H., Muranaka, H., Mori, N., Hosoh, S., Ichihara, Y., Kagawa, S., Wang, X., Toyooka, N., Takamura, Y., Uwano, T., Nishijo, H., Wada, T., & Sasaoka, T. (2010). The inositol phosphatase SHIP2 negatively regulates insulin/IGF-I actions implicated in neuroprotection and memory function in mouse brain. *Molecular Endocrinology*, *24*(10), 1965–1977. https://doi.org/10.1210/me.2010-0163

Song, J., & Tanouye, M. A. (n.d.). *From bench to drug: Human seizure modeling using Drosophila*.

Stark, A., Brennecke, J., Bushati, N., Russell, R. B., & Cohen, S. M. (2005). Animal microRNAs confer robustness to gene expression and have a significant impact on 3′UTR evolution. *Cell*, *123*(6), 1133–1146. https://doi.org/10.1016/j.cell.2005.11.023

Statello, L., Guo, C. J., Chen, L. L., & Huarte, M. (2021). Gene regulation by long non-coding RNAs and its biological functions. In *Nature Reviews Molecular Cell Biology* (Vol. 22, Issue 2, pp. 96–118). Nature Research. https://doi.org/10.1038/s41580-020-00315-9

Strazisar, M., Cammaerts, S., van der Ven, K., Forero, D. A., Lenaerts, A. S., Nordin, A., Almeida-Souza, L., Genovese, G., Timmerman, V., Liekens, A., de Rijk, P., Adolfsson, R., Callaerts, P., & Del-Favero, J. (2015). MIR137 variants identified in psychiatric patients affect synaptogenesis and neuronal transmission gene sets. *Molecular Psychiatry*, *20*(4), 472–481. https://doi.org/10.1038/mp.2014.53

Strilbytska, O. M., Semaniuk, U. V., Storey, K. B., Yurkevych, I. S., & Lushchak, O. (2020). Insulin Signaling in Intestinal Stem and Progenitor Cells as an Important Determinant of Physiological and Metabolic Traits in Drosophila. *Cells*, *9*(4). https://doi.org/10.3390/cells9040803

Sun, G., Ye, P., Murai, K., Lang, M. F., Li, S., Zhang, H., Li, W., Fu, C., Yin, J., Wang, A., Ma, X., & Shi, Y. (2011). MiR-137 forms a regulatory loop with nuclear receptor TLX and LSD1 in neural stem cells. *Nature Communications*, *2*(1). https://doi.org/10.1038/ncomms1532

Szulwach, K. E., Li, X., Smrt, R. D., Li, Y., Luo, Y., Lin, L., Santistevan, N. J., Li, W., Zhao, X., & Jin, P. (2010). Cross talk between microRNA and epigenetic regulation in adult neurogenesis. *Journal of Cell Biology*, *189*(1), 127–141. https://doi.org/10.1083/jcb.200908151

Takagawa, K., & Salvaterra, P. (1996). NEUROSCI ENCE RESERRCH Analysis of choline acetyltransferase protein in temperature sensitive mutant flies using newly generated monoclonal antibody. In *Neuroscience Research* (Vol. 24). ELSEVIER.

Tatar, M., Kopelman, A., Epstein, ^ D, Tu, M.-P., Yin, C.-M., & Garofalo^, =^ R S. (n.d.). *A Mutant Drosophila Insulin Receptor Homolog That Extends Life-Span and impairs Neuroendocrine Function*. www.5dencemag.org

Tchankouo-Nguetcheu, S., Udinotti, M., Durand, M., Meng, T. C., Taouis, M., & Rabinow, L. (2014). Negative regulation of MAP kinase signaling in Drosophila by Ptp61F/PTP1B. *Molecular Genetics and Genomics : MGG*, *289*(5), 795–806. https://doi.org/10.1007/s00438-014-0852-2

Teleman, A. A., Chen, Y. W., & Cohen, S. M. (2005a). 4E-BP functions as a metabolic brake used under stress conditions but not during normal growth. *Genes and Development*, *19*(16), 1844–1848. https://doi.org/10.1101/gad.341505

Teleman, A. A., Chen, Y. W., & Cohen, S. M. (2005b). 4E-BP functions as a metabolic brake used under stress conditions but not during normal growth. *Genes and Development*, *19*(16), 1844–1848. https://doi.org/10.1101/gad.341505

Teleman, A. A., & Cohen, S. M. (2006). Drosophila lacking microRNA miR-278 are defective in energy homeostasis. *Genes and Development*, *20*(4), 417–422. https://doi.org/10.1101/gad.374406

Teleman, A. A., Hietakangas, V., Sayadian, A. C., & Cohen, S. M. (2008). Nutritional Control of Protein Biosynthetic Capacity by Insulin via Myc in Drosophila. *Cell Metabolism*, *7*(1), 21–32. https://doi.org/10.1016/j.cmet.2007.11.010

Tennessen, J. M., Barry, W. E., Cox, J., & Thummel, C. S. (2014). Methods for studying metabolism in Drosophila. *Methods*, *68*(1), 105–115. https://doi.org/10.1016/j.ymeth.2014.02.034

Tettweiler, G., Miron, M., Jenkins, M., Sonenberg, N., & Lasko, P. F. (2005a). Starvation and oxidative stress resistance in Drosophila are mediated through the eIF4E-binding protein, d4E-BP. *Genes and Development*, *19*(16), 1840–1843. https://doi.org/10.1101/gad.1311805

Tettweiler, G., Miron, M., Jenkins, M., Sonenberg, N., & Lasko, P. F. (2005b). Starvation and oxidative stress resistance in Drosophila are mediated through the eIF4E-binding protein, d4E-BP. *Genes and Development*, *19*(16), 1840–1843. https://doi.org/10.1101/gad.1311805

Thalyana, S. V., & Slack, F. J. (2012). MicroRNAs and their roles in aging. In *Journal of Cell Science* (Vol. 125, Issue 1, pp. 7–17). https://doi.org/10.1242/jcs.099200

Thomas, K. T., Anderson, B. R., Shah, N., Zimmer, S. E., Hawkins, D., Valdez, A. N., Gu, Q., & Bassell, G. J. (2017). Inhibition of the Schizophrenia-Associated MicroRNA miR-137 Disrupts Nrg1α Neurodevelopmental Signal Transduction. *Cell Reports*, *20*(1), 1–12. https://doi.org/10.1016/j.celrep.2017.06.038

Thomas, K. T., Gross, C., & Bassell, G. J. (2018). MicroRNAs sculpt neuronal communication in a tight balance that is lost in neurological disease. In *Frontiers in Molecular Neuroscience* (Vol. 11). Frontiers Media S.A. https://doi.org/10.3389/fnmol.2018.00455

Tiganis, T. (2013). PTP1B and TCPTP - Nonredundant phosphatases in insulin signaling and glucose homeostasis. In *FEBS Journal* (Vol. 280, Issue 2, pp. 445–458). https://doi.org/10.1111/j.1742-4658.2012.08563.x

Toprak, U. (2020). The Role of Peptide Hormones in Insect Lipid Metabolism. In *Frontiers in Physiology* (Vol. 11). Frontiers Media S.A. https://doi.org/10.3389/fphys.2020.00434

Tsai, N. P., Lin, Y. L., & Wei, L. N. (2009). MicroRNA mir-346 targets the 5′-untranslated region of receptor-interacting protein 140 (RIP140) mRNA and up-regulates its protein expression. *Biochemical Journal*, *424*(3), 411–418. https://doi.org/10.1042/BJ20090915

Tsokanos, F., Albert, M., Demetriades, C., Spirohn, K., Boutros, M., & Teleman, A. A. (2016). eIF 4A inactivates TORC 1 in response to amino acid starvation . *The EMBO Journal*, *35*(10), 1058–1076. https://doi.org/10.15252/embj.201593118

Ueki, K., Kondo, T., & Kahn, C. R. (2004). Suppressor of Cytokine Signaling 1 (SOCS-1) and SOCS-3 Cause Insulin Resistance through Inhibition of Tyrosine Phosphorylation of Insulin Receptor Substrate Proteins by Discrete Mechanisms. *Molecular and Cellular Biology*, *24*(12), 5434–5446. https://doi.org/10.1128/mcb.24.12.5434-5446.2004

Um, S. H., D'Alessio, D., & Thomas, G. (2006). Nutrient overload, insulin resistance, and ribosomal protein S6 kinase 1, S6K1. In *Cell Metabolism* (Vol. 3, Issue 6, pp. 393–402). https://doi.org/10.1016/j.cmet.2006.05.003

van Rooij, E., Sutherland, L. B., Qi, X., Richardson, J. A., Hill, J., & Olson, E. N. (n.d.). *Control of Stress-Dependent Cardiac Growth and Gene Expression by a MicroRNA*. https://www.science.org

Varghese, J., Lim, S. F., & Cohen, S. M. (2010). Drosophila miR-14 regulates insulin production and metabolism through its target, sugarbabe. *Genes and Development*, *24*(24), 2748–2753. https://doi.org/10.1101/gad.1995910

Vasudevan, S. (2012). Posttranscriptional Upregulation by MicroRNAs. In *Wiley Interdisciplinary Reviews: RNA* (Vol. 3, Issue 3, pp. 311–330). https://doi.org/10.1002/wrna.121

Venkatachalam, K., Luo, J., & Montell, C. (2014). Evolutionarily conserved, multitasking TRP channels: Lessons from worms and flies. *Handbook of Experimental Pharmacology*, *223*, 937–962. https://doi.org/10.1007/978-3-319-05161-1_9

Venken, K. J. T., Schulze, K. L., Haelterman, N. A., Pan, H., He, Y., Evans-Holm, M., Carlson, J. W., Levis, R. W., Spradling, A. C., Hoskins, R. A., & Bellen, H. J. (2011). MiMIC: A highly versatile transposon insertion resource for engineering Drosophila melanogaster genes. *Nature Methods*, *8*(9), 737–747. https://doi.org/10.1038/nmeth.1662

Wahid, F., Shehzad, A., Khan, T., & Kim, Y. Y. (2010). MicroRNAs: Synthesis, mechanism, function, and recent clinical trials. In *Biochimica et Biophysica Acta - Molecular Cell Research* (Vol. 1803, Issue 11, pp. 1231–1243). https://doi.org/10.1016/j.bbamcr.2010.06.013

Wang, I. F., Ho, P. C., & Tsai, K. J. (2022). MicroRNAs in Learning and Memory and Their Impact on Alzheimer's Disease. In *Biomedicines* (Vol. 10, Issue 8). MDPI. https://doi.org/10.3390/biomedicines10081856

Wang, J., Wang, Z., Yuan, J., Wang, Q., & Shen, X. (2021). Upregulation of mir-137 expression suppresses tumor growth and progression via interacting with DNMT3A through inhibiting the PTEN/AKT signaling in HCC. *OncoTargets and Therapy*, *14*, 165–176. https://doi.org/10.2147/OTT.S268570

Wang, J., & Zhao, J. (2021). MicroRNA Dysregulation in Epilepsy: From Pathogenetic Involvement to Diagnostic Biomarker and Therapeutic Agent Development. In *Frontiers in Molecular Neuroscience* (Vol. 14). Frontiers Media S.A. https://doi.org/10.3389/fnmol.2021.650372

Wang, L., Harris, T. E., Roth, R. A., & Lawrence, J. C. (2007). PRAS40 regulates mTORC1 kinase activity by functioning as a direct inhibitor of substrate binding. *Journal of Biological Chemistry*, *282*(27), 20036–20044. https://doi.org/10.1074/jbc.M702376200

Wang, W., Guo, Y., He, L., Chen, C., Luo, J., Ma, Y., Li, J., Yang, Y., Yang, Q., Du, C., Zhang, Y., Li, Z., Xu, X., Tian, X., & Wang, X. (2018). Overexpression of miRNA-137 in the brain suppresses seizure activity and neuronal excitability: A new potential therapeutic strategy for epilepsy. *Neuropharmacology*, *138*, 170–181. https://doi.org/10.1016/j.neuropharm.2018.06.010

Wang, Y., Chen, R., Zhou, X., Guo, R., Yin, J., Li, Y., & Ma, G. (2020). miR-137: A Novel Therapeutic Target for Human Glioma. In *Molecular Therapy - Nucleic Acids* (Vol. 21, pp. 614–622). Cell Press. https://doi.org/10.1016/j.omtn.2020.06.028

Watson, L. S., Wilken-Resman, B., Williams, A., DiLucia, S., Sanchez, G., McLeod, T. L., & Sims-Robinson, C. (2022). Hyperinsulinemia alters insulin receptor presentation and internalization in brain microvascular endothelial cells. *Diabetes and Vascular Disease Research*, *19*(4). https://doi.org/10.1177/14791641221118626

Webb, A. E., & Brunet, A. (2014). FOXO transcription factors: Key regulators of cellular quality control. In *Trends in Biochemical Sciences* (Vol. 39, Issue 4, pp. 159–169). Elsevier Ltd. https://doi.org/10.1016/j.tibs.2014.02.003

West, A. E., & Greenberg, M. E. (2011). Neuronal activity-regulated gene transcription in synapse development and cognitive function. In *Cold Spring Harbor Perspectives in Biology* (Vol. 3, Issue 6, pp. 1–21). https://doi.org/10.1101/cshperspect.a005744

Weye, N., Momen, N. C., Christensen, M. K., Iburg, K. M., Dalsgaard, S., Laursen, T. M., Mortensen, P. B., Santomauro, D. F., Scott, J. G., Whiteford, H. A., McGrath, J. J., & Plana-Ripoll, O. (2020). Association of Specific Mental Disorders with Premature Mortality in the Danish Population Using Alternative Measurement Methods. *JAMA Network Open*, *3*(6). https://doi.org/10.1001/jamanetworkopen.2020.6646

When microRNAs activate translation. (2008). http://www.nature.com/naturemethods

Willoughby, L. F., Manent, J., Allan, K., Lee, H., Portela, M., Wiede, F., Warr, C., Meng, T. C., Tiganis, T., & Richardson, H. E. (2017a). Differential regulation of protein tyrosine kinase signalling by Dock and the PTP61F variants. *FEBS Journal*, *284*(14), 2231–2250. https://doi.org/10.1111/febs.14118

Willoughby, L. F., Manent, J., Allan, K., Lee, H., Portela, M., Wiede, F., Warr, C., Meng, T. C., Tiganis, T., & Richardson, H. E. (2017b). Differential regulation of protein tyrosine kinase signalling by Dock and the PTP61F variants. *FEBS Journal*, *284*(14), 2231–2250. https://doi.org/10.1111/febs.14118

Wright, C., Gupta, C. N., Chen, J., Patel, V., Calhoun, V. D., Ehrlich, S., Wang, L., Bustillo, J. R., Perrone-Bizzozero, N. I., & Turner, J. A. (2016). Polymorphisms in MIR137HG and microRNA-137-regulated genes influence gray matter structure in schizophrenia. *Translational Psychiatry*, *6*. https://doi.org/10.1038/tp.2015.211

Wright, C., Turner, J. A., Calhoun, V. D., & Perrone-Bizzozero, N. (2013). Potential Impact of miR-137 and Its Targets in Schizophrenia. *Frontiers in Genetics*, *4*. https://doi.org/10.3389/fgene.2013.00058

Wu, C. L., Buszard, B., Teng, C. H., Chen, W. L., Warr, C. G., Tiganis, T., & Meng, T. C. (2011a). Dock/Nck facilitates PTP61F/PTP1B regulation of insulin signalling. *Biochemical Journal*, *439*(1), 151–159. https://doi.org/10.1042/BJ20110799

Wu, C. L., Buszard, B., Teng, C. H., Chen, W. L., Warr, C. G., Tiganis, T., & Meng, T. C. (2011b). Dock/Nck facilitates PTP61F/PTP1B regulation of insulin signalling. *Biochemical Journal*, *439*(1), 151–159. https://doi.org/10.1042/BJ20110799

Wu, L., Chen, J., Ding, C., Wei, S., Zhu, Y., Yang, W., Zhang, X., Wei, X., & Han, D. (2015). MicroRNA-137 contributes to dampened tumorigenesis in human gastric cancer by targeting AKT2. *PLoS ONE*, *10*(6). https://doi.org/10.1371/journal.pone.0130124

Xu, Y., & Fisher, G. J. (2012). Receptor type protein tyrosine phosphatases (RPTPs) - Roles in signal transduction and human disease. In *Journal of Cell Communication and Signaling* (Vol. 6, Issue 3, pp. 125–138). Kluwer Academic Publishers. https://doi.org/10.1007/s12079-012-0171-5

Xue, Y., & Zhang, Y. (2018). Emerging roles for microRNA in the regulation of Drosophila circadian clock. In *BMC Neuroscience* (Vol. 19, Issue 1). BioMed Central Ltd. https://doi.org/10.1186/s12868-018-0401-8

Yang, Z., Yu, Y., Zhang, V., Tian, Y., Qi, W., & Wang, L. (2015). Octopamine mediates starvation-induced hyperactivity in adult Drosophila. *Proceedings of the National Academy of Sciences of the United States of America*, *112*(16), 5219–5224. https://doi.org/10.1073/pnas.1417838112

Yi, R., Qin, Y., Macara, I. G., & Cullen, B. R. (2003). Exportin-5 mediates the nuclear export of pre-microRNAs and short hairpin RNAs. *Genes and Development*, *17*(24), 3011–3016. https://doi.org/10.1101/gad.1158803

Yin, J., Lin, J., Luo, X., Chen, Y., Li, Z., Ma, G., & Li, K. (2014a). MiR-137: A new player in schizophrenia. In *International Journal of Molecular Sciences* (Vol. 15, Issue 2, pp. 3262–3271). Molecular Diversity Preservation International. https://doi.org/10.3390/ijms15023262

Yin, J., Lin, J., Luo, X., Chen, Y., Li, Z., Ma, G., & Li, K. (2014b). MiR-137: A new player in schizophrenia. In *International Journal of Molecular Sciences* (Vol. 15, Issue 2, pp. 3262–3271). Molecular Diversity Preservation International. https://doi.org/10.3390/ijms15023262

Yuan, L., Li, J., Yang, Y., Chen, Y., Bu, Y., Ye, M., Mao, X., Ma, T., Yu, L., & Nan, Y. (2021). LINC00514 promotes gastric cancer cell growth and EMT progression via miR-204-3p/KRAS. *Aging*, *13*(8), 12007–12015. https://doi.org/10.18632/aging.202905

Zhong, L., Bellemer, A., Yan, H., Honjo, K., Robertson, J., Hwang, R. Y., Pitt, G. S., & Tracey, W. D. (2012). Thermosensory and Nonthermosensory Isoforms of

Drosophila melanogaster TRPA1 Reveal Heat-Sensor Domains of a ThermoTRP Channel. *Cell Reports*, *1*(1), 43–55. https://doi.org/10.1016/j.celrep.2011.11.002

Zhou, S., Mackay, T. F. C., & Anholt, R. R. H. (2014). Transcriptional and epigenetic responses to mating and aging in Drosophila melanogaster. *BMC Genomics*, *15*(1). https://doi.org/10.1186/1471-2164-15-927